U.S. Department
of Transportation
Federal Railroad
Administration

Office of Research,
Development and Technology
Washington, DC 20590

Locomotive Crash Energy Management Vehicle-to-Vehicle Tests 1 & 2: Analyses and Test Results

DOT/FRA/ORD-23/20

Final Report | July 2023

REPORT DOCUMENTATION PAGE

Form Approved
OMB No. 0704-0188

1. REPORT DATE *(DD-MM-YYYY)*	2. REPORT TYPE	3. DATES COVERED *(From - To)*
9/9/2022	Technical Report	8/24/2018–5/10/2022

4. TITLE AND SUBTITLE
Locomotive Crash Energy Management Vehicle-to-Vehicle Tests 1 & 2: Analyses and Test Results

5a. CONTRACT NUMBER
6913G618F500083

5b. GRANT NUMBER

5c. PROGRAM ELEMENT NUMBER

6. AUTHOR(S)

Patricia Llana (ORCID 0000-0003-0885-4951)
Dr. Richard Stringfellow* (ORCID 0000-0003-3730-0851)

5d. PROJECT NUMBER

5e. TASK NUMBER

5f. WORK UNIT NUMBER

7. PERFORMING ORGANIZATION NAME(S) AND ADDRESS(ES)
Volpe National Transportation Systems Center
55 Broadway
Cambridge, MA 02142

*CAMX Power LLC
35 Hartwell Avenue
Lexington, MA 02421

8. PERFORMING ORGANIZATION REPORT NUMBER

9. SPONSORING/MONITORING AGENCY NAME(S) AND ADDRESS(ES)
U.S. Department of Transportation
Federal Railroad Administration
Office of Railroad Policy and Development
Office of Research, Development, and Technology
Washington, DC 20590

10. SPONSOR/MONITOR'S ACRONYM(S)
FRA

11. SPONSOR/MONITOR'S REPORT NUMBER(S)
DOT/FRA/ORD-23/20

12. DISTRIBUTION/AVAILABILITY STATEMENT

This document is available to the public through the FRA eLibrary.

13. SUPPLEMENTARY NOTES
COR: Patricia Llana (Volpe Center), Jeff Gordon (FRA)

14. ABSTRACT
Crash energy management (CEM) components which can be integrated into the end structure of a locomotive were developed: a push-back coupler and a deformable anti-climber. These components are designed to inhibit override and improve crashworthiness for equipped locomotives in a wide range of collisions. A full-scale dynamic impact test program has been designed to evaluate the CEM system. Two sets of coupling tests validated finite element models. Two CEM locomotive vehicle-to-vehicle collision tests and a train-to-train collision test are planned. This report describes the analyses and test results of both the first and second vehicle-to-vehicle impact tests.

15. SUBJECT TERMS
Locomotives, crashworthiness, railcars, couplers, crash energy management, push-back coupler, deformable anti-climber, override, collision, injury, impacts

16. SECURITY CLASSIFICATION OF:			17. LIMITATION OF ABSTRACT	18. NUMBER OF PAGES	19a. NAME OF RESPONSIBLE PERSON
a. REPORT	b. ABSTRACT	c. THIS PAGE			Jeff Gordon
Unclassified	Unclassified	Unclassified		118	19b. TELEPHONE NUMBER *(Include area code)* 617-494-2303

METRIC/ENGLISH CONVERSION FACTORS

ENGLISH TO METRIC	METRIC TO ENGLISH
LENGTH (APPROXIMATE)	**LENGTH (APPROXIMATE)**
1 inch (in) = 2.5 centimeters (cm)	1 millimeter (mm) = 0.04 inch (in)
1 foot (ft) = 30 centimeters (cm)	1 centimeter (cm) = 0.4 inch (in)
1 yard (yd) = 0.9 meter (m)	1 meter (m) = 3.3 feet (ft)
1 mile (mi) = 1.6 kilometers (km)	1 meter (m) = 1.1 yards (yd)
	1 kilometer (km) = 0.6 mile (mi)
AREA (APPROXIMATE)	**AREA (APPROXIMATE)**
1 square inch (sq in, in^2) = 6.5 square centimeters (cm^2)	1 square centimeter (cm^2) = 0.16 square inch (sq in, in^2)
1 square foot (sq ft, ft^2) = 0.09 square meter (m^2)	1 square meter (m^2) = 1.2 square yards (sq yd, yd^2)
1 square yard (sq yd, yd^2) = 0.8 square meter (m^2)	1 square kilometer (km^2) = 0.4 square mile (sq mi, mi^2)
1 square mile (sq mi, mi^2) = 2.6 square kilometers (km^2)	10,000 square meters (m^2) = 1 hectare (ha) = 2.5 acres
1 acre = 0.4 hectare (he) = 4,000 square meters (m^2)	
MASS - WEIGHT (APPROXIMATE)	**MASS - WEIGHT (APPROXIMATE)**
1 ounce (oz) = 28 grams (gm)	1 gram (gm) = 0.036 ounce (oz)
1 pound (lb) = 0.45 kilogram (kg)	1 kilogram (kg) = 2.2 pounds (lb)
1 short ton = 2,000 pounds (lb) = 0.9 tonne (t)	1 tonne (t) = 1,000 kilograms (kg) = 1.1 short tons
VOLUME (APPROXIMATE)	**VOLUME (APPROXIMATE)**
1 teaspoon (tsp) = 5 milliliters (ml)	1 milliliter (ml) = 0.03 fluid ounce (fl oz)
1 tablespoon (tbsp) = 15 milliliters (ml)	1 liter (l) = 2.1 pints (pt)
1 fluid ounce (fl oz) = 30 milliliters (ml)	1 liter (l) = 1.06 quarts (qt)
1 cup (c) = 0.24 liter (l)	1 liter (l) = 0.26 gallon (gal)
1 pint (pt) = 0.47 liter (l)	
1 quart (qt) = 0.96 liter (l)	
1 gallon (gal) = 3.8 liters (l)	
1 cubic foot (cu ft, ft^3) = 0.03 cubic meter (m^3)	1 cubic meter (m^3) = 36 cubic feet (cu ft, ft^3)
1 cubic yard (cu yd, yd^3) = 0.76 cubic meter (m^3)	1 cubic meter (m^3) = 1.3 cubic yards (cu yd, yd^3)
TEMPERATURE (EXACT)	**TEMPERATURE (EXACT)**
[(x-32)(5/9)] °F = y °C	[(9/5) y + 32] °C = x °F

QUICK INCH - CENTIMETER LENGTH CONVERSION

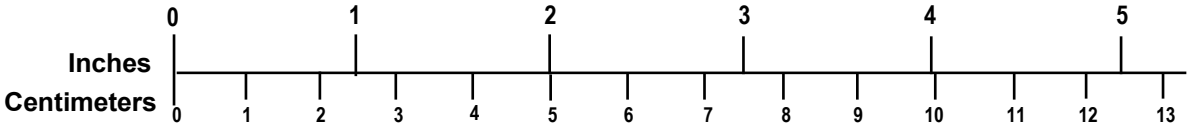

QUICK FAHRENHEIT - CELSIUS TEMPERATURE CONVERSIO

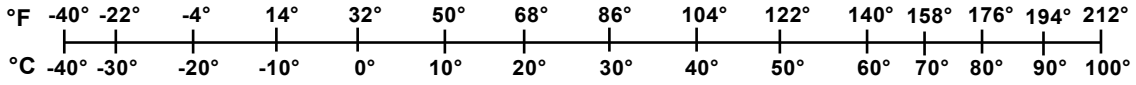

For more exact and or other conversion factors, see NIST Miscellaneous Publication 286, Units of Weights and Measures. Price $2.50 SD Catalog No. C13 10286

Updated 6/17/98

Acknowledgements

This work was performed as part of the Equipment Safety Research Program of the Federal Railroad Administration (FRA) Office of Research, Development, and Technology (RD&T). The authors appreciate the technical support and guidance provided by Jeff Gordon, Program Manager, RD&T. FRA staff at the Transportation Technology Center (TTC) in Pueblo, Colorado, helped coordinate efforts between FRA and Transportation Technology Center, Inc. (TTCI). The authors appreciate the technical support and efforts of both FRA staff and TTCI staff at TTC in conducting the equipment tests. The authors would also like to acknowledge Volpe National Transportation Systems Center colleague A. Benjamin Perlman for his ongoing technical advice and support in the research discussed in this report.

Contents

Illustrations

Tables

Executive Summary

The Federal Railroad Administration (FRA), with support of the Volpe National Transportation Systems Center, is conducting research on the implementation of CEM features on locomotives. This report summarizes activities that supported full-scale vehicle-to-vehicle tests that evaluated two components retrofitted onto a conventional passenger locomotive to enhance its crashworthiness: a push-back coupler (PBC) and a deformable anti-climber (DAC). The modified locomotive design was based on the concepts generally referred to as "crash energy management," (CEM) and thus has been termed a "CEM locomotive."

The work plan for the program called for four key activities:

- Pre-test analysis for Vehicle-to-Vehicle Test 1 (V2VT1) — a collision between a moving CEM locomotive and a standing conventional locomotive
- Post-test evaluation for V2VT1
- Pre-test analysis for Vehicle-to-Vehicle Test 2 (V2VT2) — a collision between a moving CEM locomotive and a standing consist with a lead cab car and trailing freight car
- Post-test evaluation for V2VT2

Researchers focused pre-test activities for both tests on developing and implementing finite element (FE) models that simulated the test collision and, in particular, helped determine the target speeds for the collisions. They chose the target speeds so that certain aspects of the CEM design could be assessed in the tests. Specifically, it was set at a speed that would cause complete exhaustion of the PBC system, failure of the shear bolts connecting the sliding lug to the side plates of the draft pocket, and crush of DAC elements to an extent that 50 percent of the required energy absorption capacity would be absorbed. Pre-test activities for both tests also included support of various aspects of test preparation, including the test implementation plan.

Based on pre-test activities in support of V2VT1, researchers identified a target speed of 21 mph ±1 mph that would meet test objectives, with some margin of error. The actual test speed was only 19.3 mph, less than the minimum expected speed of 20 mph. At 19.3 mph, the kinetic energy of the impact is only 93 percent of that at 20 mph, and only 84 percent of that at 21 mph (the target speed). The test was successful in that the various components performed as designed, and the stroke of the PBC deformation tube appeared to have been exhausted. However, there was not enough energy to fail the shear bolts of the PBC. Researchers identified two discrepancies between the test conditions and the model as factors that led to recommended target collision speeds being lower than they otherwise would have been, and thus also contributed to insufficient collision energy to cause the shear bolts to fail. Post-test assessment of damage uncovered one issue regarding the design of the CEM locomotive support structure that needed to be addressed prior to V2VT2. Post-test FE analyses conducted at the actual test speed were in very good agreement with the test data, an indication of the reliability and fidelity of the FE models.

Due to the COVID-19 pandemic, V2VT2 was postponed approximately 18 months.

Pre-test support for VTVT2 focused on modifying the FE model to address the repairs made, modifying the cab car model and adding a freight car. Researchers made several modifications to the FE models to improve their fidelity.

Pre-test simulations of VTVT2 indicated the couplers must be closed for the PBC system to exhaust the stroke of the deformation tube and fail the shear bolts. A target speed of 33 mph ± 2 mph was chosen to meet test objectives of complete PBC stroke with shear bolt failure and energy absorption in the DAC of at least 50 percent of the design specification, with some margin for error. Due to the removal of the original flooring in the asbestos remediation process, the models indicated the collision forces that would arise in this test might challenge the buckling resistance of the cab car.

The actual collision speed was 32.8 mph – very close to the target. The test was successful, with all of the key test objectives met, including exhaustion of the PBC deformation tube stroke and failure of the shear bolts. The colliding vehicles did not derail, nor did one override the other. However, the cab car was "crippled," with a large buckle forming in the underframe just forward of the rear side doors. After impact, the wheels of the rear truck of the cab car lifted slightly and fell back onto the rail without causing a derailment. Overall, the vehicle-to-vehicle impact tests together were successful in demonstrating the effectiveness of the components of the CEM system working in tandem to absorb impact energy and to prevent override in two different vehicle-to-vehicle collision scenarios.

1. Introduction

Research to develop new technologies for increasing the safety of passengers and crew in rail equipment is being directed by the Federal Railroad Administration (FRA) Office of Research, Development, and Technology (RD&T). To that end, two crash energy management (CEM) components that can be integrated into the end structure of a locomotive have been developed: a push-back coupler (PBC) and a deformable anti-climber (DAC). These components are designed to inhibit override in the event of a collision. The results of vehicle-to-vehicle override, where the strong underframe of one vehicle, typically a locomotive, impacts the weaker superstructure of the other vehicle, can be devastating and compromise the occupied space. The objective of this research project is to demonstrate the feasibility of using these components to improve crashworthiness of equipped locomotives in a wide range of potential collisions, including collisions with conventional locomotives, conventional cab cars, and freight equipment.

1.1 Background

RD&T and the Volpe National Transportation Systems Center (Volpe Center) continue to evaluate new technologies for increasing the safety of rail passengers and crew. In recognition of the importance of override prevention in train-to-train collisions in which one of the vehicles is a locomotive [1][2][3], and in light of the success of crash energy management technologies in passenger trains [4], FRA seeks to evaluate the effectiveness of crashworthy components that are integrated into the end structure of a locomotive. These components are specifically designed to mitigate the effects of a collision and, in particular, to prevent override of one of the lead vehicles onto the other [5].

In prior Volpe Center research, designs for two CEM components for retrofit onto the forward end of a locomotive, a DAC and PBC, were developed, fabricated, and tested [6][7]. The performance of each design was evaluated through large deformation dynamic finite element (FE) analysis. Two test articles were fabricated and dynamically tested individually by means of a railcar impact into a test wall to independently verify performance characteristics of the two components relative to specific requirements. The tests were successful in demonstrating the effectiveness of the two design concepts. Test results were consistent with FE model predictions in terms of energy absorption capability, force-displacement behavior, and modes of deformation.

In a follow-on program, the two CEM components were integrated into the end structure of a conventional locomotive (see Figure 1) to demonstrate, through a series of full-scale vehicle collision tests, that these components work together to mitigate the effects of a collision and prevent override [8]. Each of these tests were designed to evaluate the performance of the CEM locomotive in head-on collision scenarios in which a moving CEM locomotive (or CEM locomotive-led consist) collides with a stationary vehicle or consist. The stationary vehicle (or lead vehicle in a consist) may be a conventional locomotive, a CEM locomotive, a cab car, or a freight car. The overall objective of these tests is to demonstrate the effectiveness of a locomotive CEM system comprised of a PBC and a DAC.

Figure 1. CEM locomotive comprising a DAC and PBC retrofit onto an F40 locomotive

In a first series of tests, both conventional and CEM coupling tests were conducted. The conventional coupling tests, between a conventional locomotive and a standing M1 cab car, were conducted to establish the speed at which coupling does not cause damage to either of the colliding vehicles [9][10]. The CEM coupling tests evaluated the performance of the PBC at collision speeds ranging from 2 mph to 9 mph [9]. In these tests, the CEM locomotive impacted a standing M1 cab car. Two reports detail the test instrumentation and provide the raw test data for both the conventional [10] and CEM coupling tests [11].

In this program, sub-contractor CAMX (formerly TIAX) provided consulting services to the Volpe Center in support of two vehicle-to-vehicle collision tests — one with a CEM locomotive impacting a standing conventional locomotive, and one with a CEM locomotive impacting a standing consist led by an M1 cab car with trailing freight cars. These services included FE analyses, review of test implementation plans, troubleshooting of the CEM systems used in the tests, post-test data review, and repair recommendations for the equipment.

1.2 Objectives

The objective of this effort was to provide engineering evaluation and program management, including FE analyses and troubleshooting, for two CEM locomotive vehicle-to-vehicle tests.

Prior to the tests, these services included making modifications to FE models, as needed, and simulation of test collisions to help determine test parameters (particularly impact speed) and to predict the behavior of the vehicles during the impact. The services also included solving structural and logistical issues that arose with the CEM components and their retrofit to the locomotive. Following each test, these services included evaluation of test results, evaluation of vehicle damage, and recommendations for vehicle repair in preparation of subsequent tests. Vehicle-to-Vehicle Test 2 (V2VT2) was postponed approximately 18 months due to travel restrictions caused by the COVID-19 pandemic.

1.3 Overall Approach

The approach to this effort was dependent on the nature of the issues that arose. In general, the approach included review of test plans, e-mail exchanges, telephone discussions, pre-test and post-test data and photographs of vehicle components, and the creation and execution of FE models simulating the two vehicle-to-vehicle tests.

1.4 Scope

Researchers focused on providing engineering evaluation and program management for the two CEM locomotive vehicle-to-vehicle tests in support of the objectives outlined in Section 1.2. Prior to each test, Volpe Center and CAMX personnel participated in discussions and assisted with problem-solving of structural and logistical issues that arose with the vehicles. A key component of the effort was pre-test FE analysis of the impact tests to determine test parameters and to predict the behavior of the vehicles. Following each test, damage evaluations were performed, and repair recommendations were developed for the equipment. Retrofit design modifications necessary for the repair of these components and their attachment to the main structure of the locomotive were within scope of this program; however, such modifications were kept to a minimum.

1.5 Organization of the Report

The remainder of this report is organized into eight sections that describe the activities in the test program:

- Section 2. Vehicle-to-Vehicle Test 1 Pre-Test Analysis
- Section 3. Vehicle-to-Vehicle Test 1 Test Results
- Section 4. Vehicle-to-Vehicle Test 1 Post-Test Evaluation
- Section 5. Vehicle-to-Vehicle Test 2 Pre-Test Analysis
- Section 6. Vehicle-to-Vehicle Test 1 Test Results
- Section 7. Vehicle-to-Vehicle Test 2 Post-Test Evaluation
- Section 8. Construction of Finite Element Models
- Section 9. Conclusion

Note that some of the FE model creation activities described in Section 8 were performed as part of Section 2 and Section 5 of the program.

2. Vehicle-to-Vehicle Test 1 Pre-Test Analysis

This section describes engineering evaluation and project management performed in support of the first CEM locomotive vehicle-to-vehicle test (V2VT1). These services culminated in a trip to the Transportation Technology Center (TTC) in Pueblo, Colorado, in January 2019 to witness Vehicle-to-Vehicle Test 1, a collision between a moving CEM locomotive and a standing conventional locomotive. The test was conducted by Transportation Technology Center, Inc. (TTCI), a wholly owned subsidiary of the American Association of Railroads (AAR), on behalf of FRA. A schematic of the test is shown in Figure 2. Details of the test preparation, test requirements, and instrumentation can be found in a companion ASME paper [12].

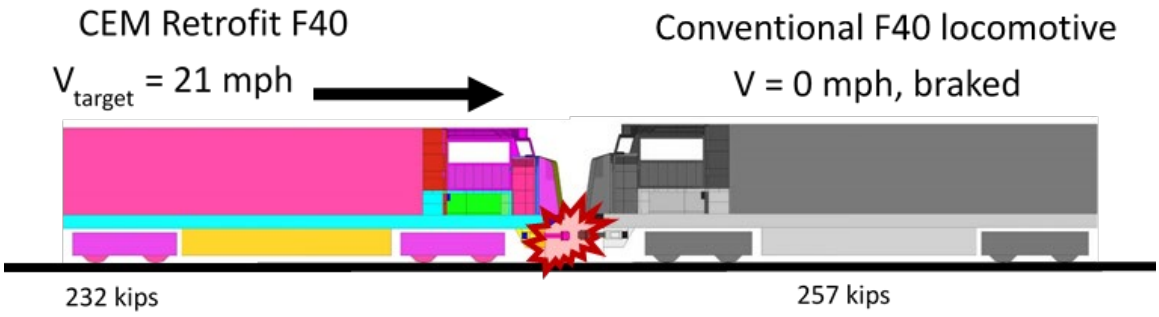

Figure 2. Schematic of CEM Vehicle-to-Vehicle Test 1 initial conditions

- Activities performed during this period included modification of FE models (described in greater detail in Section 8 of the report):
  - Modification of the FE model of the CEM locomotive to include a more explicit representation of the coupler carrier so that impact between the coupler and the coupler carrier could be realized, as well as failure of the coupler carrier.
  - Modification of the FE model of the conventional locomotive to include a plow.
  - Revision of the FE model of the conventional locomotive to include modifications to the collision post and other structures in the short hood to reflect the pre-S-580 condition of Locomotive 4117 that will be used in the upcoming collision test.
- Assembly and implementation of an FE model reflecting these modifications for impact of the CEM locomotive with a conventional locomotive at approximately 20 mph.
- Review and comment of the Test Implementation Plan (TIP) for the V2VT1 planned for January 2019.
- Participation via telephone and e-mail in a number of discussions in preparation for the January 2019 test

2.1 Pre-Test Finite Element Analysis

An FE model originally constructed as part of a prior program [8] was modified to:

(1) More explicitly model the coupler/coupler carrier interaction.

(2) Incorporate differences between the conventional locomotive planned for use in V2VT1 with the representative locomotive design used in the earlier program.

These modifications are described in more detail in Section 8. One of the primary purposes of the model was to help determine the collision speed for the test. This speed was calculated to satisfy three key test objectives:

(1) Exhaustion of push-back coupler (PBC) stroke.

(2) Failure of the shear bolts connecting the sliding lug to the sides of the draft pocket.

(3) Sufficient deformation of the deformable anti-climber (DAC) to absorb 50 percent of its specified energy absorption capacity of 600 ft-kips, i.e., 300 ft-kips.

Based on the results of prior analyses, researchers determined that a collision speed of 20 mph was sufficient to satisfy these criteria. Results from FE analyses of a collision at this speed are summarized in the next several figures.

Figure 3 shows a side view of the model for this collision scenario. The model for the CEM locomotive employed approximately 230,000 elements, with the element size defined to be progressively smaller near the colliding interface.

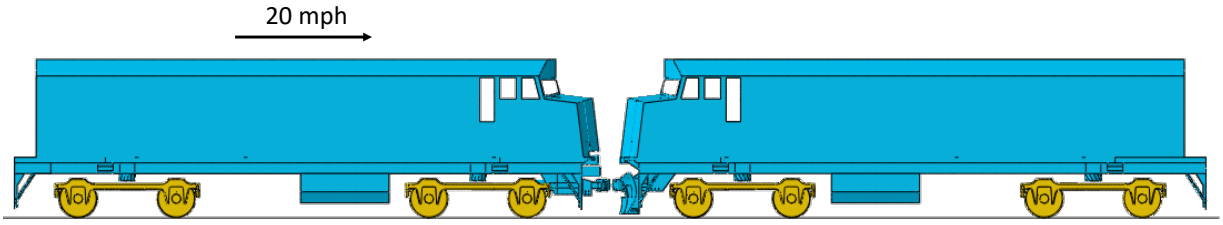

Figure 3. Side view of the model for a moving CEM locomotive (left) colliding with a conventional locomotive (right)

Figure 4 shows a side view of the colliding vehicle ends after 12.8” of crush (~0.04 seconds). At this point, the coupler carrier bolts had just failed after impact from the PBC. During the next ~0.05 seconds, the coupler continued to push back until exhausting its stroke after approximately 24.5” of crush (see Figure 5), causing the shear bolts to fail. At this level of crush, the upper DAC tube assembly had impacted the anti-climber of the conventional locomotive.

As the vehicles continued to crush, the load path shifted upward to the DAC, specifically the upper DAC tubes. The upper DAC tubes continued to crush against the anti-climber of the conventional locomotive, and the respective short hoods begin to crush. At the peak extent of crush (35”, see Figure 6), the vehicle ends were extensively engaged. Deformation of the respective vehicle ends is illustrated in Figure 7. Most of the deformation occurred in the upper DAC assembly, which crushed about 10” and rotated back as indicated, and in the central regions of the respective short hoods. A detail showing only the conventional locomotive plow and the CEM draft pocket side plates (Figure 8) indicates that there was a minimal, localized deformation of the plow due to impact with the front edges of the side plates, where the coupler carrier was mounted. Figure 9 shows a side view of the DAC at various stages of the collision. Figure 10 shows the pre-test analysis calculated force-displacement curve, indicating the force contributions from the PBC, DAC, and other end structures. As indicated in the figure, coupler

carrier failure occurred after ~12” of crush (~0.04 seconds after impact), DAC engagement occurred after ~20” of crush (~0.08 seconds after impact), and shear bolt failure occurred after ~24” of crush (~0.9 seconds after impact).

At the maximum extent of crush, the DAC absorbed approximately 420 ft-kips of energy, well above the target of 300 ft-kips. The exhausted PBC absorbed its design limit of almost 1,100 ft-kips. Other structures in the end frames of the respective vehicles, including the conventional locomotive draft gear, absorbed another 300 ft-kips.

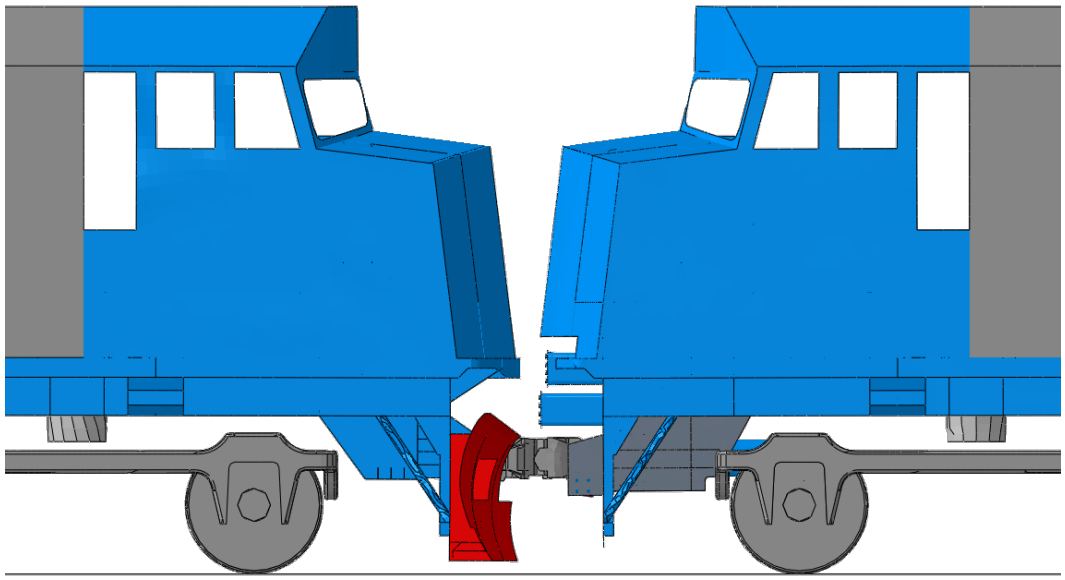

Figure 4. Detail showing colliding vehicle ends after 12.8” of crush; the coupler carrier bolts have failed

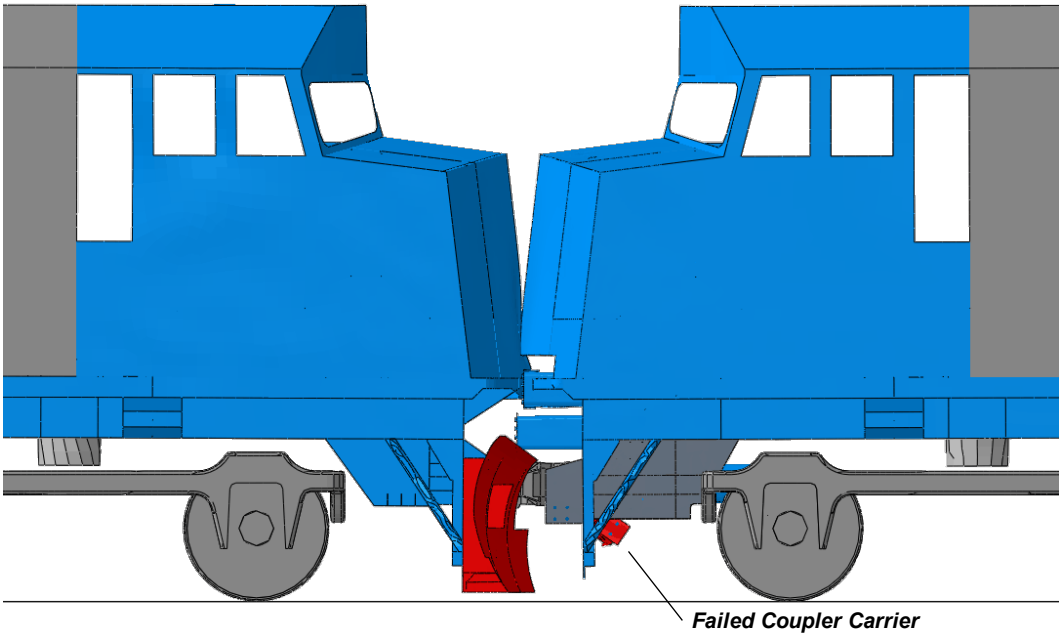

Figure 5. Detail showing colliding vehicle ends after 24.5” of crush; the shear bolts have now failed

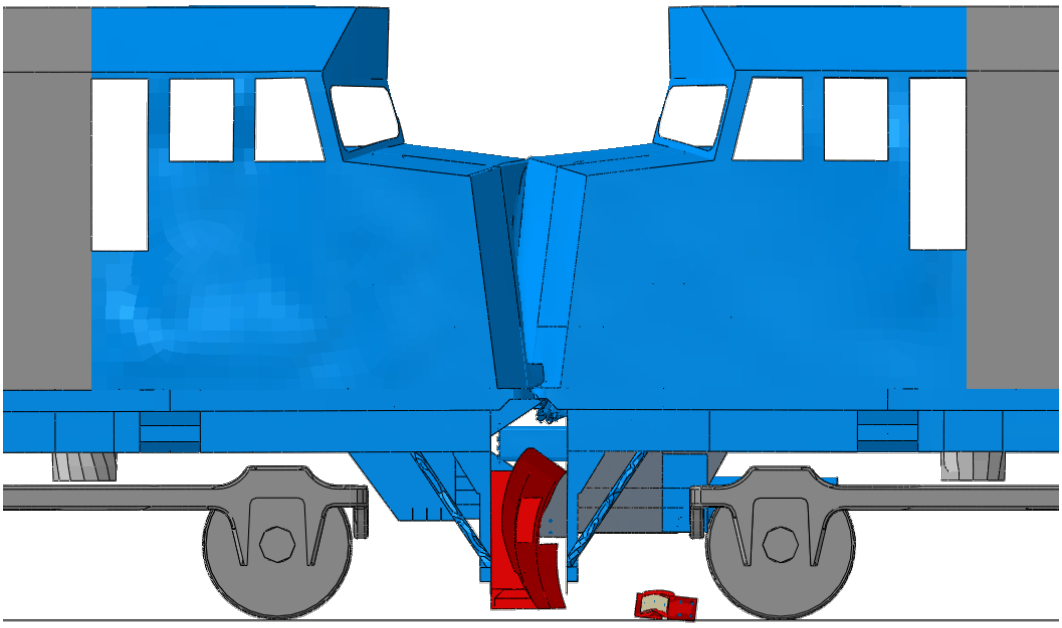

Figure 6. Detail showing colliding vehicle ends after 35” of crush (peak displacement)

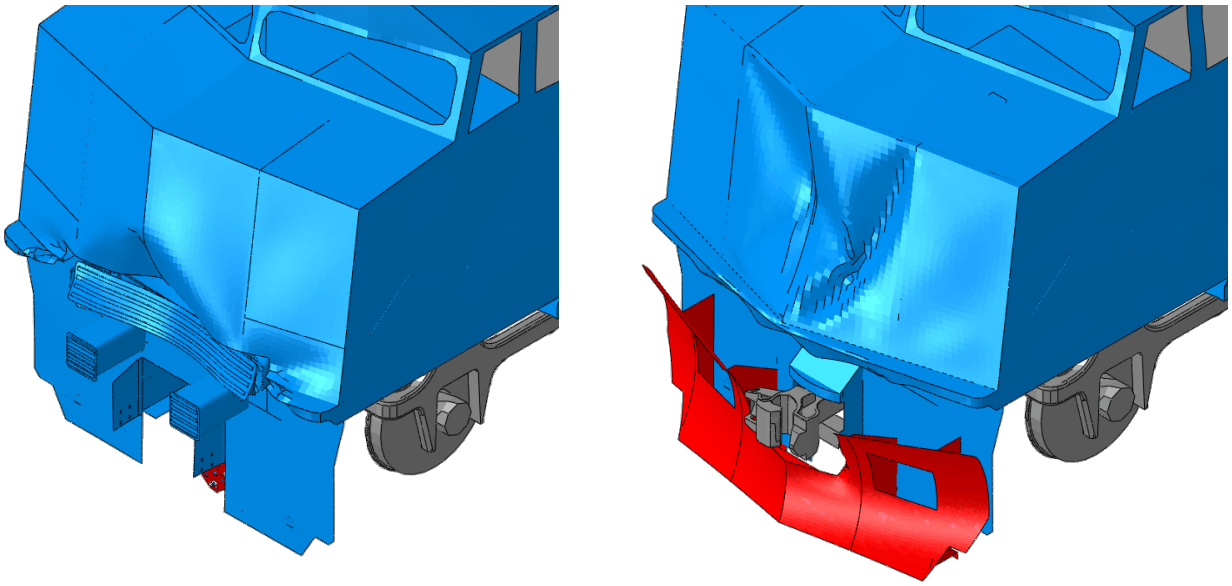

Figure 7. Deformation at 35” crush. Left — CEM locomotive; right — conventional locomotive

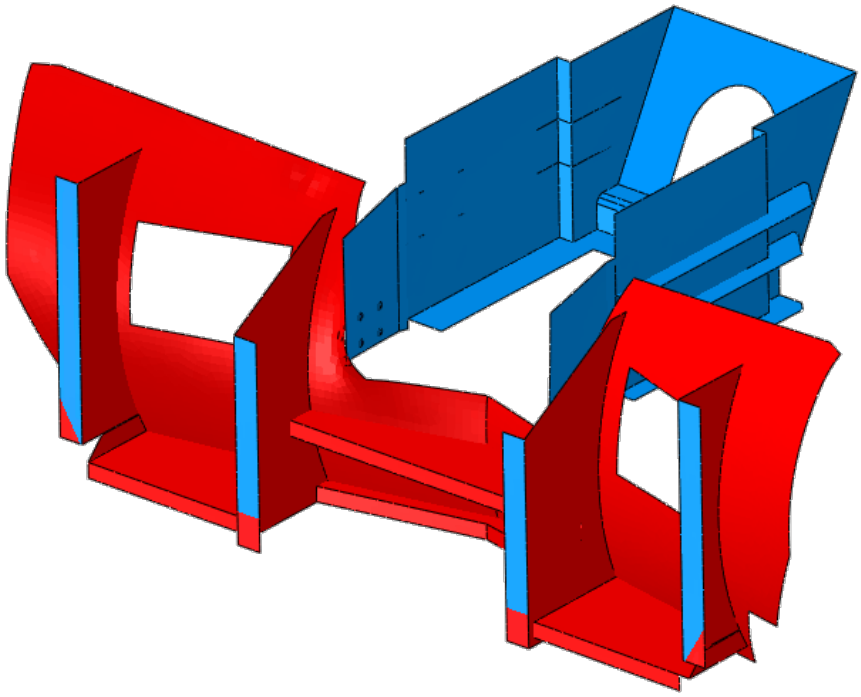

Figure 8. Detail showing minimal deformation of conventional locomotive plow (red) at 35” crush due to impact with draft pocket side plates (blue)

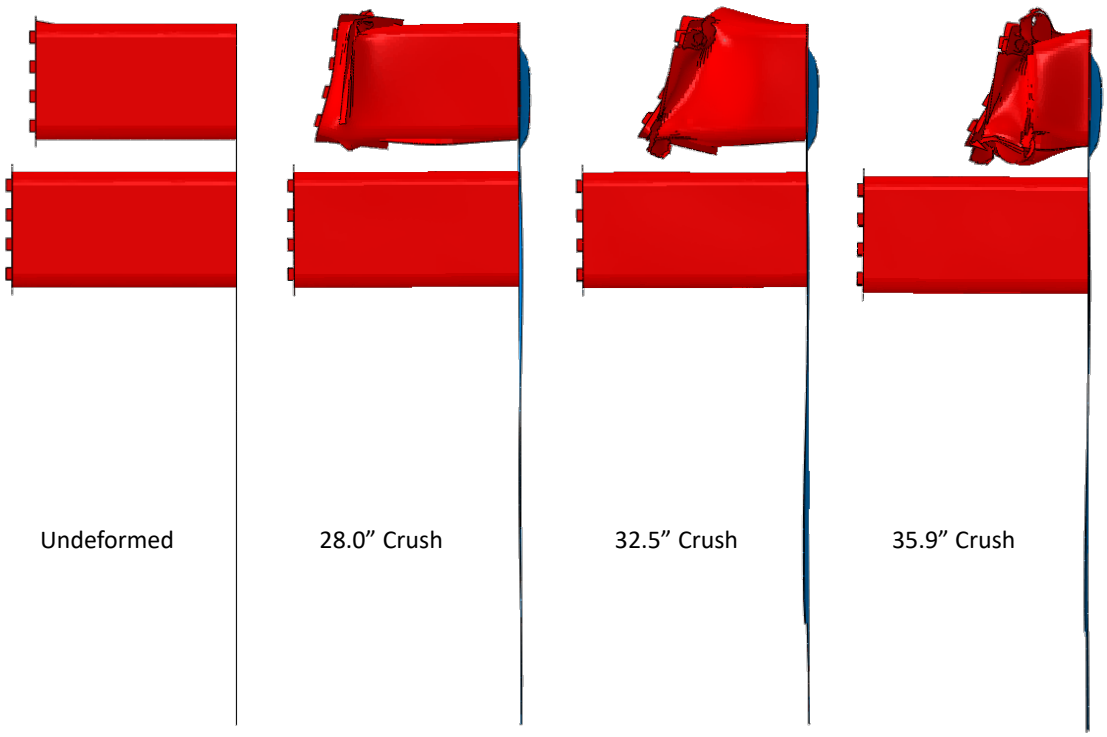

Note: elements with PEEQ > 0.3 have been removed. Not all such elements have failed, due to triaxiality dependence of failure criterion.

Figure 9. Deformation of DAC at various extents of crush

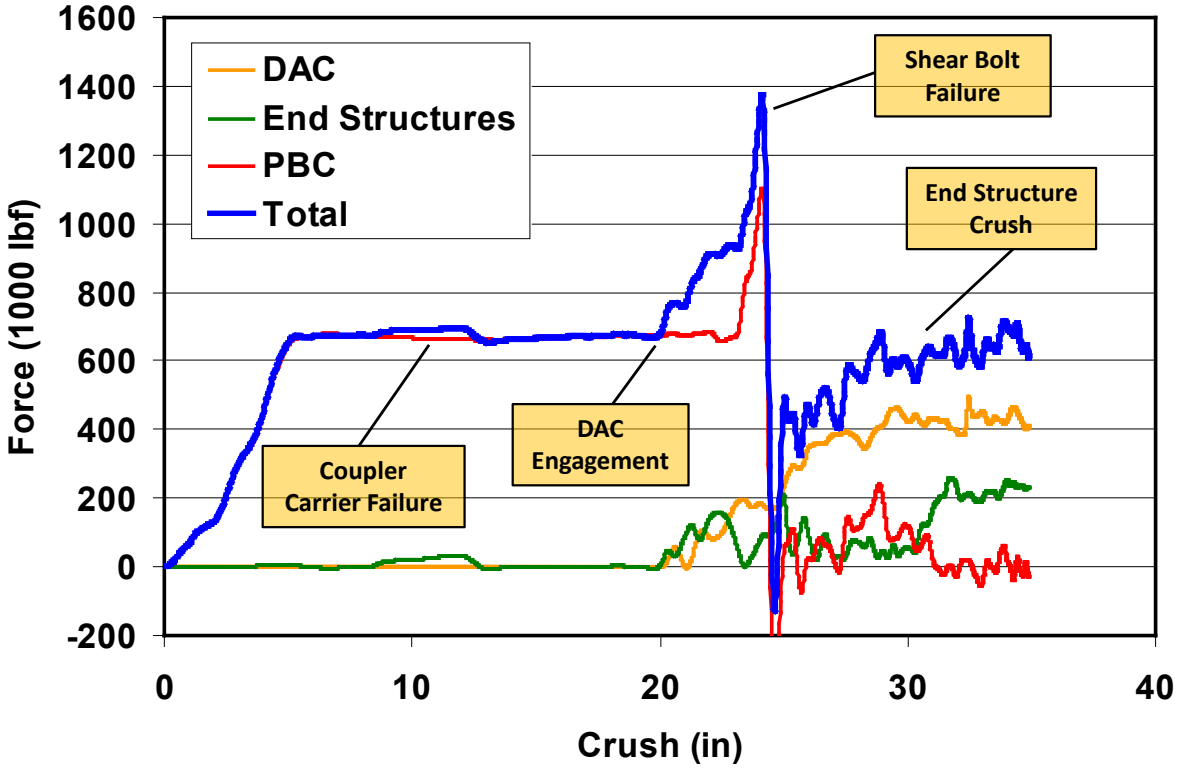

Figure 10. Force-displacement curve showing contributions from PBC, DAC and other end structures

2.2 Revised Pre-Test Analyses

Just prior to the test, informed by measurements of the actual weights of the instrumented CEM locomotive (233 kips) and conventional locomotive (257 kips), an FE analysis incorporating the measured weights was conducted at the target speed of 21 mph as well as at the limits of the expected speed range (20 mph and 22 mph). Selected results from theses analyses are presented in Figure 11 through Figure 13. Figure 11 shows the calculated force-displacement curve and the estimated contributions of the key structures for a 21-mph test speed. Results indicate that the predicted crush at 21 mph was about 37", with the shear bolts failing at a crush of 25". Figure 12 shows the respective vehicle speeds and indicate a crossover of speeds (corresponding to maximum crush) at ~0.19 seconds. Figure 13 shows calculated force-crush curves for three collision speeds — 20 mph, 21 mph and 22 mph — in the expected range for the test, with the predicted crush increasing from ~34" at 20 mph to ~39" at 22 mph. Since the desired impact speed was 20 mph, the target impact speed was set to 21 mph to take into account the ±1 mph speed tolerance.

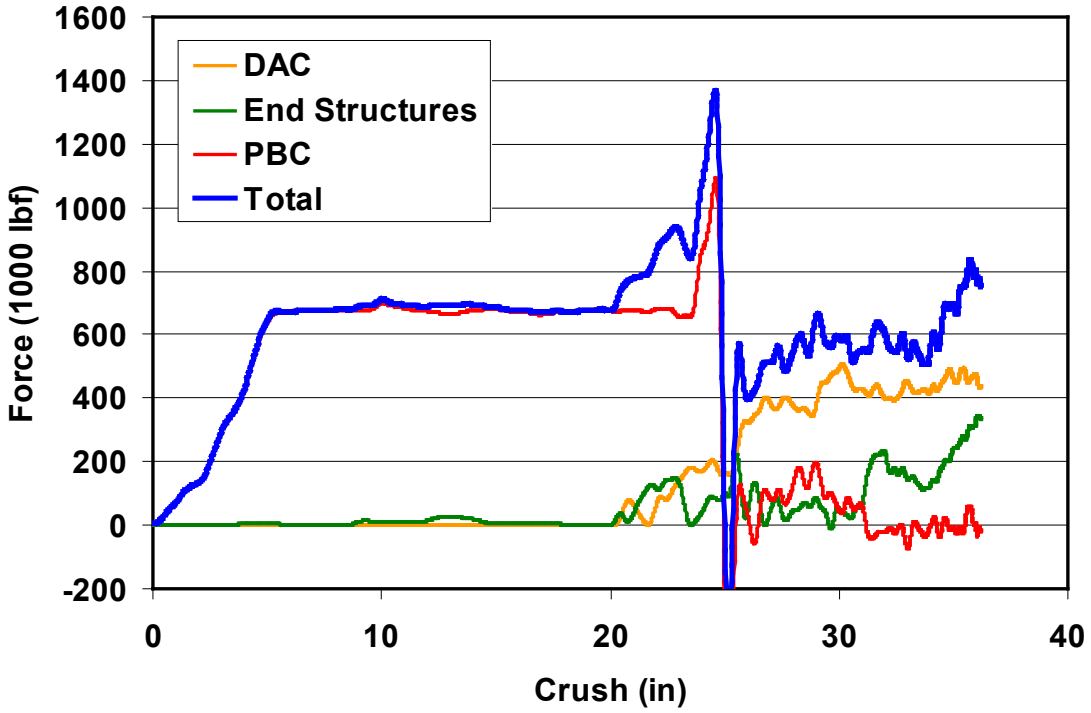

Figure 11. FE model calculated force-displacement curve at 21 mph collision for revised model using measured vehicle weights, with estimated contributions of key components

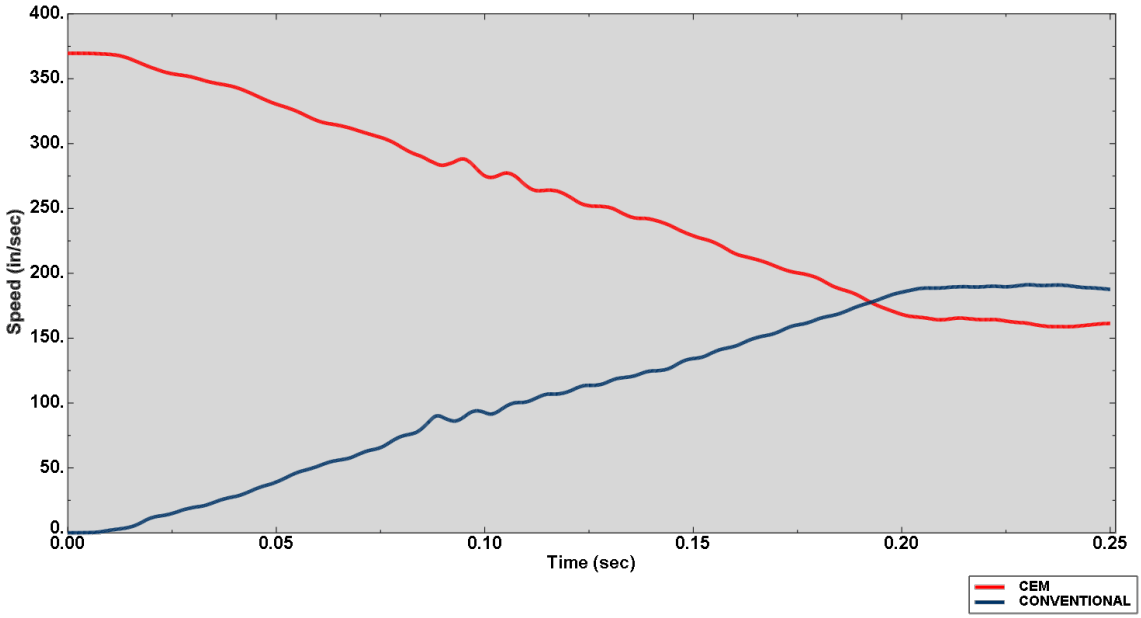

Figure 12. FE model predicted vehicle speeds at 21 mph for revised model using measured vehicle weights

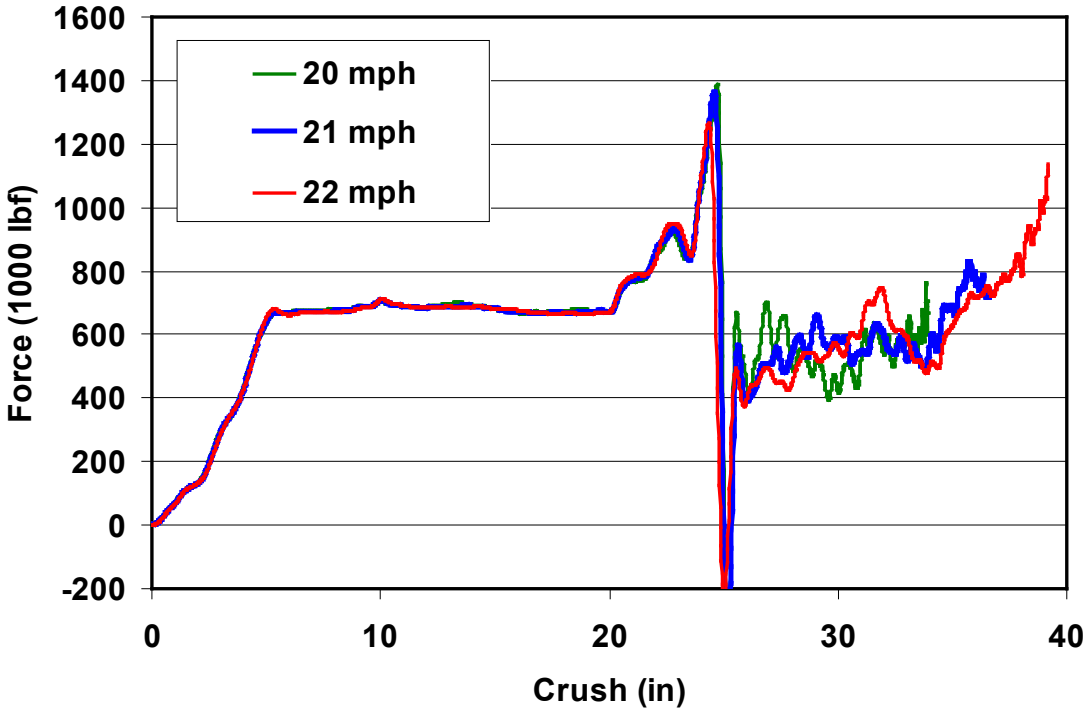

Figure 13. Comparison of revised FE model predicted force-displacement curves for collision speeds of 20 mph, 21 mph, and 22 mph

3. Vehicle-to-Vehicle Test 1 Test Results

Vehicle-to-Vehicle Test 1 was performed on January 23, 2019. The test locomotives were inspected on the afternoon of January 22. The instrumentation for the test was inspected. Positioning of strain gages on the underframes of the respective vehicles was verified. A report details the test instrumentation and provides the raw test data for this test [13]. Details and evaluation of the test results can be found in a companion ASME paper [14].

3.1 Test Outcome

On the day of the test, the weather conditions were clear with low winds. The research team decided both couplers would be left open to increase the chance of coupling, and the couplers were aligned within 1 inch vertically. The conventional locomotive's air brakes were applied, and the hand brake was secured before the impact. The target impact speed was 21 mph, and the actual impact speed was 19.3 mph. Figure 14 shows the vehicles after the test. The vehicles were kept in-line. There was no derailment of the vehicles and no sign of override.

Figure 14. Post-test photo of the locomotives

During the test, the couplers engaged at impact but did not lock together. The PBC triggered properly and moved back into the draft pocket. As the PBC moved back, the coupler carrier broke away, as designed. The intact coupler carrier before the test is shown in Figure 15. Figure 16 shows the failed coupler carrier where it fell after the PBC head moved back through it and disengaged it.

Figure 15. Pre-test photograph of the coupler carrier

Figure 16. Post-test photograph showing the coupler carrier lying on the track

After pushing through the coupler carrier, the PBC continued to move back, deforming the crush tube. Figure 17 and Figure 18 show the back of the deformation tube of the PBC before and after the impact. The deformation tube was covered in paint that was designed to peel off in strips as the exterior tube deformed. Figure 18 indicates that the stroke of the deformation tube was

almost exhausted. Figure 19 shows the deformation tube after it was removed from the draft pocket. Measurements taken confirmed that the full design stroke of the deformation tube was nearly exhausted. This was confirmed by evidence of contact between the limit stop mounted on the sliding lug and the rear of the PBC head, as shown in Figure 20 and Figure 21. This contact was designed to occur at the full stroke of the PBC.

Figure 17. Pre-test photograph of the back of the PBC deformation tube

Figure 18. Post-test photograph showing the back of the PBC deformation tube

Figure 19. Deformed PBC deformation tube removed from the draft pocket; peeled paint has been removed

Figure 20. Damage to the limit stop mounted to the front of the sliding lug due to contact by the back of the PBC coupler head

Figure 21. Damage to rear of the PBC coupler head from limit stop contact

As the PBC was pushed back, the top DAC tubes impacted the front of the conventional locomotive and began to crush. Figure 22 shows the two locomotives engaged after the impact. The photo on the right shows that only the upper DAC tubes crushed; the lower DAC tubes did not deform, as expected.

For comparison, Figure 23 shows the undeformed DAC before the test, and Figure 24 shows the deformed DAC after the test and after the vehicles had been separated. Figure 25 shows side views of both the right and left upper DAC tubes. The crush was greater on the right side than on the left — due to an approximately 2” lateral offset between the locomotives at the moment of impact.

The shear bolts connecting the sliding lug to the draft pocket did not trigger; therefore, the sliding lug did not move back into the draft pocket.

Figure 22. Post-test photo of CEM system; close-up on the right

Figure 23. Pre-test photograph of DAC

Figure 24. Post-test photograph of DAC showing that only the upper DAC tubes deformed

Figure 25. Deformed upper DAC tubes, right and left sides, respectively

3.2 Damage to the Equipment

Other than the damage to the CEM components, which was designed to occur, there was minimal damage to the CEM locomotive. Figure 26 shows the small amount of deformation of the bottom of the short hood. This was minor and easy to repair.

Figure 26. CEM locomotive damage

There was also minimal damage to the conventional locomotive. Figure 27 and Figure 28 show the dent caused by interaction with the short hood of the CEM locomotive. This was also minor and easy to repair.

Figure 27. Conventional locomotive damage

Figure 28. Close-up of conventional locomotive damage

Figure 29 shows a comparison of post-test photographs that provide evidence of the lateral offset of the colliding vehicles: matching scratches on short hoods of CEM locomotive (top left) and conventional locomotive (top right) indicate a 2.5” lateral offset. This offset resulted in less extensive crush of the left upper DAC tube (bottom left) relative to crush of the right upper DAC tube (bottom right).

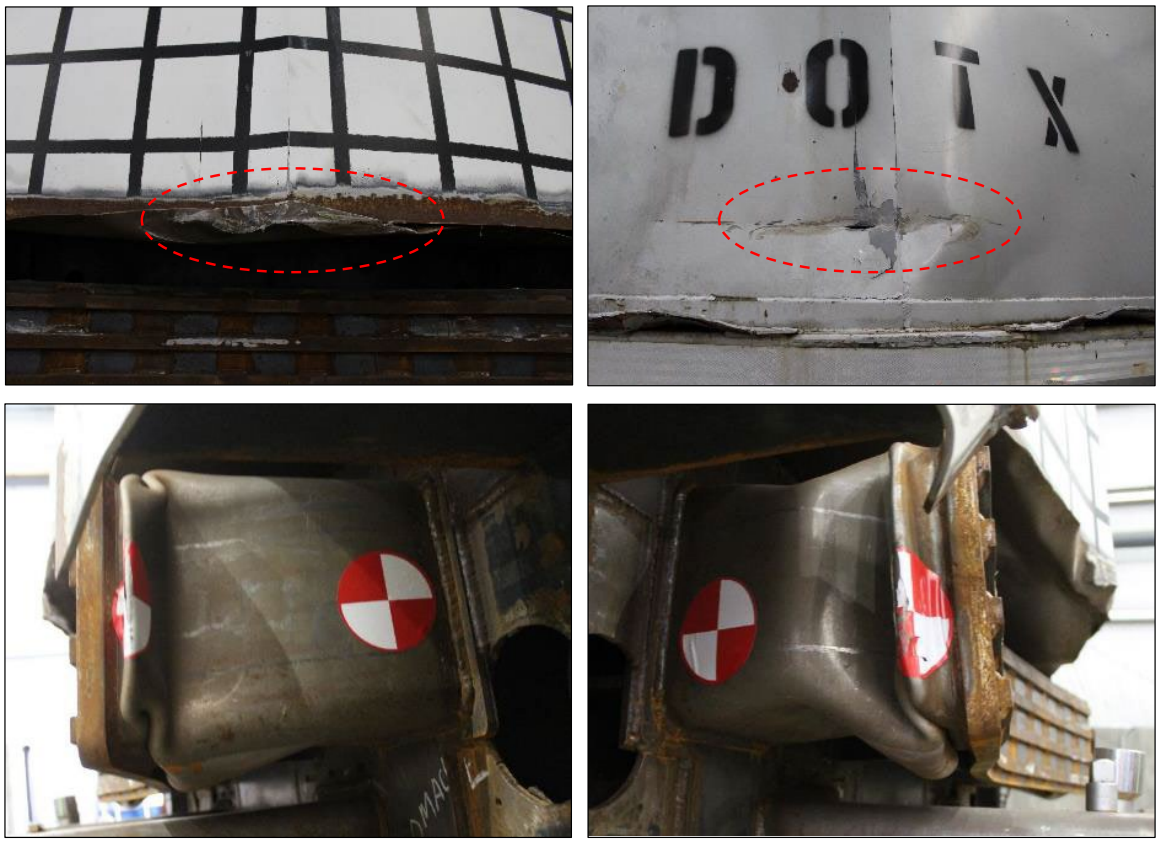

Figure 29. Post-test photographs indicating lateral offset of the colliding vehicles

4. Vehicle-Vehicle Test 1 Post-Test Evaluation

Immediately following the test, the test vehicles were inspected at the test site and measurements and photographs were taken. Both vehicles were then moved into one of the buildings, with the CEM locomotive positioned over a pit where additional measurements photographs were taken. Measurement of paint loss on the PBC deformation tube indicated that the permanent stroke was about 18.5”. This provided evidence that the shear bolts were just about to be loaded as the relative crush between the two vehicles reached its maximum. This was consistent with the presence of a scratch mark on the limit block that was added to the sliding lug to promote clean contact between the coupler and the sliding lug at the end of deformation tube stroke.

4.1 Data Review and Analysis

Test data were compiled and filtered by TTCI and provided to the Volpe Center and CAMX in a spreadsheet. The data (from accelerometers, string potentiometers, strain gages, and cameras) were reviewed relative to what they reveal about the impact sequence, vehicle motions, collision forces and strain near the shear bolts. Key results are summarized in several time-history plots. A report details the test instrumentation and provides the raw and filtered test data [13]. Post-test filtering of the data was performed using a two-pass, phaseless, four-pole digital filter algorithm consistent with the requirements of SAE J211 (CFC 60).

4.1.1 Impact Sequence

Inspection of accelerometer and strain gage data (see Figure 30) indicated that full engagement of the colliding open couplers did not occur until approximately 0.031 seconds after initial impact. At a collision speed of 19.3 mph, the 0.031-second lag between the time at which the impact tape mounted to the front surface of the conventional locomotive coupler was triggered and the time at which the couplers were fully engaged and began to transmit significant longitudinal forces indicated additional travel of approximately 10.5”.

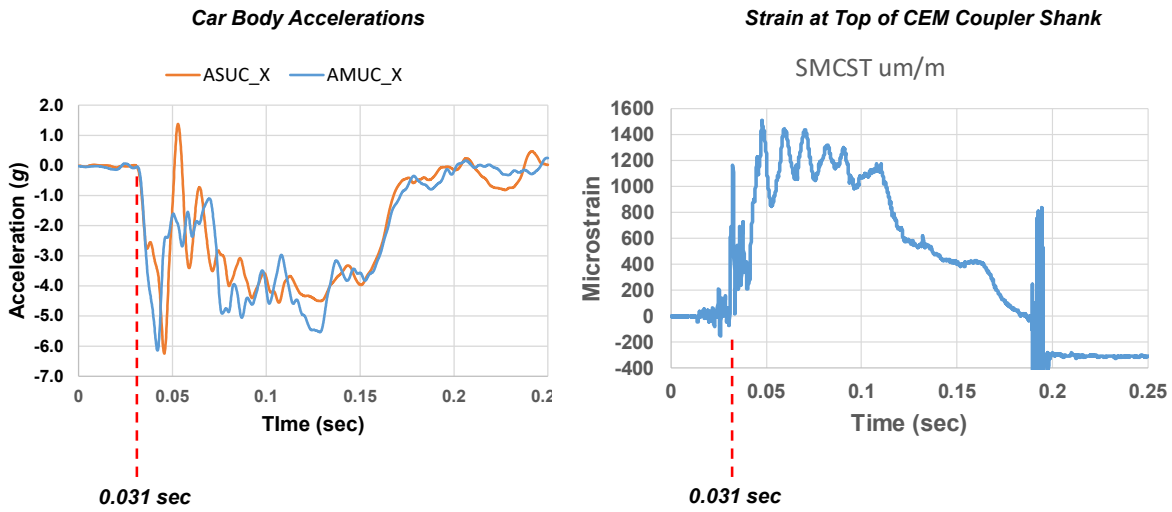

Figure 30. Left — carbody longitudinal accelerations (orange for stationary, blue for moving); right — strain at the top of the CEM coupler shank

String potentiometer data (see Figure 31, left) indicated that the upper DAC assembly impacted the skirt of the conventional locomotive after about 0.075 seconds. Note the delay of about 0.005 seconds between the initiation of motion on the left and right sides. Data from longitudinal accelerometers positioned at the center of the CEM locomotive carbody (see Figure 31, right) also indicate a significant jump after 0.075 seconds, accompanying the impact of the anti-climbers.

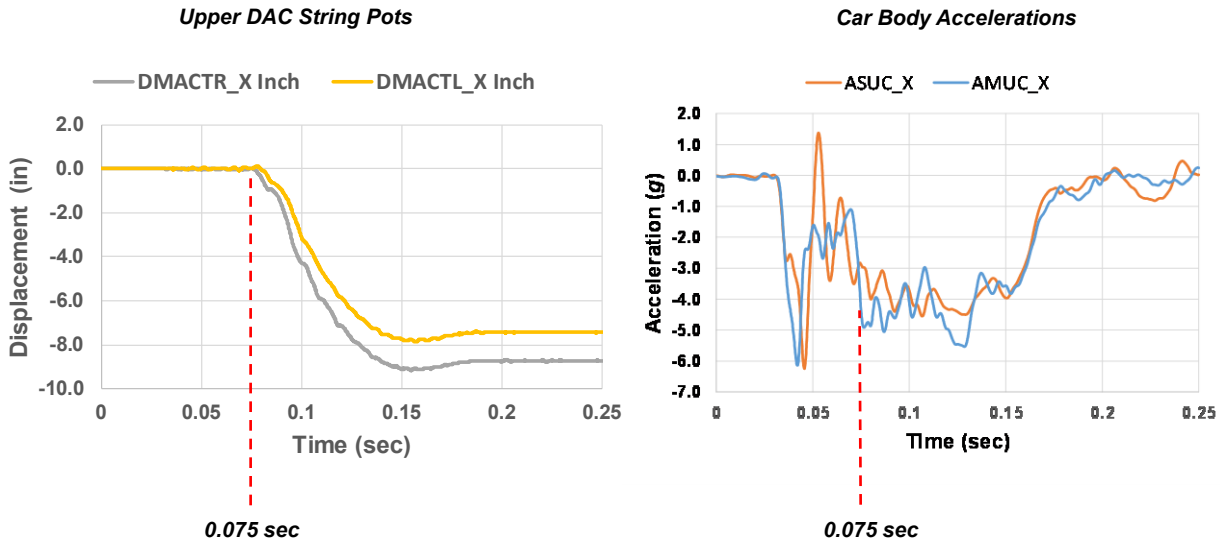

Figure 31. Left — upper DAC deformations; right — carbody longitudinal accelerations

The carbody acceleration pulse dropped to near zero after about 0.175 seconds (see Figure 32). There did not appear to be any additional pulses associated with impact of the coupler with the sliding lug.

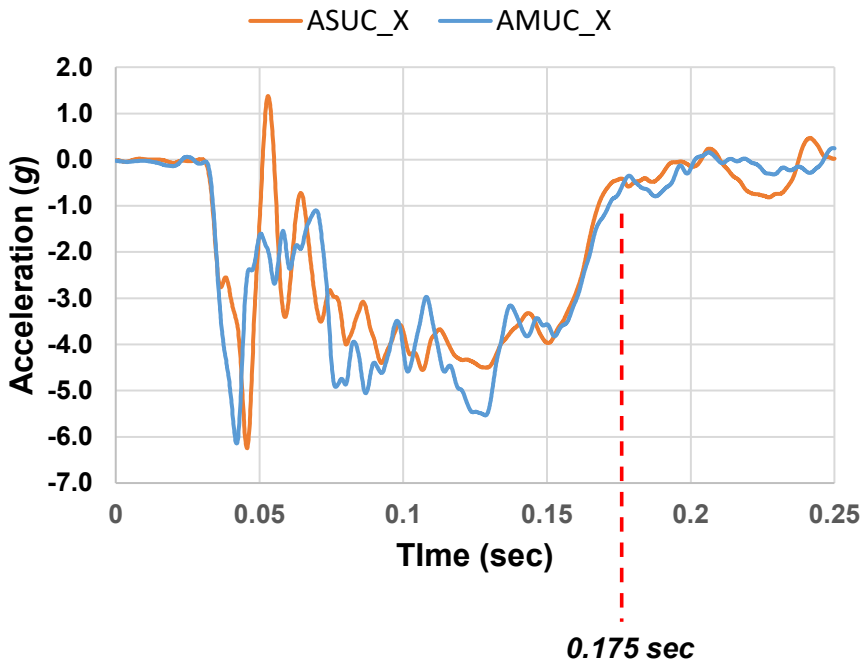

Figure 32. Carbody longitudinal acceleration pulse drops to zero after about 0.175 second

4.1.2 Vehicle Motions

Integrating the acceleration pulses for the respective vehicles and imposing a 19.3 mph initial speed for the CEM locomotive yielded speed and displacement time-histories (see Figure 33).

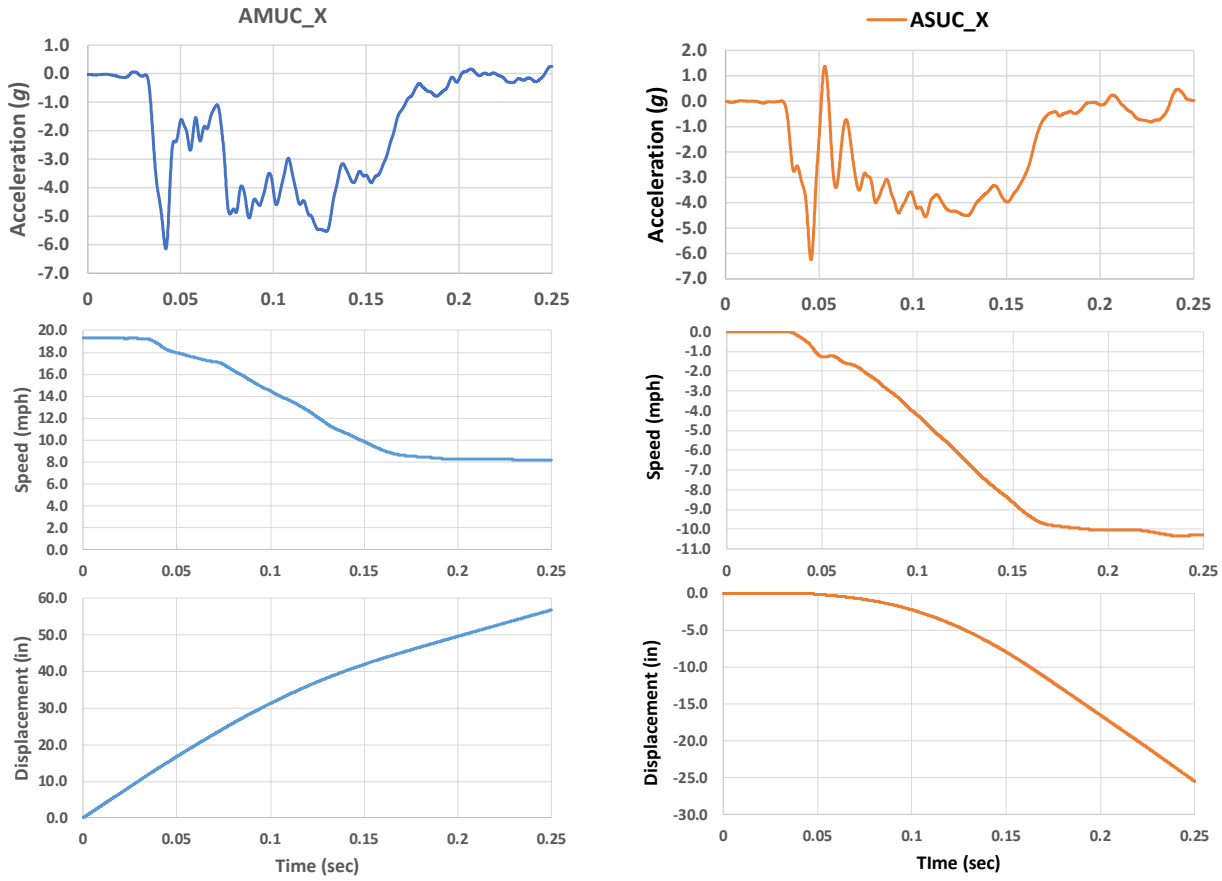

Figure 33. Successive integration of the acceleration pulses (top row) for the CEM locomotive (left) and conventional locomotive (right) yielded speed (middle row) and displacement (lower row) time-histories

Plotting the vehicle speed curves together indicated that the maximum crush of the vehicles occurred after about 0.157 seconds, shown in Figure 34. After this, the vehicles rebounded elastically. Note also the abrupt change in the rate of decrease in CEM locomotive speed at 0.075 second due to the impact of the DAC.

Calculated relative vehicle displacement and crush time-histories are plotted at the left in Figure 35. Relative vehicle displacement peaks after 0.157 seconds at 34.1”. Subtracting the displacement prior to full coupler impact yielded a peak crush distance of 23.6”. This 10.5” difference was consistent with the travel (~11”) that occurred when the couplers were open and the knuckles moved past one another and rotated before the respective vehicles fully engaged (see schematic in Figure 35, right). TTCI has verified these distances. Note that the precise distance of travel prior to full coupler engagement was likely affected by the alignment of the

couplers at impact and the positioning and thickness of the impact sensor bundle. Figure 36 shows a pre-test photograph of the couplers (left) and a photograph of the conventional locomotive coupler with the impact sensors taped to the front surface of the knuckle, just prior to running the test (right). Note also that one of the two couplers shown at left appears to have been closed.

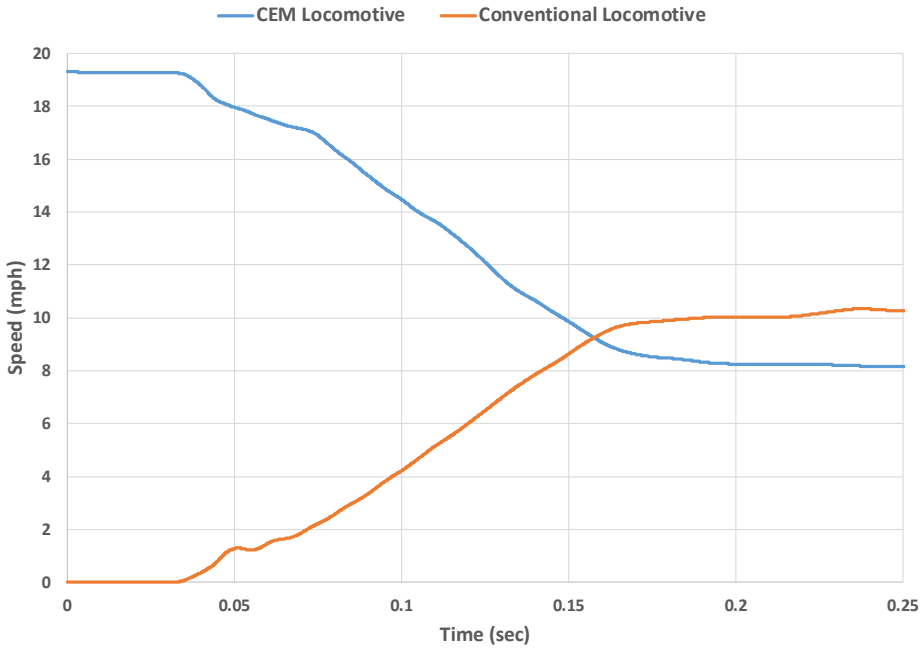

Figure 34. Calculated vehicle speed time-histories

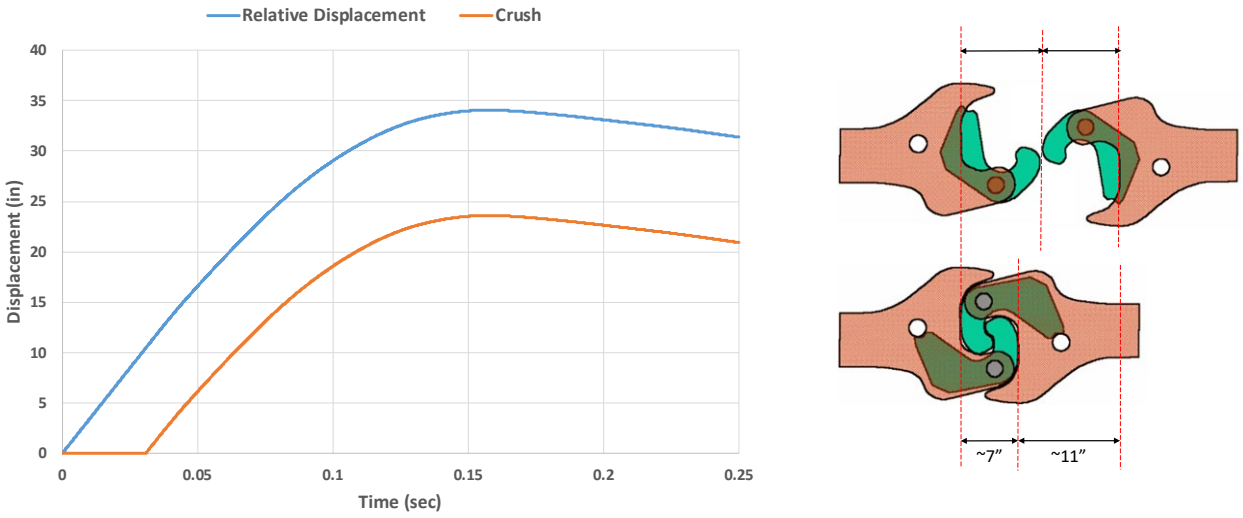

Figure 35. Left — calculated relative vehicle displacement time-histories; right — schematic illustration of additional vehicle approach prior to force build-up after initial impact when couplers are open

Figure 36. Top Left — a pre-test photograph of the couplers from above; bottom left — impact sensors affixed to the front surface of the stationary conventional locomotive; right — impact sensors affixed to the front surface of the CEM locomotive coupler

Test videos indicated a noticeable cyclic pitch (bouncing) of the CEM locomotive carbody on the suspension system of the forward truck during the collision. The vertical travel was much larger than anticipated, as the truck suspension is meant to have a limit stop of ±2”, which was included in the FE model. The vertical acceleration pulse for the CEM carbody at the forward truck (see Figure 37, upper left) was integrated to estimate the speed time-history at this location (see Figure 37, lower left). This curve was then corrected (see Figure 37, upper right) to remove drift (a common issue with these types of data) by reasoning that this curve must be near zero both at impact and after 5 seconds, when the oscillations had damped out. Finally, the corrected speed curve was integrated again to estimate the vertical displacement time-history at this location (see Figure 37, lower right). The displacement curve indicates an initial downward displacement of about 4.5” followed by continued oscillation, with an approximate magnitude of about 3” that slowly decreases over the next several seconds.

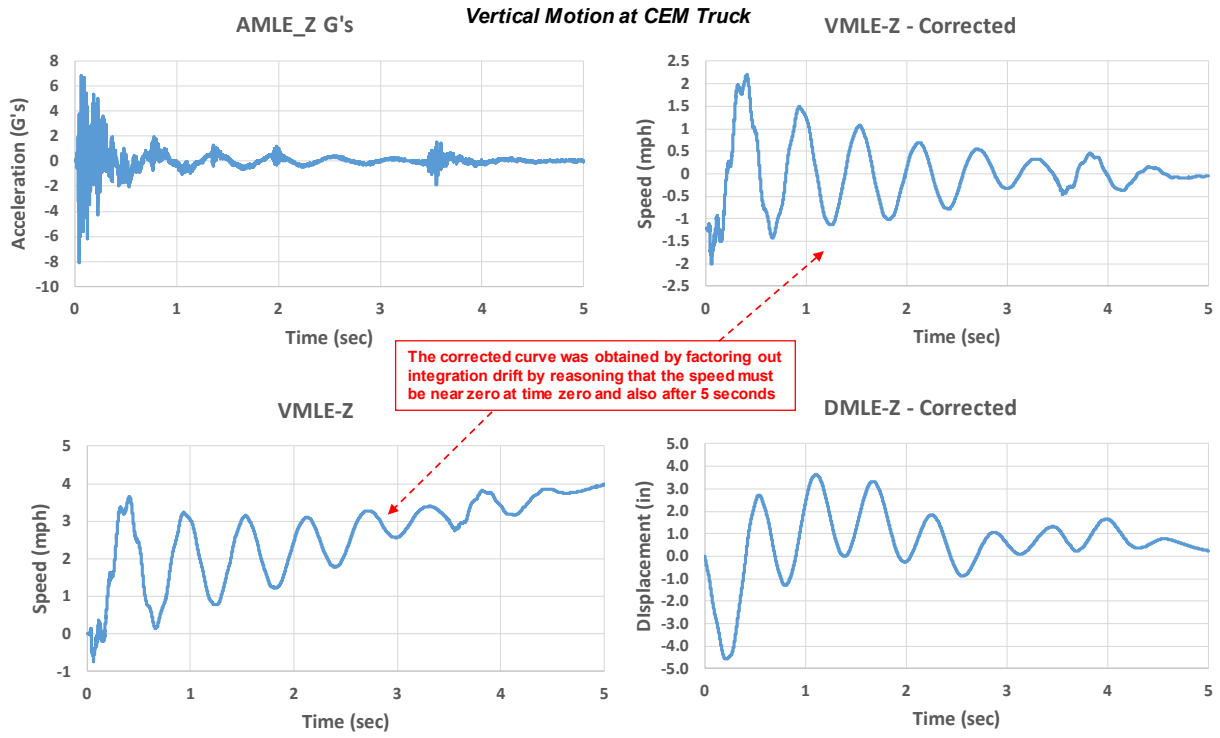

Figure 37. Upper left — vertical acceleration of carbody at CEM forward truck; lower left — integration of acceleration pulse to yield vertical speed (in mph); upper right — correction of speed curve to remove drift; lower right — integration of corrected speed curve to yield vertical displacement time-history

4.1.3 Collision Forces

The longitudinal acceleration can be multiplied by the mass of the CEM locomotive (232,600 lbs) to get an estimate of the longitudinal force, as shown in Figure 38. The resulting curve indicates that the force increased considerably — from an average of about 450 kips to an average of about 1,000 kips — when the DAC assembly was impacted. The huge peak in force after initial impact (almost 1,400 kips) and the oscillation during push-back suggest that this measure of forces must be considered approximate, at best, as it depends on the vehicle acting as a single-degree-of-freedom system.

Based on results from coupler impact studies [12], a better estimate of the force through the push-back coupler is derived from the longitudinal strains in the coupler shank. Figure 39 (left) shows estimated time-histories of the force through the coupler based on data from the five strain gages positioned on the shank (top, left, and right) and a few inches forward of the pin (left and right). The data from the five gages were somewhat noisy, so averages of the forces for the three front gages (shank) and two rear (pin) gages, as well as the overall average, were calculated. Figure 39 (right) shows the calculated averages over the first 0.08 seconds after impact. Compared to the acceleration-based estimates of force, these strain gages provided a more reasonable estimate of force when all of the force was going through the coupler (i.e., prior to DAC impact). The jump in force at impact was much smaller, and the plateau force was much more consistent with the rated push-back load of 674 kips for the PBC.

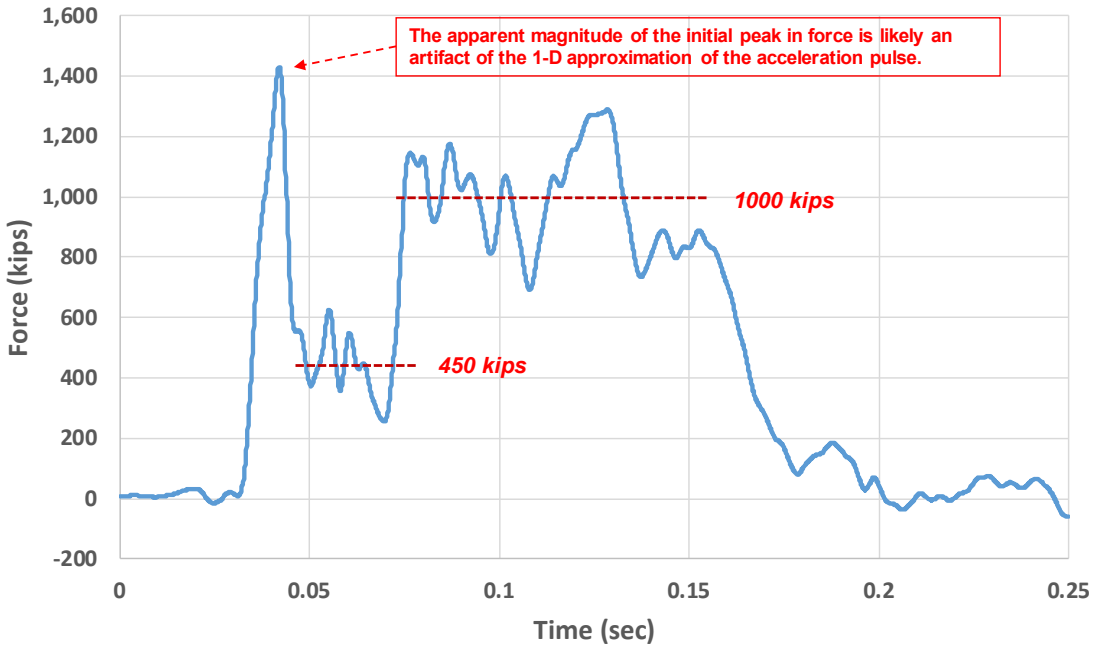

Figure 38. Force time-history based on single-degree-of-freedom approximation (F = ma) where 'm' is the mass of the CEM locomotive and 'a' is the longitudinal acceleration at the center of the vehicle

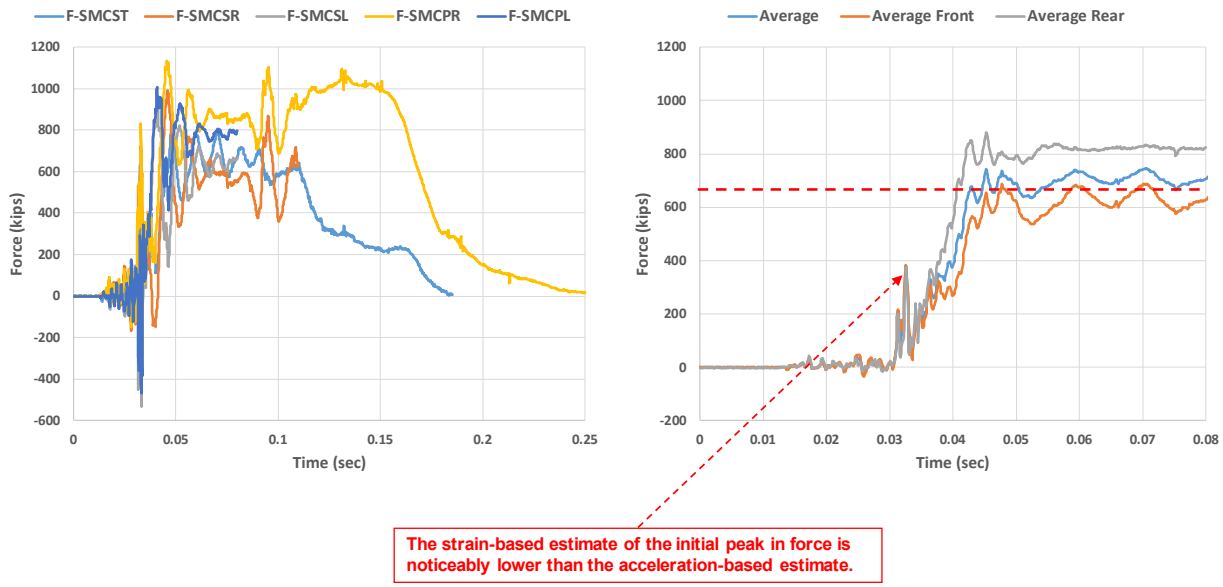

Figure 39. Left — estimated time-histories of the force through the coupler based on data from strain gages positioned on the shank and near the pin; right — calculated averages forces for the three front (shank) and two rear (pin) gages overs the first 0.08 seconds after impact

4.1.4 Strain Near Shear Bolts

Strain gage readings for the draft pocket and sliding lug bolt hole regions were consistent with results from the coupling tests [12].

Table 1 reports averaged values (front and rear, top and bottom, and left and right sides) for the eight gages mounted to the draft pocket side plates and the eight gages mounted to the sliding lug slide plates. (Note that positive readings indicate compression.) Reported values for the gages mounted to the draft pocket side plates (about 1" behind each shear bolt) indicated that the strain levels were relatively uniform, with little variation of averaged values front-to-back, side-to-side, and top-to-bottom.

Sliding lug side plate strains were generally much smaller than draft pocket side plate strains, making it difficult to infer trends from the data. It did appear, however, that the strain levels were very different front-to-back, with the front gages indicating compression and the back gages indicating tension. It was not immediately evident why these strain magnitudes changed sign, but it should be noted that previous testing and analysis on stiff bolted rail components have indicated that the transmission of force through the bolted connections can be quite complex [3].

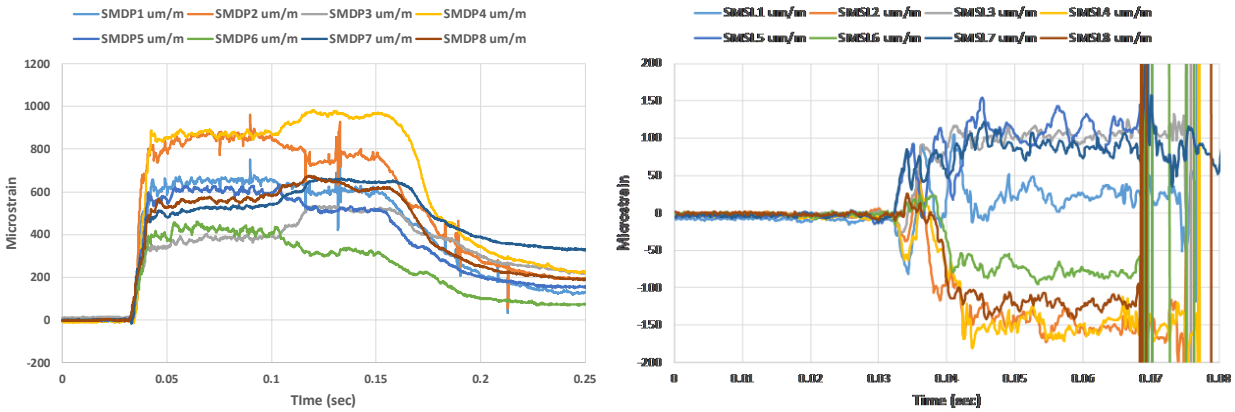

Figure 40. Left — time-histories of strain behind the eight top and bottom shear bolts on the draft pocket side plates; right — time-histories of strain ahead of the eight top and bottom shear bolts on the sliding lug side plates

Table 1. Comparison of averaged measured peak strain levels (microstrain) during vehicle-vehicle test with those from 9-mph coupling test; note that positive strain gage readings are compressive

Location	Test	Bolt Hole Locations					
		Front	Rear	Left	Right	Top	Bottom
Draft Pocket Side Plate	20 mph Impact Test	550	670	530	700	600	630
	9 mph Coupling Test	380	530	550	360	490	430
PBC Side Plate	20 mph Impact Test	80	-130	-40	0	-20	-20
	9 mph Coupling Test	40	-150	-40	-60	-30	-70

4.2 Comparison of Test Results with Pre-Test Model Predictions

Pre-test predictions of behavior during the test are compared with test results in this section. Differences between model predictions and test results can be largely attributable to two key factors:

1. The actual collision speed was 19.3 mph — a 16 percent decrease in collision energy when compared to the target speed of 21 mph and a 7 percent decrease in collision energy when compared to the minimum expected collision speed of 20 mph.
2. Having the couplers open brought the DAC system much closer (~11”) to impact with the conventional locomotive end frame prior to PBC impact; it therefore absorbed much more energy prior to shear bolt failure.

A few modeling issues were revealed as a result of the comparison with test results. For the most part, these likely had a minor influence on results, but identifying them can help improve future simulations. Of these, the issue that likely had the most influence on results was the use of shell elements to model most of the vehicle structures. It is difficult to account for certain thicknesses of structures when modeling vehicle contact using shell elements. In particular, the upper DAC assembly protruded outward by 20.875” from the end plate, but in the model this distance was only modeled as 19.5” because the 1”-thick front plate and the 0.375” back bearing pad were modeled as shell elements, reducing the extent that the upper DAC assembly protruded forward off the end plate of the CEM locomotive. This 1.375” difference added to the 10.5” difference attributable to open coupler impact, so the DAC impact occurred about 12” sooner than the model would indicate. As a result, much of the collision energy that otherwise would have been

directed into the PBC was instead directed into the DAC, increasing the collision speed needed to fail the shear bolts.

With these issues in mind, several comparisons between model predictions and test results are highlighted below.

4.2.1 Vehicle Motion

Comparing the relative displacement (or crush) and speed time-histories derived from test results with model predictions (Figure 41) indicated that the CEM locomotive slowed down more quickly than pre-test model results would indicate, especially when the first 0.031 seconds after impact are neglected (allowing the open couplers to fully engage). This difference in behavior was indicative of higher collision forces and became more pronounced at about 0.075 seconds when the DAC tubes began to crush. These differences were likely attributable to the much earlier impact of the DAC (relative to the extent of PBC crush) during the test than was modeled, as noted above. Accounting for the 10.5" travel of the couplers prior to impact in the model, as well as the 1.375" additional protrusion of the DAC, as noted, will likely improve agreement.

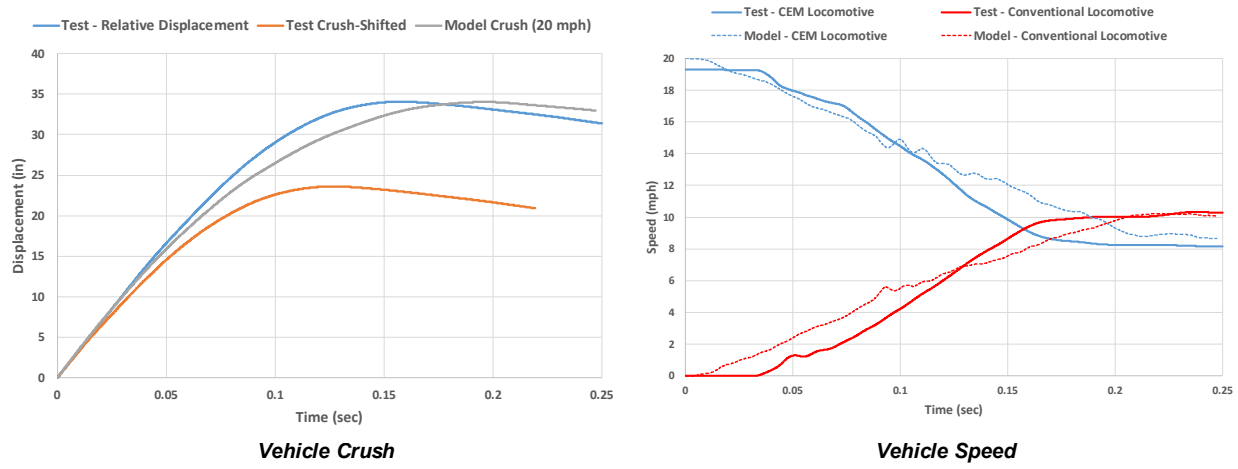

Figure 41. Left — comparison of measured displacement time-histories with model predictions; right — comparison of measured speed time-histories with model prediction

4.2.2 Force-Displacement Curve

Figure 42 shows the force versus crush through the carbody and through the coupler, from both the pre-test prediction and the test data. The solid blue line is the accelerometer-based force from the longitudinal center of the underframe. The solid red line is the strain-based force from the coupler shank, which gives a better estimate of the force through the push-back coupler. As seen in the figure, the average force through the CEM locomotive carbody (solid blue line) increases considerably — from an average of about 450 kips (when the PBC deformation tube alone was absorbing energy) to an average of about 1,000 kips (when the DAC assembly was impacted). While the estimated carbody force was about 450 kips during the PBC deformation, the coupler force (solid red line) was approximately 670 kips — the designed force level for PBC pushback. A comparison of test/model force-crush behavior (Figure 42) indicates that, in the test, the DAC tubes began to absorb collision energy much earlier than in the model. As noted, this was

primarily due to the 10.5” or so of travel prior to loading the push-back coupler system, which caused the DAC assembly to engage earlier relative to PBC crush.

Note that while the early engagement of the DAC likely prevented shear bolt failure at this test speed, it nonetheless contributed significantly to energy absorption.

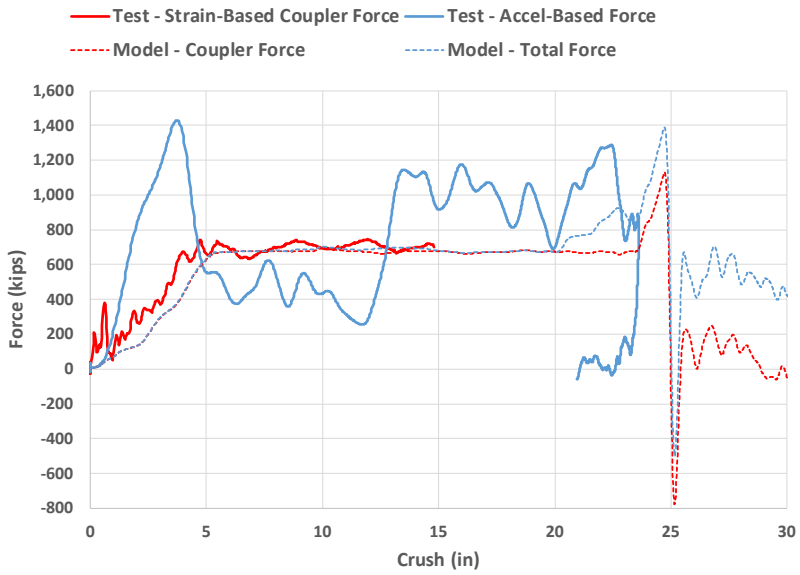

Figure 42. Left — comparison of calculated test/model force crush curves (coupler only and total)

4.2.3 Energy Absorption

Calculated/estimated energy absorption totals for the test and the model are compared in Table 2. The PBC stroke was limited to 21”, but 2.7” of that was compression of the PBC draft gear. Assuming that the full stroke of the PBC was exhausted during the test, as evidenced by the scratch on the limit stop, then the model and test values for these energies were, for all intents and purposes, equal. The extent of energy absorption in the PBC and conventional locomotive draft gears was estimated by subtracting the design deformation tube energy (1,030 kips) from the FE model calculation of energy for the connector elements representing the PBC and the conventional locomotive draft gear. Note that each of the draft gears absorbed about 70 ft-kips of energy.

Table 2. Comparison of calculated energy absorption levels from the test with model predictions

Component	Test (ft-kips)	Model (ft-kips)
PBC Deformation Tube	1,030[1]	1,030[1]
PBC/Conventional Locomotive Draft Gears	140[2]	140[2]
DAC	260[3]	340[6]
Other Vehicle End Structures	70[4]	200[6]
Total	1,500[5]	1,710[6]

1. 675 kips x 18.3" stroke (remaining 2.7" PBC stroke prior to bolt failure is in draft gear)
2. Model calculation of total PBC energy minus deformation tube energy — assumed to be the same for the test.
3. Estimate based on model DAC energy × test DAC stroke/model DAC stroke (340 x 10/13.5)
4. Subtraction of DAC and PBC energy from total energy
5. Integration of area under acceleration-based force vs. displacement curve
6. Model calculation of respective energies

4.2.4 Strain Near Shear Bolts

A contour plot of longitudinal strain in the draft pocket side plate (see Figure 43) during PBC pushback indicates that the model predicted smaller strain levels than were measured in the test (see Table 1). The strain levels were greater near the forward bolt holes — also contrary to test results which indicate that they were about the same. Note that the use of connector elements to define the shear bolts likely detracted from the accuracy of predicted strain levels in the region of the bolts, as it was difficult to determine their influence on the stiffness of the structures surrounding the bolts.

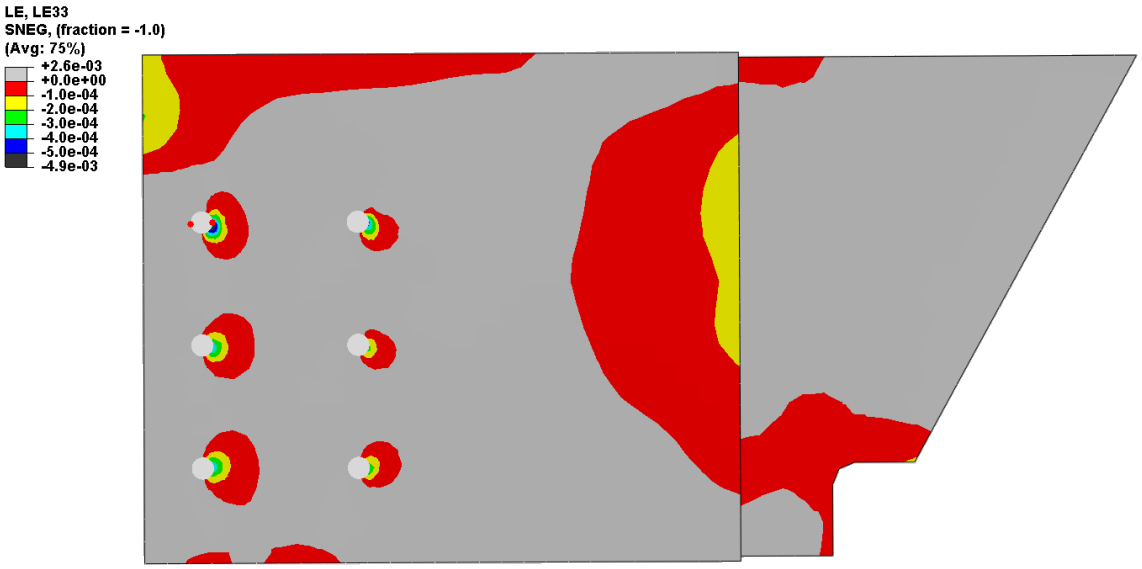

Figure 43. Left — contours of strain on the side of the draft pocket during deformation tube stroke

4.2.5 Mode of Deformation

The predicted mode of deformation of the top DAC assembly appeared to be very consistent with test results, as shown in Figure 44. The model did not, of course, pick up the side-side variation in crush due to the ~2" lateral motion following impact. The much greater predicted extent of crush of the nose of the short hood was consistent with the much more extensive predicted crush of the DAC (13.5" in the FE model vs. 10" in the test) due to the higher target speed versus actual test speed.

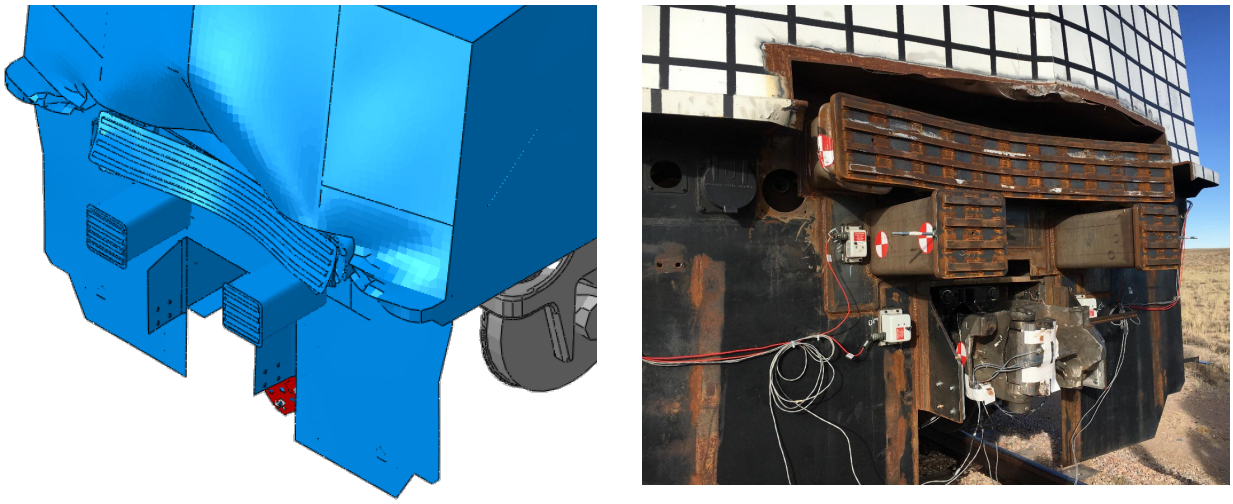

Figure 44. Comparison of FE model prediction of CEM end frame mode of deformation with post-test photograph of the end frame (right)

4.3 Comparison of Test Results with Post-Test Model Predictions

Informed by the post-test data review/analysis and inspection of the damaged vehicles, a few modifications were made to the FE model for V2VT1:

- The impact speed was lowered to 19.3 mph.
- The DAC tubes and angled gusset plates were extended by 1.125” so that the distance between the DAC and the conventional locomotive end frame matched that of the test. The extensions were modeled to be effectively rigid so that they did not change the energy absorption characteristics of the DAC. This modification is described in detail in Section 8.4.
- The initial position of the CEM locomotive was adjusted so that, at impact of the fully engaged couplers, the end structures of respective vehicles were the appropriate distance from one another. At impact, the vehicle end plates were assumed to be 53.5” from one another. This distance was based on lengths of 31” and 28.5”, respectively, for the CEM locomotive and conventional locomotive couplers, with coupler pins positioned 3.5” behind the respective end plates, and a 1” gap between the locomotives (53.5” = 28.5” + 31” – 2 × 3.5” + 1”). This was modified because the couplers were open for the test, as opposed to closed for the pre-test analysis. In the test, the couplers were not fully engaged until approximately 0.031 seconds.
- The connector that governs impact of the two vehicles was modified so that the impact of fully engaged couplers occurred at approximately 0.031 seconds, as in the test (after ~10.5” of free CEM locomotive travel following initial impact).

FE model predictions for relative vehicle displacement, vehicle speed, and force-vs.-crush are compared with test results in Figure 45 through Figure 47. Predictions of relative vehicle displacement (Figure 45) compare quite favorably to test results, with the prediction of final vehicle crush only about 1” different than the test result. Similarly, predictions of vehicle speeds (Figure 46) are in excellent agreement with test results, particularly with respect to the time at which the vehicle speeds were determined to be equal (at maximum relative displacement).

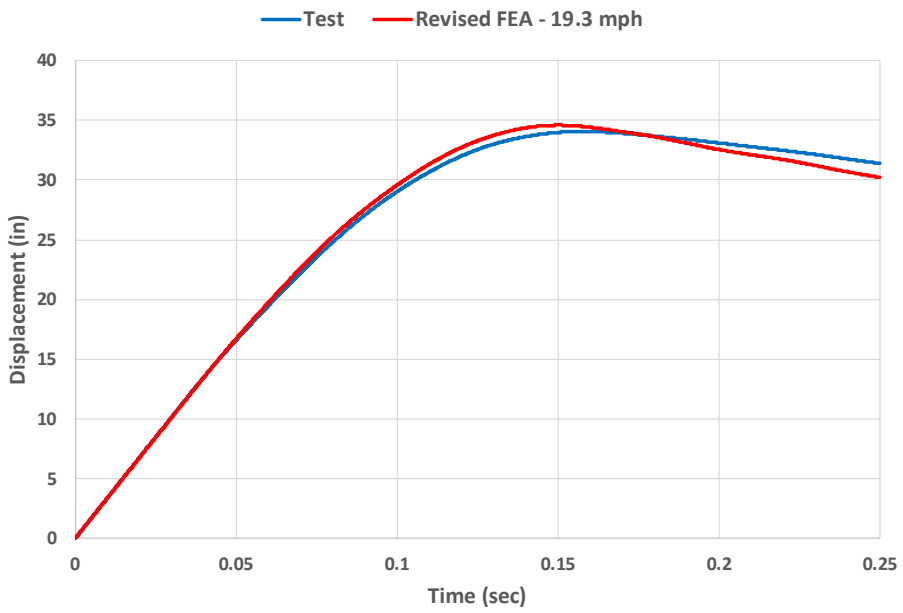

Figure 45. Comparison of revised FE model prediction of relative vehicle displacement with test results

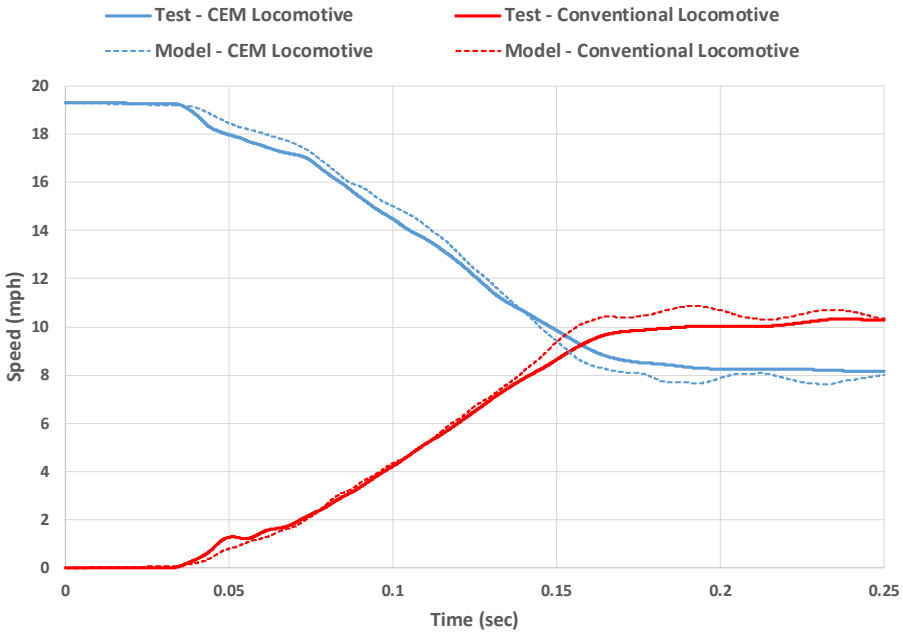

Figure 46. Comparison of revised FE model prediction of vehicle speeds displacement with test results

Comparison of the predicted force-crush curve with test results (Figure 47) was a little more difficult because the force-crush curve for the test was not measured but had to be calculated from acceleration or strain data based on simplifying assumptions regarding vehicle behavior, as discussed in Section 4.2.2. Again, the solid red line is the strain-based coupler force, the solid blue line is the acceleration-based force at the CG of the CEM locomotive, the red dashed line is

the model coupler force, and the dashed blue line is the model total force. As seen in the figure, the initial peak in the strain-based force (solid red line) indicates the coupler impact. The acceleration-based estimate (solid blue line) of peak force at impact was delayed with respect to the strain-based estimate. The acceleration-based estimate of force was not as reliable as the strain-based estimate of force, particularly in the early stages of the collision. It relied on the assumption that the locomotive was behaving as a single-degree-of-freedom system, with force equal to mass multiplied by acceleration. When the vehicles first impacted one another, the effective mass associated with the measured acceleration of the vehicle center of gravity was likely much lower than the total mass of the locomotive. However, the acceleration-based estimate was more reliably predicting the total force by the time the DAC was engaged.

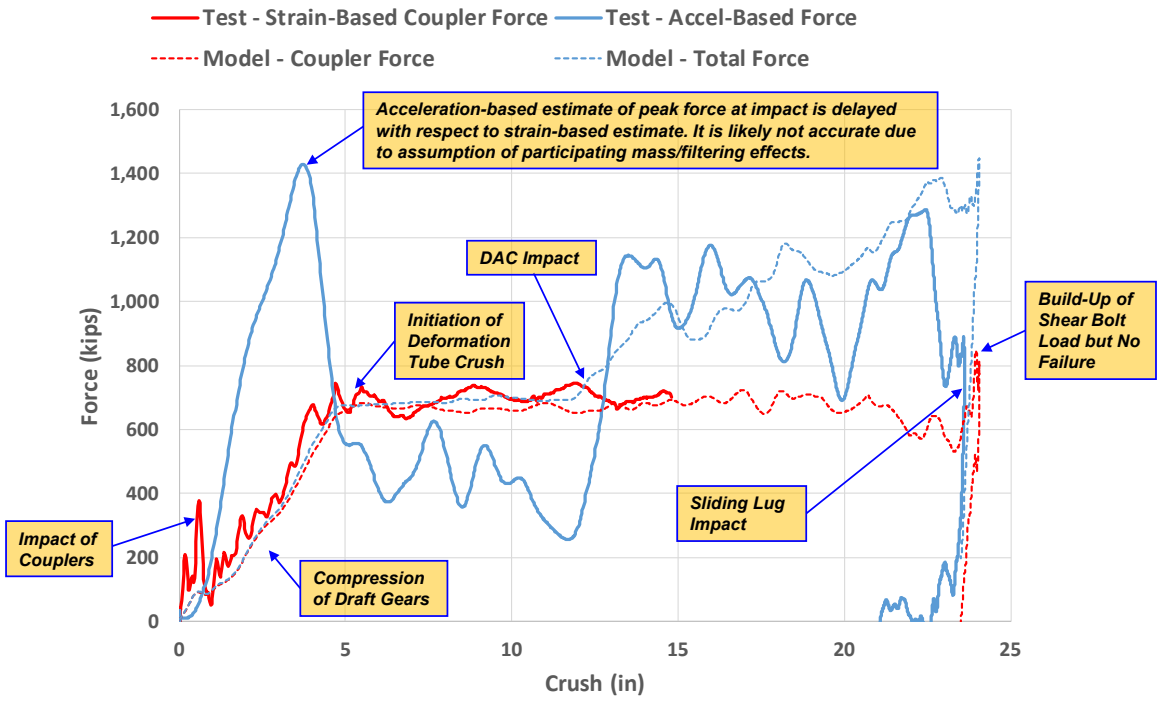

Figure 47. Comparison of FE model prediction of force-vs.-crush with values calculated based on test results

There was good agreement between the model and the strain-based measurement during the compression of the draft gears of both locomotives. Then the PBC triggered and the deformation tube began to crush. Again, there was good agreement here between the model and the strain-based measurement. Once the DAC was impacted by the conventional locomotive, the force levels increased. This was captured by the model and the acceleration-based measurement, but not in the strain-based measurement through the coupler shank, as expected. The force levels and the fluctuation in amplitude due to the DAC tubes deforming were very similar when comparing the model and the acceleration-based measurement. The model results also indicate a build-up of force near the end of crush, indicating the load on the shear bolts was increasing, but not by enough to cause failure.

The post-test predictions of force-crush behavior were in much better agreement than pre-test predictions due to the modification of the collision speed, the correction of the distance the DAC

extended forward of the end plate, and accounting for the period of free travel that followed initial impact/triggering of impact tape sensors prior to full coupler engagement.

Aside from the PBC deformation tube, most of the deformation that occurred was, by design, concentrated in the DAC. Predictions of DAC deformation are compared with test results in Figure 48. As is evident, the model appeared to capture quite well the deformation of the upper DAC tubes, which crushed and rotated upwards during the collision. The deformation at the center of the DAC was predicted to decrease the distance from the DAC plate to the end plate of the locomotive from 18.875” to about 6.5”, i.e., about 12.4” of crush. The post-test measured distance was determined to be about 7.5” at this location, indicating a total crush of about 11.4”. Part of this 1” difference may be attributable to the lateral offset of the impact.

The FE model also predicted some deformation of the conventional locomotive anti-climber gusset plates, as illustrated in Figure 49. This did not appear to have occurred during the test.

At the time of this post-test FE analysis, TTCI researchers had not removed the collision posts to inspect damage to the supporting structures. When they did so, they discovered some damage where the angled gusset plate of the DAC was welded to the end frame. The FE model also predicted damage in this area. This is discussed further in the next section.

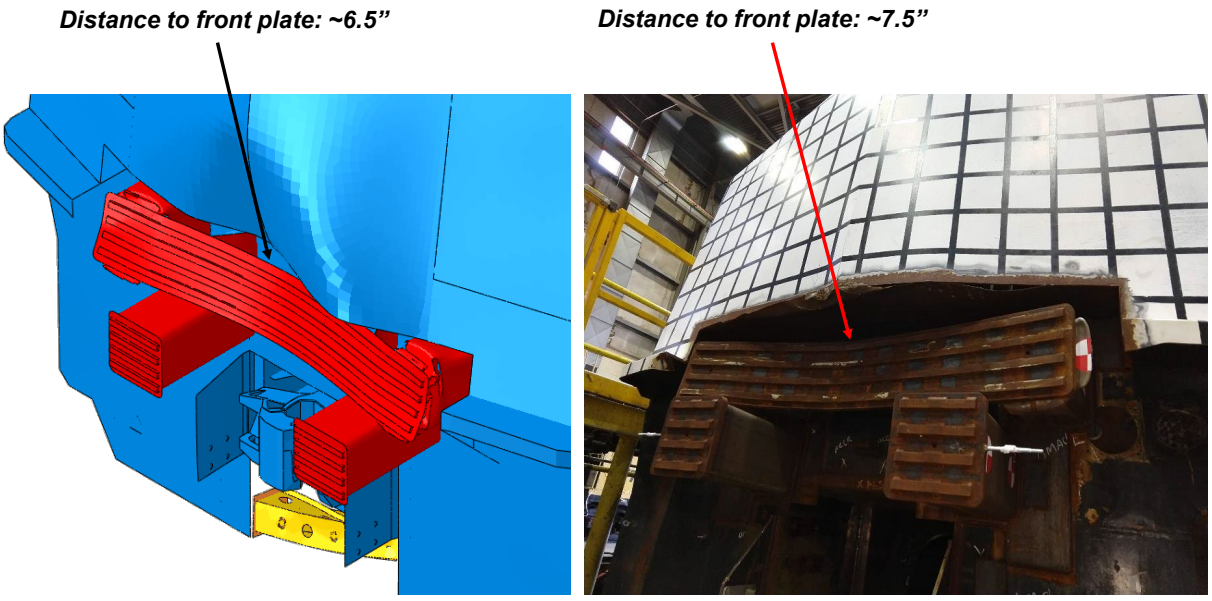

Figure 48. Comparison of predicted DAC deformation with test results

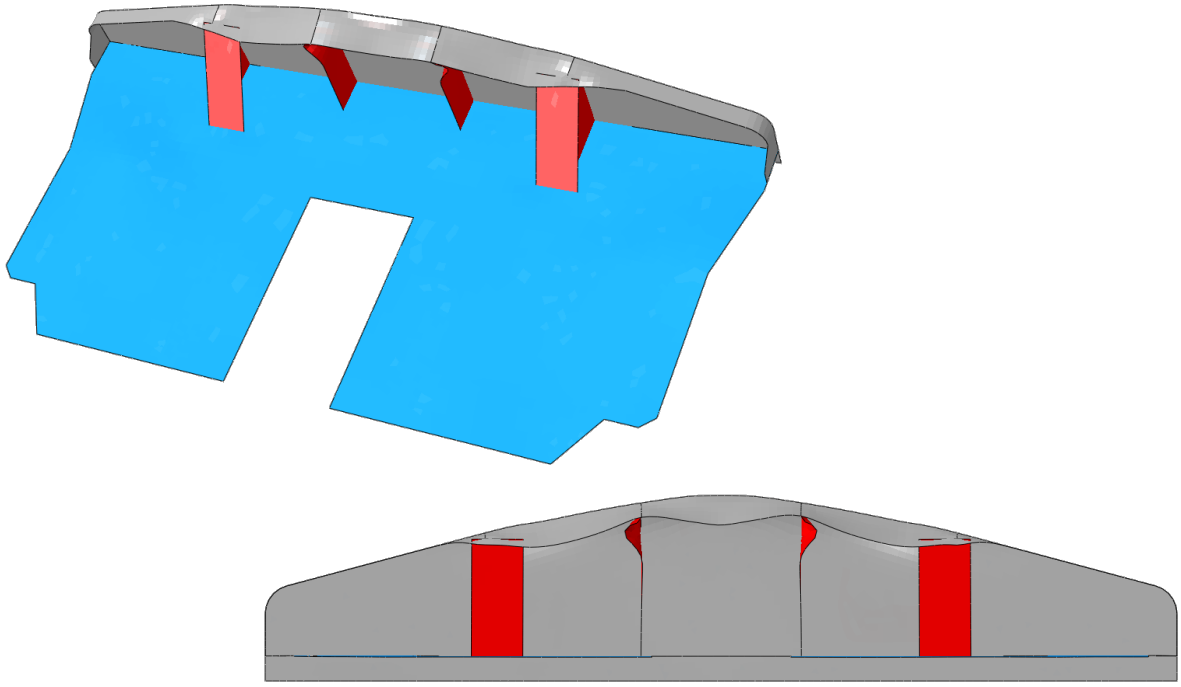

Figure 49. Predicted deformation of conventional locomotive anti-climber apron and inner gusset plates

Overall, the agreement between model predictions and test results was good:

- The timing of DAC engagement was similar.
- The extent of push-back coupler deformation was similar.
- The mode of DAC deformation was similar; note that the FE model predicted build-up of shear bolt force to about 80 kips in each bolt, indicating they were very close to failing (88 kips) but did not fail.

There were a few potential causes for the small discrepancies present, including:

- Different extents of conventional locomotive draft gear compression prior to load build-up to 674 kips
- The actual strength of DAC component materials versus that modeled
- Lateral offset of the vehicles (appeared to be 2” to 3”)
- Extra pitching of the CEM locomotive due to the lack of limit stops on the forward truck-to-body connection
- Underframe height mismatch (the CEM locomotive appeared to be about 3” higher)

4.4 Assessment of CEM Locomotive Damage/Repair Needs

Due to the low impact speed, damage to the CEM locomotive was limited. Following a post-test inspection of the vehicle, the following replacement/repair activities were recommended in preparation for the next test, Vehicle-to-Vehicle Test 2 (V2VT2):

- Replace the PBC.
- Replace the shear bolts and bushings.
- Inspect the sliding lug and draft pocket for damage.
- Replace the upper DAC assembly.
- Replace the coupler carrier.
- Design and fabricate a retention system for the coupler carrier so it does not fall onto the track during a collision.
- Inspect the upper DAC support structures and the modified collision posts.
- Repair the short hood nose and apron side plates.

After removing the DAC assembly and inspecting the DAC support structures, one further area of damage was revealed where the angled, upper DAC support plate on the left side of the CEM locomotive was welded to the front plate, as is illustrated on the left in Figure 50. The front plate did not have a doubling plate at this location, as it did behind the DAC tubes. There was clear evidence of damage at the top of the welded connection between the angled support plate and the end plate, as shown at right in Figure 50.

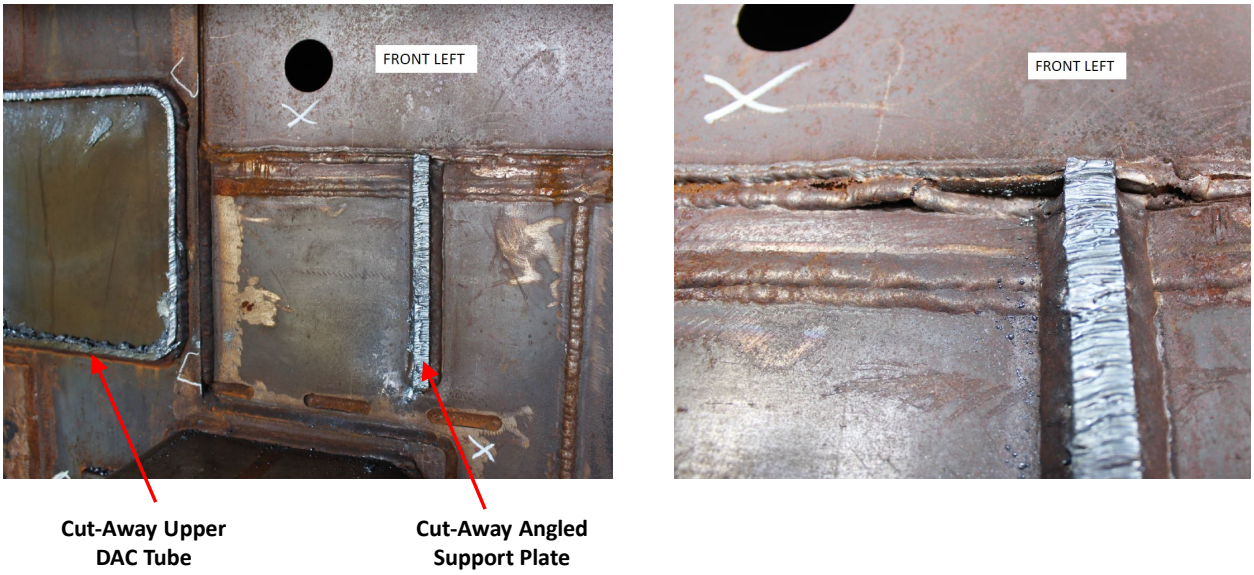

Figure 50. Left — photograph showing cut-away left upper DAC tube and angled support plate; right — detail showing damage at top of connection between angled support plate and front plate

The damage in this area was consistent with pre-test model predictions which indicated high levels of plastic strain in this region prior to folding of the angle support plates, as shown in Figure 51.

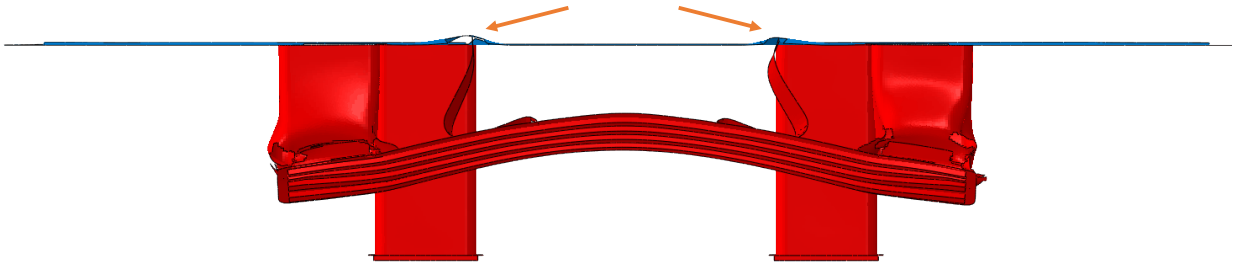

Figure 51. Detail of deformed CEM locomotive at the end of the simulation of V2VT1 showing plastic deformation at the top of the welded connection of the angled support plate to the end plate, as indicated

4.5 CEM Locomotive Repair

As noted in Section 4.4, when the damaged upper DAC assembly was removed from the CEM locomotive after V2VT1, damage was evident where the DAC angled support plates were welded to the end plate.

Following discussions with the Volpe Center and CAMX, site technicians suggested and later implemented two modifications to remediate this issue. The first was to weld a 0.375”-thick bearing plate, as outlined in yellow at the left in Figure 52, onto the end plate. This plate, which extended upward a little beyond the level of the floor, would be welded to the front of the end plate along its sides and bottom and welded to the back of the front plate along its top. The second modification was to install a 1”-thick by 4”-wide by 9”-tall plate, oriented as shown in red at the right in Figure 52, behind the end plate of the locomotive at the location where the angled support gusset was welded to the front of the end plate.

The FE model of the CEM locomotive was updated to include these modifications, as is discussed in Section 4.4. Note that, since the post-test FE analysis had already been conducted when these repairs were made, the FE analysis for the V2VT1 collision was not re-run. Based on the very localized area of damage, it is not likely that these modifications would have had a significant effect on the results of the analysis.

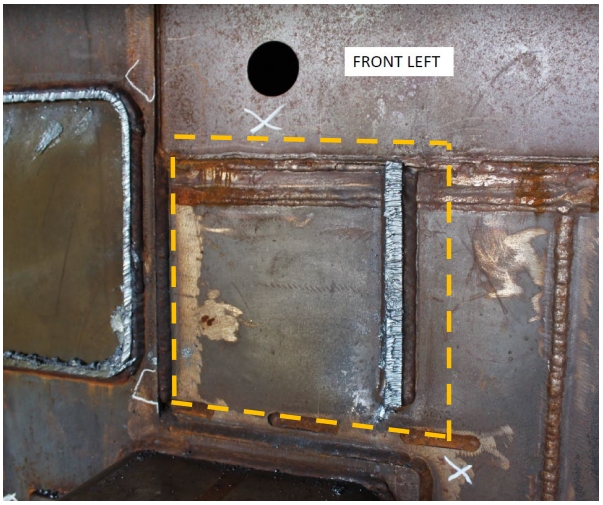

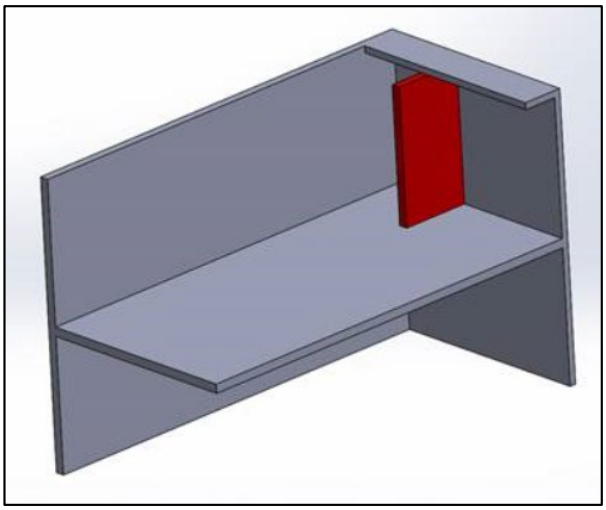

Figure 52. Left — outline of the bearing plate which will be welded to the front of the CEM locomotive end plate and onto which the angled gusset will be welded; right — illustration of the reinforcement gusset to be welded behind the end plate where the angled gusset plate was welded to the end plate

In addition to these repairs, the PBC was replaced, and the coupler carrier was rebuilt. Small cables were connected to the sides of the coupler carrier to prevent its interfering with instrumentation wiring or falling to the ground after failing and becoming a derailment trigger. Inspection of the draft pocket and sliding lug bolt holes revealed minimal damage.

Further damage to the CEM locomotive was also minimal and included a small dent in the nose of the short hood.

5. Vehicle-to-Vehicle Test 2 Pre-Test Analysis

This section describes engineering evaluations and project management performed in support of V2VT2, conducted November 17, 2021, at TTC. In this test, a moving CEM locomotive collided with a standing consist comprising a cab car and two trailing hopper cars. A schematic of the test is shown in Figure 53.

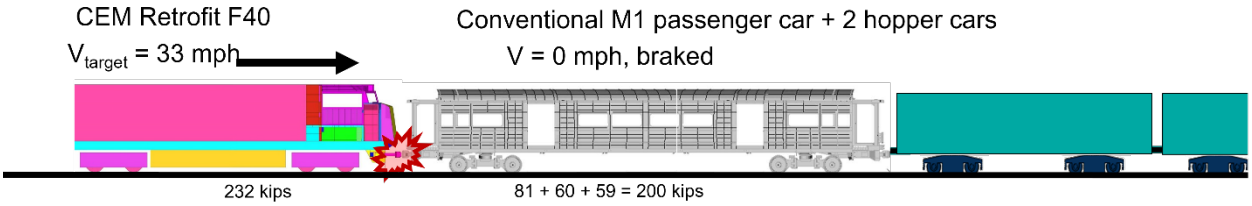

Figure 53. Schematic of CEM Vehicle-to-Vehicle Test 2 initial conditions

Key objectives for the test included the following:

- Activation and complete operation of the PBC system:
  - Complete push-back of the CEM coupler deformation tube
  - Impact of the CEM coupler head with the sliding slug
  - Failure of the shear bolts connecting the sliding lug to the draft pocket.
  - Push-back of the sliding lug to accommodate complete push-back of the CEM coupler to allow the vehicle ends to engage.
- Impact of the DAC components, with a target energy absorption of 300 ft-kips (50 percent of its design capacity).
- Controlled motion and deformation for all impacting vehicles:
  - Engagement of colliding vehicle end structures
  - No override
  - No derailment
  - Minimal loss of occupant volume in the cab car

5.1 Identification of Cab Car Test Vehicle

TTCI and Volpe agreed to use an M1 cab car that was onsite at TTC and available for use in VTVT2. Two considerations related to this vehicle affected the pre-test FE modeling effort:

- This cab car has a buffer beam extending forward below the doorway at the end of the car, as pictured in Figure 54. The beam is open at the back and is connected to the end beam behind it, with two cylindrical spring/damper components. The FE model developed for the coupling tests (see Section 8.6) did not include this component, as it was missing. It needed to be modeled and integrated into the cab car model.
- This cab car had not been remediated to remove asbestos. It therefore had interior components, including a composite floor covering.

Figure 54. Buffer beam at forward end of M1 cab car selected for VTVT2

The FE model was revised based on measurements taken from a buffer beam on a different M1 cab car during an earlier visit to TTC and is described in Section 8.6 of this report.

It was initially determined that the asbestos should be removed only from the front vestibule forward, i.e., the first 3' or so of the vehicle. Later, based on the results of preliminary FE models that indicated significant floor deformation further back in the cab car, it was decided that the entire vehicle should be remediated. A preliminary FE model had been constructed for the cab car based on the assumption that only the front part of the cab car floor would be removed during the remediation (see Section 8.6). The model was later revised to remove the floor covering that had been added.

5.2 Pre-Test Finite Element Analyses

A series of pre-test FE analyses were conducted, with the primary objective of estimating a collision speed that would allow for meeting the key objectives of the test while minimizing the risk of an undesired test outcome, particularly a derailment.

Site engineers indicated they could control the collision speed to within ±2 mph. For this reason, the pre-test FE calculations focused on identifying a target speed range where:

- At its minimum value (target speed minus 2 mph), the PBC system would activate and operate to the point where the shear bolts would fail, the sliding lug would push back, and the DAC would absorb 300 ft-kips of energy (50 percent of its design capacity).
- At its maximum value (target speed plus 2 mph), the additional collision energy brought about by the higher speed would be accommodated in a controlled manner.

An FE model originally developed in a prior program was modified to include a second freight car, as shown in Figure 55. Note that the structure representing the plymetal cab car flooring was removed from this model in accordance with the complete removal of the flooring for asbestos remediation.

Figure 55. FE model for CEM locomotive impact of a consist comprising a lead M1 cab car with two trailing hopper cars

Preliminary analyses using this model indicated that, without the stabilization provided by flooring, the cab car is susceptible to buckling, particularly when the collision speed is not enough to cause shear bolt failure, as illustrated in Figure 56.

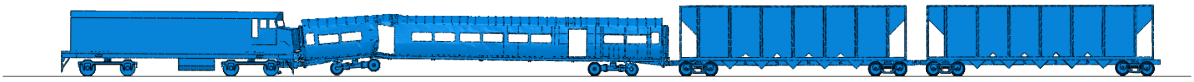

Figure 56. Predicted deformation after 0.25 seconds for a collision speed of 27.5 mph

Based on the outcome of this simulation, flooring was added back into the model, but only just past the forward side door opening. Subsequent results from simulations at this same collision speed of 27.5 mph indicate this only moved the buckle to the rear door opening, as illustrated in Figure 57.

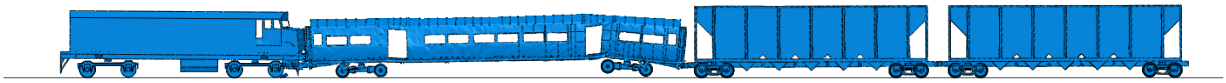

Figure 57. Predicted deformation after 0.25 seconds for a collision speed of 27.5 mph for model with flooring added back into the model, but only just past the forward door opening

Based on these results and the desire to minimize the risk of derailment, Volpe instructed the TTCI engineers to retrofit the entire cab car with plywood panels to mimic the original flooring. A total thickness of 1.0” of plywood was added; however, because panels of such thickness were not readily available, an overlapping series of half-inch thick plywood panels were used. These panels were fastened to the steel sheet floor understructure panels using screw fasteners.

The FE model was modified accordingly. In addition, the model was revised to allow for yaw rotation of the impacting couplers to ensure that such motion did not hinder the activation and complete push back of the PBC. FE results with the modified model indicated the minimum speed at which the shear bolts are predicted to fail is 29 mph. At this speed, a desirable outcome was achieved, in the sense that all the key objectives of the test were predicted to be met. A side view showing the predicted deformation at the end of the analysis (0.25 seconds) is shown in Figure 58, and indicates that localized deformation at the forward side door is minimal, and the cab car truck wheels do not lift off the rail.

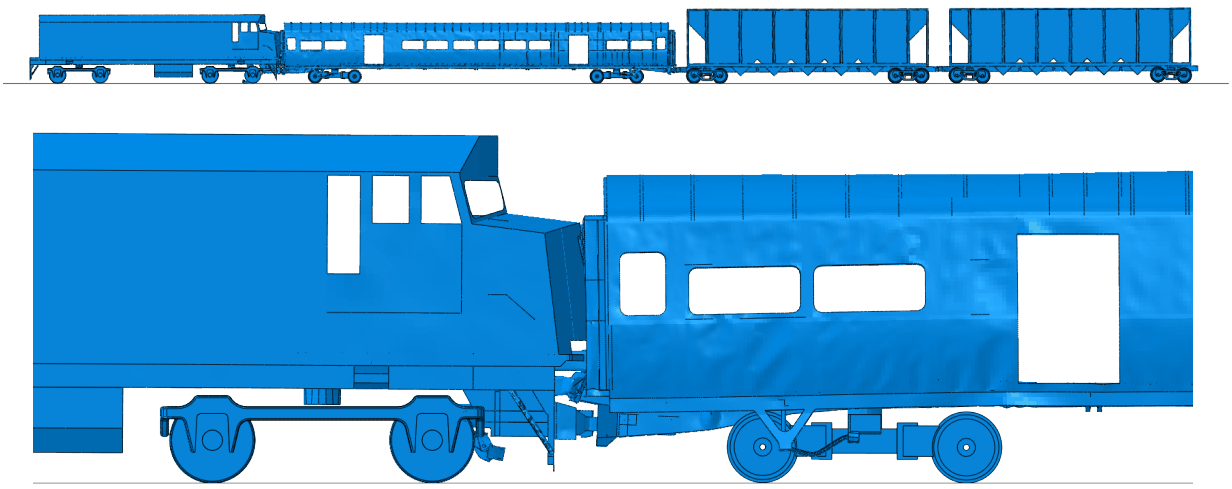

Figure 58. Predicted results for FE model with retrofit plywood flooring and coupler yaw rotation during impact at 29 mph collision speed: top — a side view showing all vehicles; bottom — a detailed side view showing the impacting CEM locomotive and cab car

Interestingly, at 28 mph, the outcome of the test was less desirable. The deformation tube of the PBC was fully exhausted, but the impact of the PBC against the sliding lug was not sufficient to fail the shear bolts. Instead, the load through the coupler gradually began to drop. Simultaneous with the drop in load was the formation of a buckle in the underframe of the cab car, near the front side door openings (see Figure 59). This seems to have occurred because a sizable load was still being transmitted through the coupler as another large load built up in the DAC. These two loads acting in parallel became greater than the cab carbody could withstand, particularly at the door opening, where the strength of the carbody cross-section was weakened. At this speed, the forward wheel was predicted to rise, but only by a few tenths of an inch, far less than predicted when the flooring had been removed.

Note that the interaction of the PBC and the sliding lug is defined in the model through the force-displacement behavior of a connector element. Once the full 21” of deformation tube crush is exhausted, the load between these two components is defined to rise rapidly. However, it is difficult to accurately capture the dynamics of the impact of these two stiff components. It is quite possible that the bolts would fail even at 28 mph, particularly if the couplers remain in-line and do not fail.

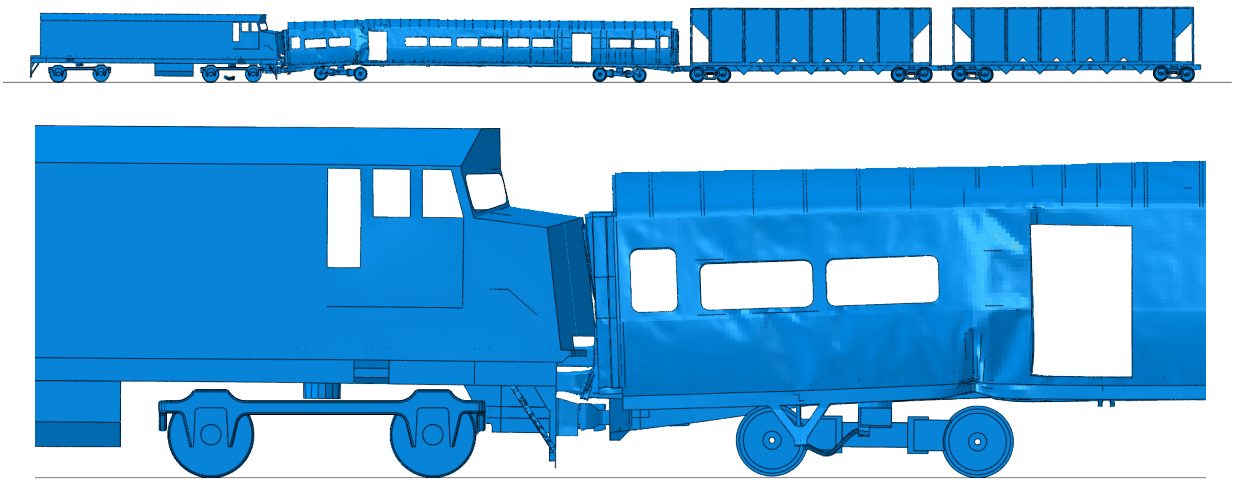

Figure 59. Predicted deformation at 28 mph collision speed: top — a side view showing all vehicles; bottom — a detailed side view showing the impacting CEM locomotive and cab car

Because the FE model predicts an abrupt change in behavior between 28 and 29 mph, and because it seems prudent to provide a "cushion" that accounts for potential inaccuracies in FE model predictions, researchers decided to increase the minimum acceptable test speed to 31 mph and, accordingly, increase the target speed to 33 mph. The predicted deformation at the target speed is shown in Figure 60. At this speed, there was substantial deformation in both the CEM and the cab car end structures, and the predicted extent of energy absorption in the DAC (710 ft-kips) was well above the 300 ft-kip target.

The predicted force-crush curve at the target speed of 33 mph is shown in Figure 61. The estimated force associated with key contributors to the total force is also shown.

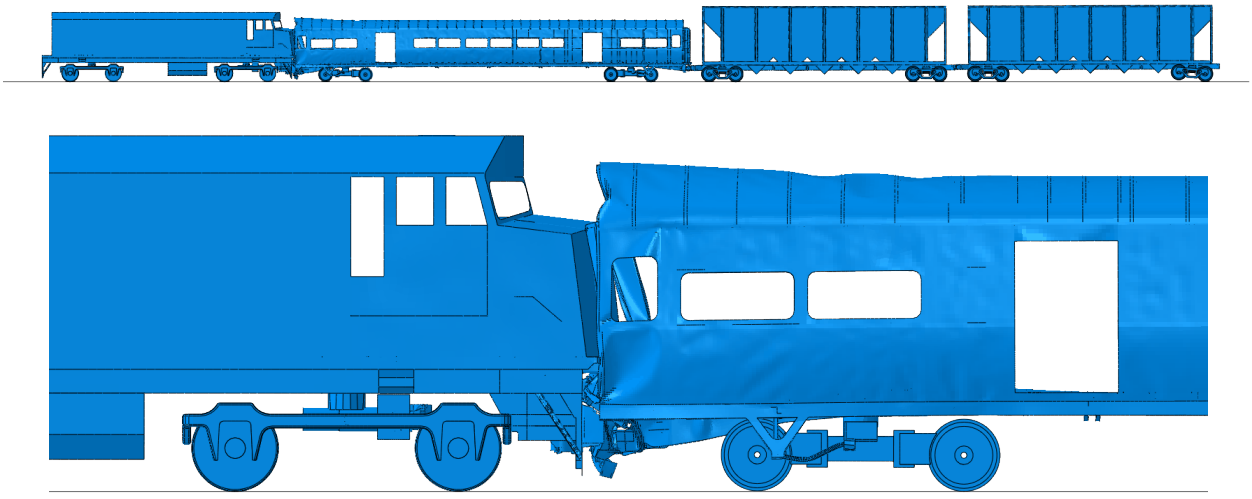

Figure 60. Predicted deformation at the target collision speed of 33 mph: Top — a side view showing all vehicles; bottom — a detailed side view showing the impacting CEM locomotive and cab car

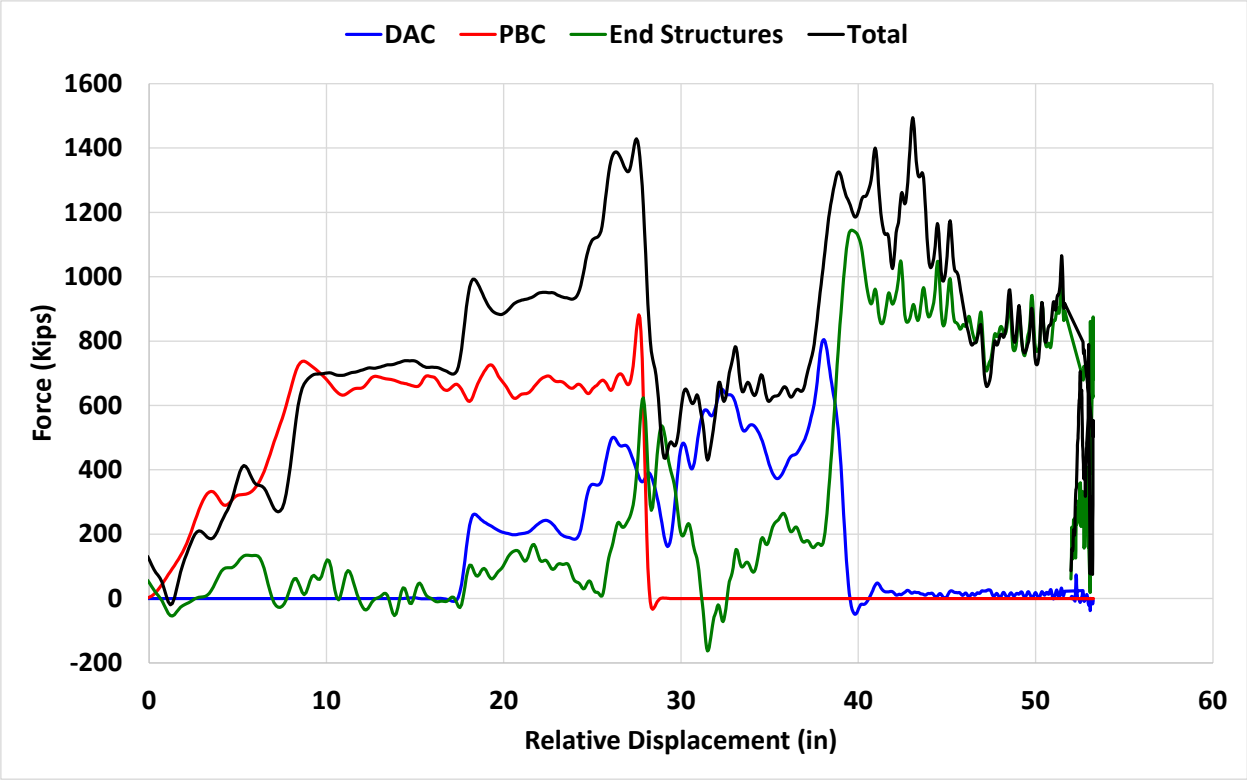

Figure 61. Predicted force crush curve at the target speed of 33 mph and a breakdown of the key contributions to the total force, including the PBC, the DAC assembly, and deformation of colliding end structures

FE results at 35 mph (see predicted deformation in Figure 60) indicate there was substantial additional end structure deformation but no undesired modes of motion or deformation, such as buckling of the cab car underframe or lifting of truck wheels.

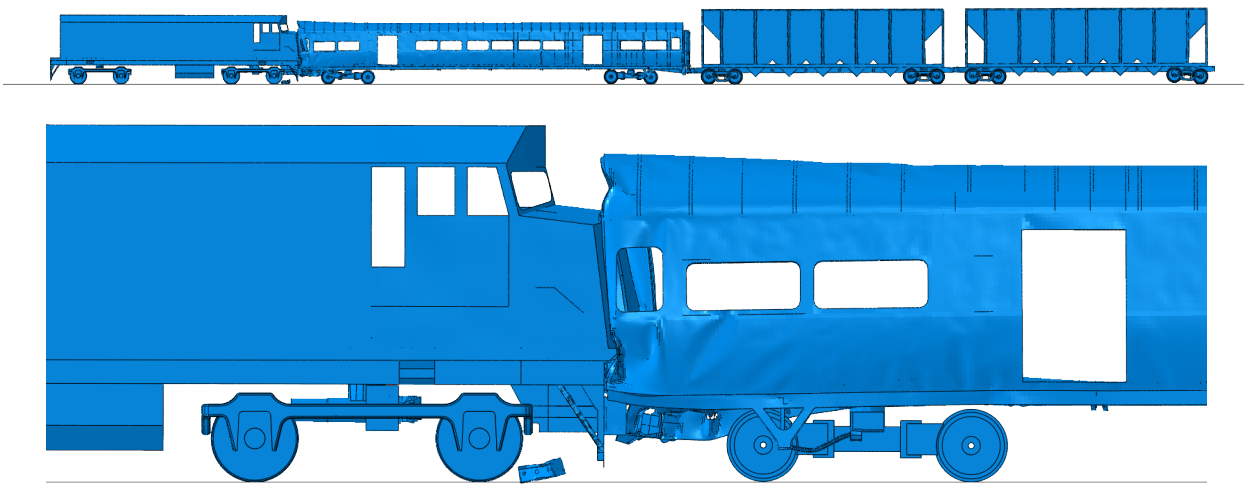

Figure 62. Predicted deformation at the estimated upper limit of collision speed (35 mph): top — a side view showing all vehicles; bottom — a detailed side view showing the impacting CEM locomotive and cab car

6. Vehicle-to-Vehicle Test 2 Test Results

Vehicle-to-Vehicle Test 2 was conducted on November 17, 2021. The test vehicles, instrumentation, and camera views were inspected on November 16. Positioning of strain gages and displacement transducers on the underframes of the respective vehicles were verified. A report details the test instrumentation and provides the raw test data for this test [15].

6.1 Test Outcome

On the day of the test, the weather conditions were clear with low winds. Both couplers were left closed, and the couplers were aligned within 1" vertically. Figure 63 is a pre-test photo of the impact interface. The target impact speed was 33 mph, and the actual impact speed was 32.8 mph. Figure 64 shows the impact interface after the test. The vehicles were kept in-line. There was no derailment of the vehicles and no override.

Prior to the impact, the two impacting couplers were set to their "closed" position, which was expected to maximize the extent of PBC stroke prior to DAC engagement, thereby reducing the time during which collision loads acted in parallel through both components. During the test, the closed couplers engaged at impact and the knuckle of the cab car coupler fractured. It appeared that the knuckle of the CEM locomotive pushed past the vertically oriented split in the cab car coupler knuckle and seated against the back of the coupler head, as if the couplers had been open prior to impact, as can be seen in Figure 65.

The PBC then triggered properly and the PBC head began to move back into the draft pocket. The PBC head continued to push back as the deformation tube deformed, and the bottom DAC tubes impacted the M1 buffer beam. The bottom DAC tubes deformed against the shape of the M1 underframe, as shown in Figure 66.

Figure 63. Pre-test photo of the impact interface

Figure 64. Post-test photo of the impact interface

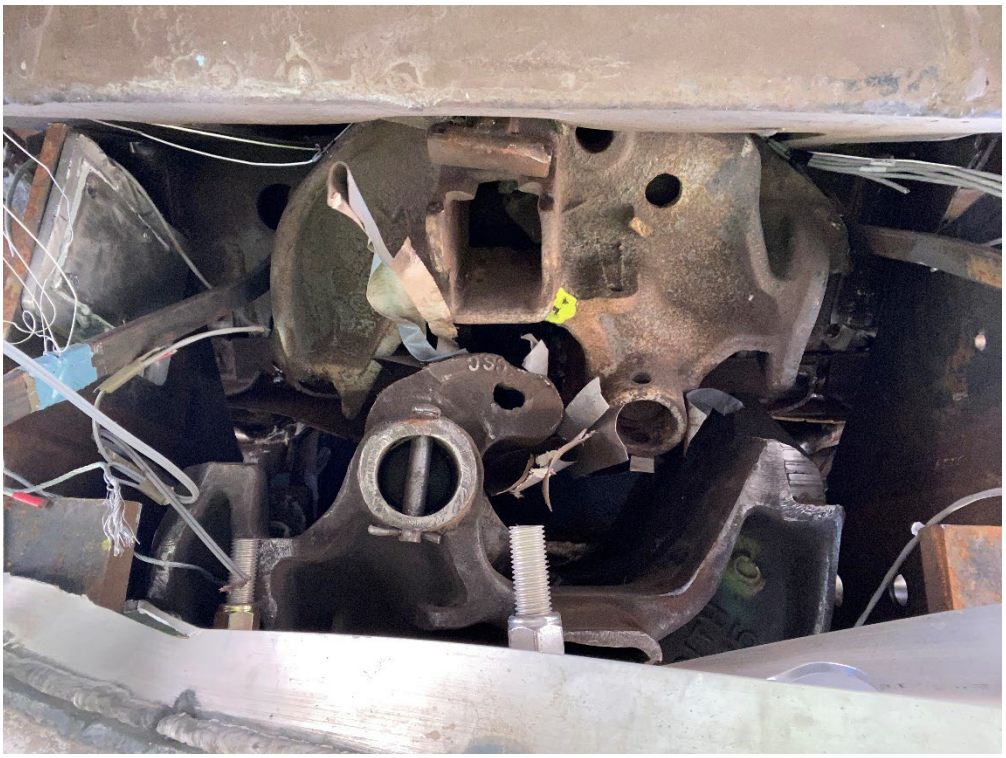

Figure 65. View of impacting couplers from below: M1 coupler on top, CEM loco coupler on bottom

Figure 66. DAC tubes after impact, before the vehicles were separated

As the PBC head moved back, the coupler carrier broke away, as designed. To prevent the frangible coupler carrier from interfering with instrumentation wiring, both sides were tethered to the draft pocket side plates. However, the tethers might not have been long enough, and one side of the damaged coupler carrier became caught between the sliding lug and a sliding lug support plate, as shown in Figure 67, causing damage to the sliding lug support plates.

At this point in the collision, the top DAC tubes impacted the end frame of the M1, causing the M1 collision posts to deform inward, as seen in Figure 66 and from inside the M1 in Figure 68. The PBC head continued to move back and the deformation tube was expanded along its entire stroke of 21", as shown in Figure 69. This was confirmed by evidence of contact between the limit stop mounted on the sliding lug and the rear of the PBC head, as shown in Figure 70. This contact was designed to occur at the full stroke of the PBC.

Figure 67. The deformed coupler carrier caught between the sliding lug and a bottom plate of the draft pocket

Figure 68. The view from inside the M1, looking at the CEM locomotive, before the vehicles were separated

Figure 69. The PBC deformation tube was expanded along its entire stroke of 21”

Figure 70. Damage to the limit stop mounted to the front of the sliding lug due to contact by the back of the PBC coupler head

Once the deformation tube had expanded along its full stroke, impact between the limit stop mounted on the sliding lug and the rear of the PBC head caused the shear bolts to break, and the sliding lug moved back into the draft pocket, as shown in Figure 71. The sliding lug pushed back the full extent (10”) of the pocket behind it and impacted the back plate. The front of the CEM locomotive continued to deform the front of the M1. The engaged vehicles continued to move backward on the track together, then came to a stop approximately 575’ from the impact point.

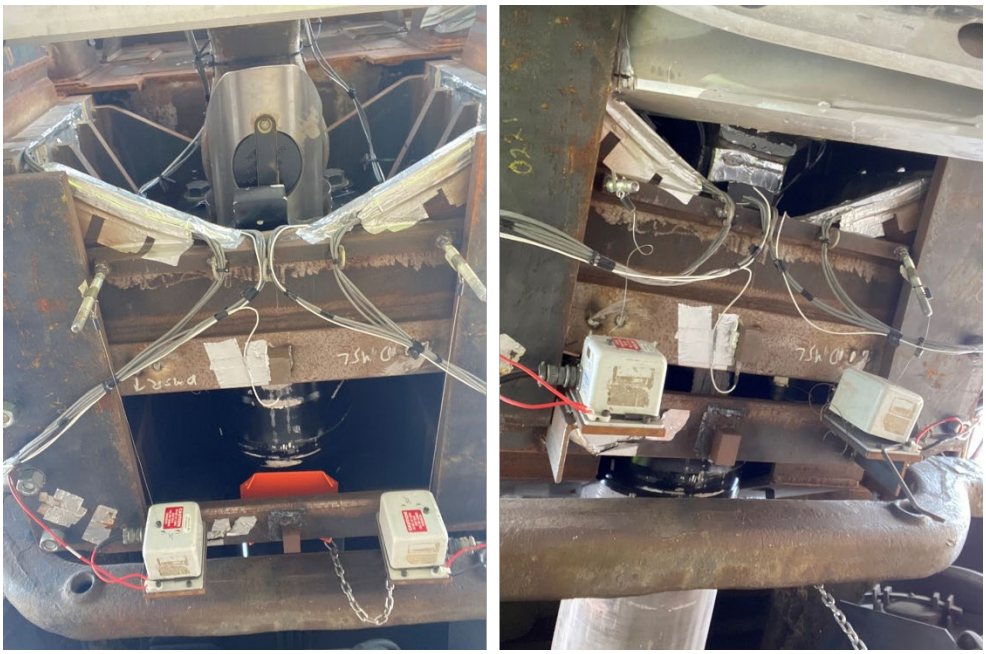

Figure 71. Sliding lug position before (left) and after (right) the impact

6.2 Damage to the Equipment

After the test, the vehicles were pulled apart. Figure 72 shows the post-test impact interface of both vehicles.

Figure 72. Post-test impact vehicles: CEM locomotive (left), M1 cab car (right)

6.2.1 Damage to the CEM Locomotive

The upper DAC plate and tubes were barely damaged. It appeared that the collision posts of the cab car folded back at such a low load that the energy absorption in the upper DAC tubes was minimal. The lower DAC tubes were impacted and deformed considerably. The deformation was not uniform, as was expected, with the bottom insides of the tubes deforming considerably more than the upper outsides of the tube. Both sets of DAC tubes can be seen in Figure 73. Post-test estimates based on the measured deformation of the four corners of each of the tubes and results from previous dynamic impact tests of the DAC system indicate that the energy absorption of the DAC was approximately 300 ft-kips, thus meeting the performance target.

After the bottom DAC tubes were removed, the support plate behind the DAC was found to have deformed approximately 0.375” on the right side, and slightly less than that on the left side. This is shown in Figure 74.

Figure 73. Upper and lower DAC tubes, post-test

Figure 74. Post-impact deformation of bottom DAC tubes support plate, left (left) and right (right) sides

All shear bolts broke, but one (#5) did not break as cleanly as the others, as shown in Figure 75. This caused some damage to its draft pocket bolt hole, as shown in Figure 76. No damage was imparted to the corresponding bolt hole in the sliding lug.

Figure 75. All shear bolts broke cleanly, except #5 (bottom row, second from right)

Figure 76. Draft pocket deformed bolt hole

As mentioned previously, one of the sliding lug support plates was deformed as a result of the coupler carrier getting caught between the sliding lug and the support plate, as shown in Figure 77.

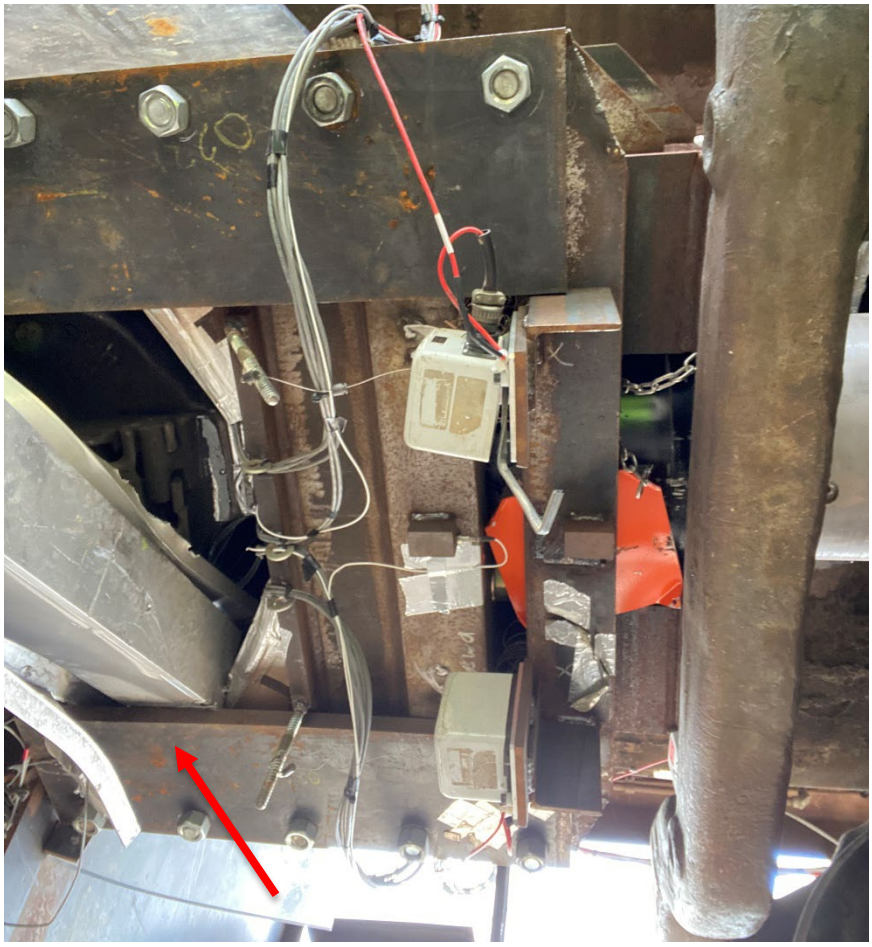

Figure 77. One of the two sliding lug support plates was deformed

The front plate of the locomotive was bent backwards on both sides by several inches, as seen in Figure 78. Note the angled pipes that support the front plate had been removed from the forward end of the CEM locomotive some time before the test. (In fact, photographs indicate they had been removed prior to VTVT1.)

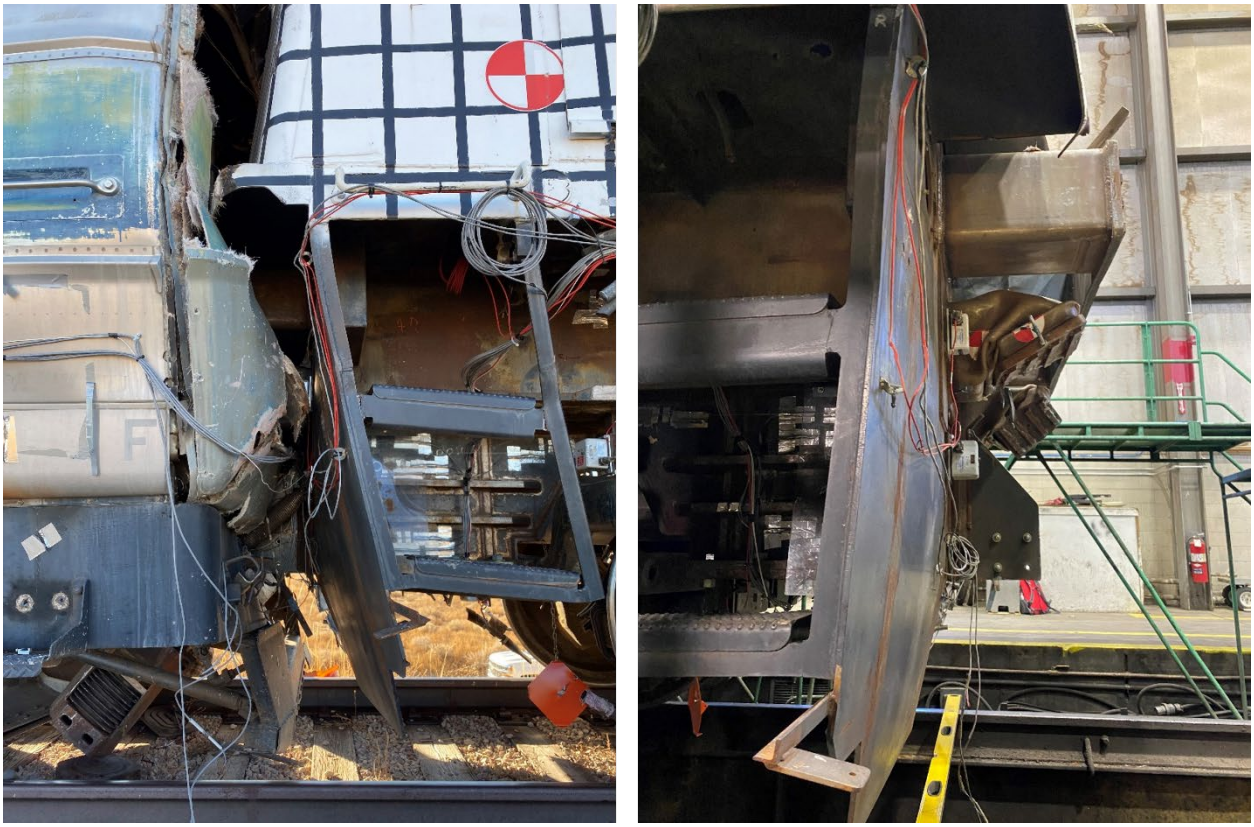

Figure 78. CEM locomotive end plate deformation on left (left) and right (right) sides

6.2.2 Damage to the M1 Cab Car

As mentioned previously, the M1 coupler knuckle fractured at impact. The knuckle of the CEM locomotive pushed past the vertically oriented split in the cab car coupler knuckle and seated against the back of the coupler head as if the couplers had been open prior to impact. The fracture can be seen in Figure 79.

The collision posts of the cab car folded back due to impact by the upper DAC plate, as seen in Figure 68. Measurements indicated that the posts intruded into the vestibule of the cab car by about 29”. Figure 80 shows the damage to the end frame of the M1. Both the coupler and the bellmouth ended up tilted upward, as seen in the photo. This was due to the M1 draft sill buckling. The draft sill deformed downward by about 15”, as shown in Figure 81.

Figure 79. M1 coupler knuckle fracture (left), and a close-up of the fracture (right)

Figure 80. Post-test damage to M1 end frame

Figure 81. M1 draft sill before impact (top) and after impact (bottom)

The cab car was “crippled,” with a large buckle forming in the underframe just forward of the rear side doors, as shown in Figure 82. The center sill of the cab car buckled downward by about 9”, just forward of the rear door, and upward by about 6”, near the center of the rear door. Severe folds arose in the floor, side walls, and roof in the area of the buckle. Figure 83 shows the damage in the interior at the rear door buckle.

Figure 82. M1 carbody buckled inboard of rear doors

Figure 83. M1 interior damage, buckle at rear door

7. Vehicle-Vehicle Test 2 Post-Test Evaluation

7.1 Data Review and Analysis

Test data were compiled and filtered by TTCI and provided to Volpe and CAMX in an Excel file. A report provides the raw test data for this test [15]. Data from accelerometers, string potentiometers, and strain gages were reviewed relative to what they reveal about the impact sequence, vehicle motions, collision forces, and strain near shear bolts. Key results are summarized in several time-history plots and, together, provide a sense of both the magnitude and timing of key events during the impact.

Note that, in contrast to VTVT1, it is difficult to determine the timing of key impact events based on longitudinal acceleration data. For this reason, a discussion of the impact sequence is presented at the end of this section, informed by an analysis of collision forces, string potentiometer data, and video evidence.

7.1.1 Longitudinal Vehicle and Component Motions

Inspection of the CEM locomotive and cab car underframe center longitudinal accelerometer data (AMUC_X and ASUC_X, respectively, as shown in Figure 84) indicates there was much more high-frequency content in the respective signals compared to the same pulses for VTVT1, making it difficult to pinpoint the timing of the sequence of key events. The signal for the lighter cab carbody was particularly noisy. Some of the early oscillation of the signal was likely due to the fracture of the cab car coupler knuckle.

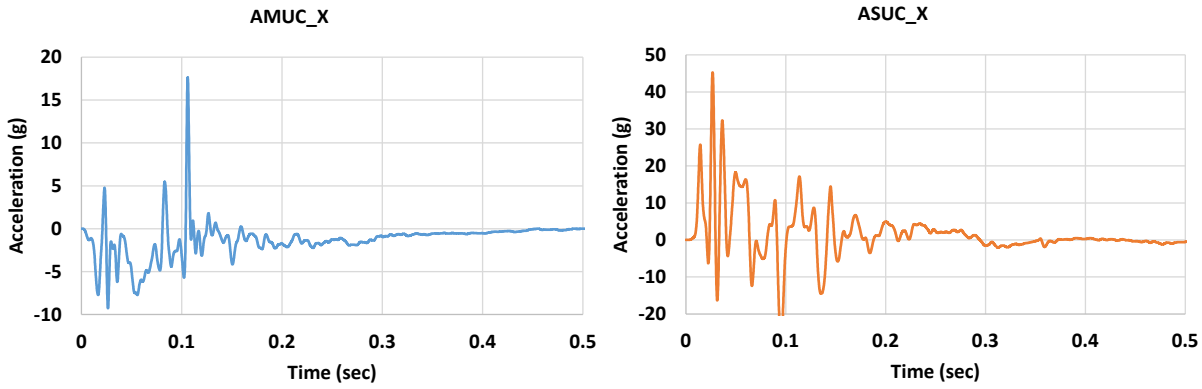

Figure 84. CEM locomotive (left) and carbody underframe (right) center longitudinal accelerations ('S' for stationary, 'M' for moving)

Integrating the acceleration pulses and applying an initial speed of 32.8 mph to the CEM locomotive yielded vehicle speed vs. time curves, as shown in Figure 85. Note that there was an offset between the speeds of the two vehicles that was evident at about 0.3 seconds after impact. Video and post-test photographic evidence clearly indicated that the vehicle ends remained locked together following impact, so it was likely that this offset was the result of signal drift.

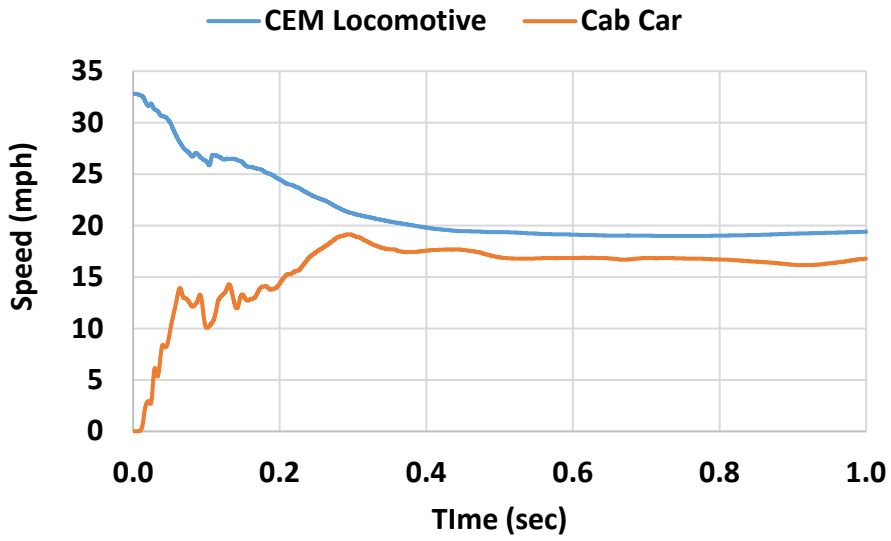

Figure 85. Calculated vehicle speed time-histories

Integrating the respective speed vs. time curves yielded vehicle displacement time-histories. Subtracting the derived displacements of the respective vehicles provided an indication of the relative displacement between the vehicle centers, or "crush." The relative impacting vehicle displacement time-history calculated in this manner is shown in the left plot in Figure 86. This curve indicates the relative displacement was still increasing after 0.5 seconds — clearly not consistent with the noted evidence that the vehicle ends locked together shortly after impact. A better estimate of the displacement time-history can be obtained by subtracting what is likely signal drift that can be identified through the difference between the velocities of the respective vehicles shown in Figure 85 (known to be essentially the same since they were locked together). Using the average value of this difference between 0.3 seconds and 1 second (ΔV=2.42 mph) and subtracting a displacement equal to t*ΔV yields the corrected relative displacement time-history shown at the right in Figure 86, indicating the maximum crush was about 57".

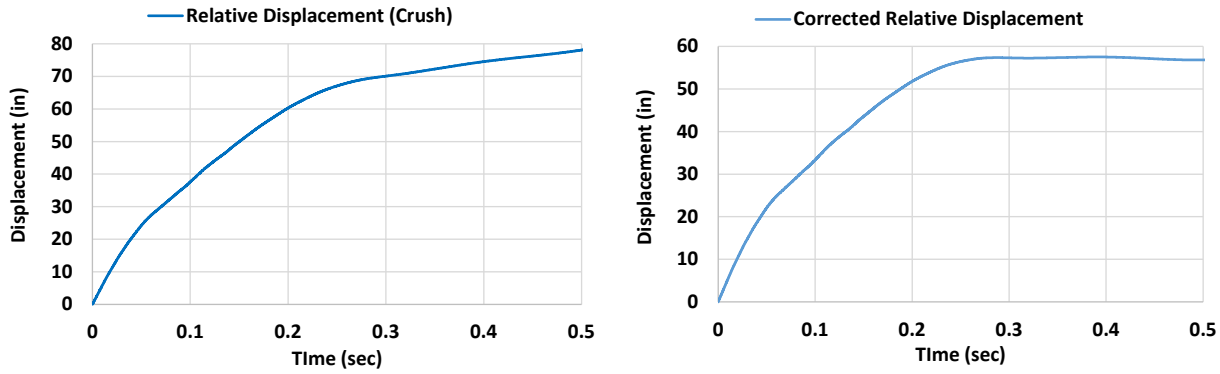

Figure 86. Vehicle relative displacement obtained from integration of the speed pulses shown in Figure 85 and subtraction of the respective vehicle displacement time-histories (left) and correction (right)

A better indicator of the total crush of the vehicle ends are post-test measurements made between different points on the colliding vehicles, as well as video evidence. Two post-test measurements were made while the vehicles were still on the track: the distance between the center of the front

wheels of the respective forward trucks (146” right side; 148” left side — 147” average), and the distance between the front plate of the locomotive and the end of the side wall/side sill of the cab car (13” right side; 15” left side — 14” average). Note that neither of these distances were measured prior to the test; however, FE model coordinates indicated that the undeformed distances were 198” and 59.6”, respectively. Subtracting the measured values from these presumed undeformed distances yielded the following estimates of crush: 51” and 45.6”, respectively. The 5.4” difference between these two measures was likely an indication that the end frame of the cab car pushed back a few inches.

High-speed videos provided another indication of total crush. Images shown in Figure 87 and Figure 88, taken from one of the high-speed videos (“East Iso.mp4”), give a clear indication of the extent of crush between the end structures of the CEM locomotive and the cab car.

Figure 87 shows an image made just before impact. The image is annotated with dashed yellow lines, indicating distinct longitudinal reference points on each of the respective vehicles: the top-front left corner of the locomotive hood and the end of the cab car side wall/side sill, where the cladding becomes rounded. Dimensions taken from the FE model indicate that this distance is approximately 64” at impact. (The indicated distance of 64.9” takes into account about 0.6” of pre-impact travel at 32.8 mph over 1.045 msec). The image in Figure 88, from a high-speed test video taken about 280 msec after impact, clearly shows these two longitudinal reference points to be effectively coincident, indicating that the maximum crush was about 64”. In the figure, the top-front corner of the locomotive hood has been pushed all the way to the end of the side wall of the cab car, where the cladding begins to curve inward at the forward end of the vehicle.

Figure 89 shows still images from the overhead standing drone video taken: (1) near the point of maximum crush and (2) after elastic rebound (i.e., close to a state where the post-test photographs were taken). These images are consistent with the model results shown in Figure 59, and further indicate an extent of rebound that appears to be 12” to 15” (note that the grid on the locomotive hood is 6” x 6”).

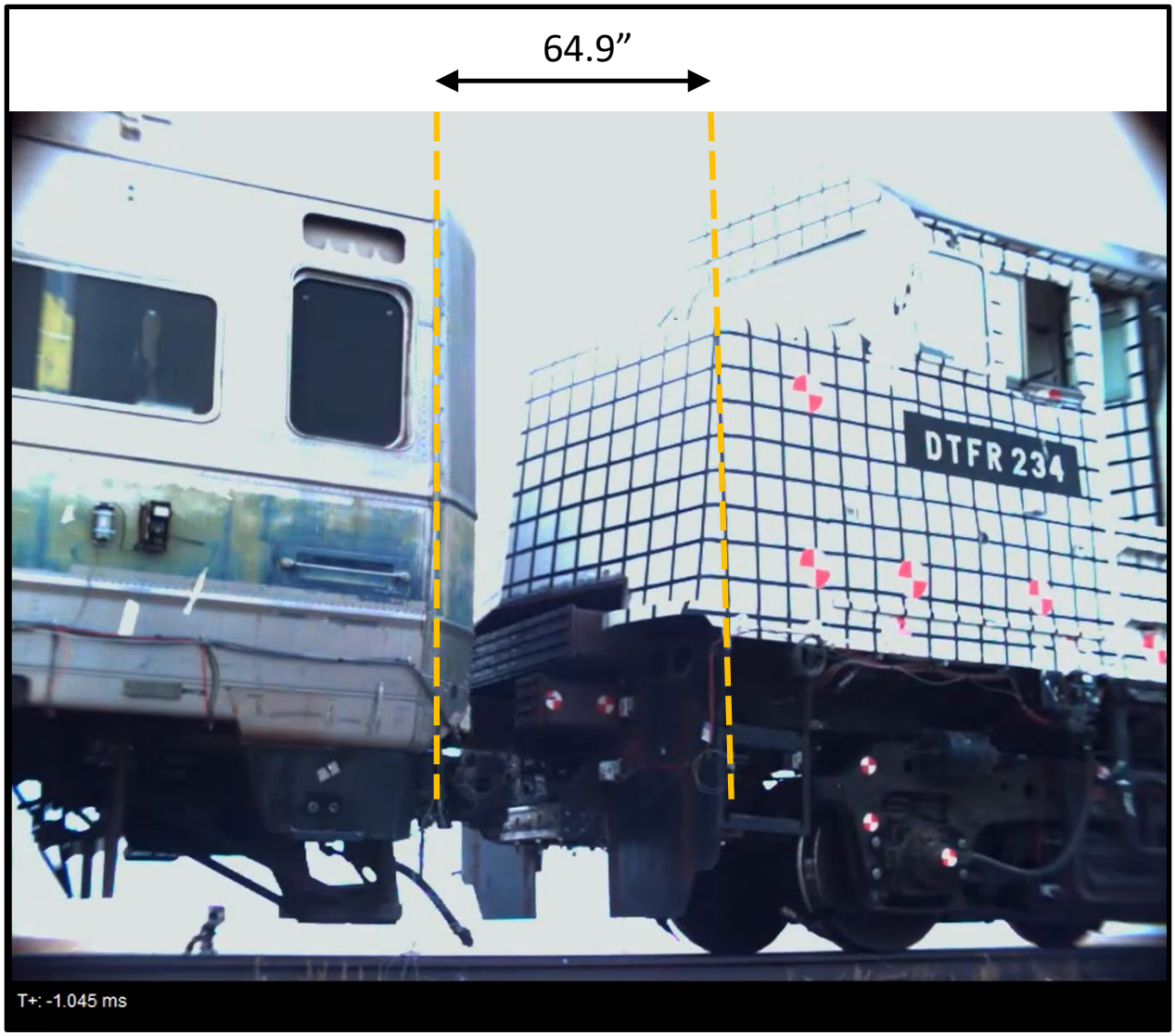

Figure 87. Image from high-speed video annotated to indicate the distance just prior to impact between reference points on each vehicle.

Figure 88. Image taken from a high-speed test video (approximately 280 msec after impact)

Figure 89. Still images from the overhead standing drone taken near the point of maximum crush (top) and after elastic rebound (bottom)

The string potentiometer data measuring CEM coupler motion are plotted in Figure 90 and indicate displacements rose to about 18” after 0.070 seconds, at which point the shear bolts failed. It is not clear why the measured stroke was less than the 21” stroke of the PBC. It is worth noting, however, that these string potentiometers also underestimated the extent of PBC stroke during VTVT1, indicated by deformation tube markings. Also note the rise and fall of coupler displacement after 0.020 to 0.025 seconds that was clearly associated with initial coupler impact followed by the failure of the cab car coupler knuckle.

Further evidence of the timing of shear bolt failure and sliding lug sill impact with the back of the draft pocket can be gleaned from the string potentiometers that measure longitudinal motion of the sliding lug. As illustrated in Figure 91, string pot displacement began to rise after 0.070 to 0.080 seconds and smoothly increased until 0.105 to 0.110 seconds, at which point there was a sharp jump in displacement, followed by a much noisier response. It is not clear from these curves why the displacement continued to increase beyond the 10” depth of the draft pocket, but it is clear from photographs that at least one of the two string potentiometers was damaged during the collision.

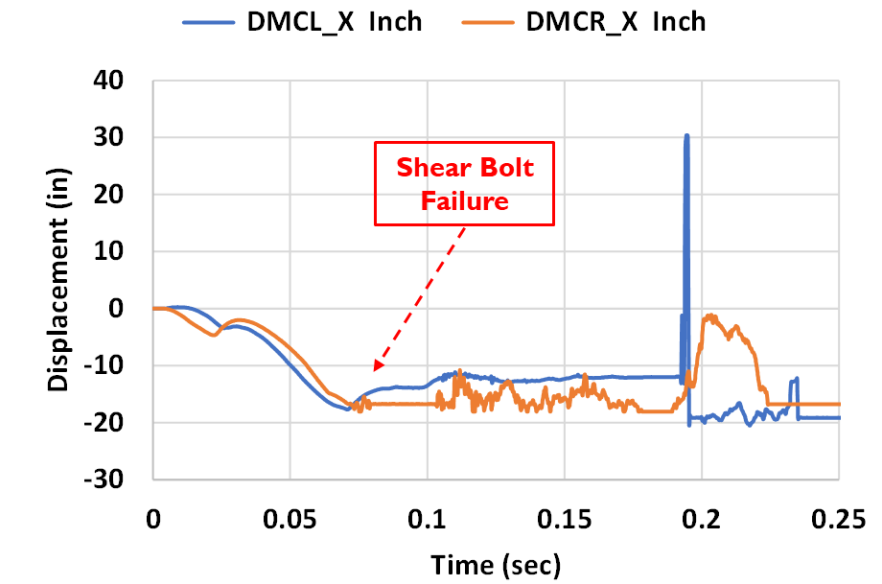

Figure 90. CEM coupler longitudinal motion, as measured by string potentiometers DMCL_X and DMCR_X

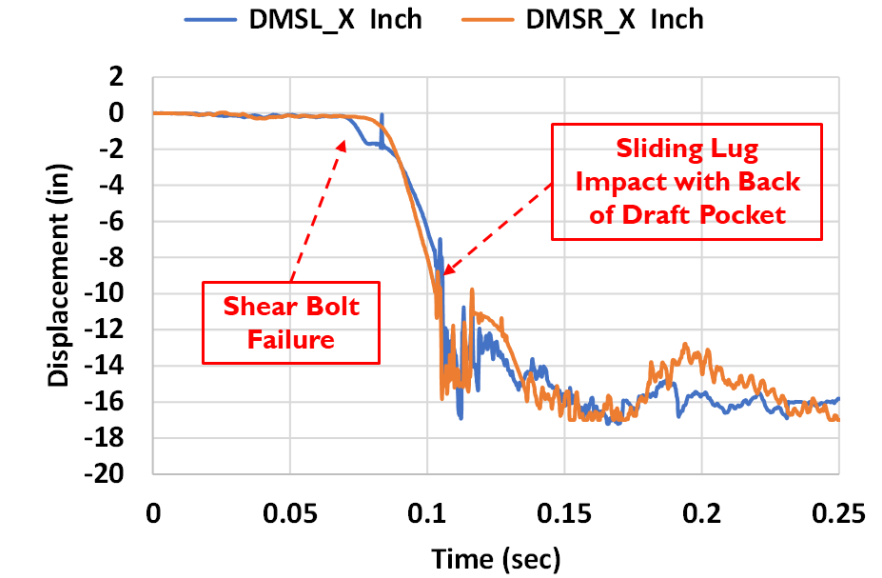

Figure 91. Sliding lug longitudinal motion, as measured by string potentiometers DMSL_X and DMSR_X

String potentiometers measuring DAC crush (see Figure 92) indicated that the crush of the lower DAC tubes began about 0.045 seconds after impact. Interestingly, there was a slight lengthening of the string just after impact, likely due to the rotation of the DAC tube end plates that occurred due to the vertical offset of the lower DAC with respect to the buffer beam of the cab car. High-speed video evidence (e.g., “East Wide-View.mp4”) suggests that the initial impact of the lower DAC tubes with the M1 spring-loaded buffer beam likely occurred between 0.019 and 0.025 seconds after impact, but the DAC tubes did not appear to begin to deform until the springs were compressed and the stiffer end beam of the cab car is loaded. There was a low-magnitude signal from the DAC string pot that was consistent with this video evidence, and further suggests that

the energy-absorbing capacity of these springs was minimal. Note that because the cab car knuckle failed, allowing the couplers to move another 7” closer to one another before PBC force build-up, the PBC stroke was only about 6” to 8” when the DAC engaged. For this reason, there was a period of about 0.04 seconds during which the PBC and DAC components acted in parallel. Video evidence supports pre-test FE predictions (consistent with end structure geometric features) that impact of the upper DAC tubes with the cab car collision posts occurred about 0.02 seconds after impact of the end beam and the lower DAC tubes. As is evident from post-test photographs, there was little deformation of the upper DAC tubes — perhaps 0.3” or so at the left tube, most of which appeared to be elastic, dropping to about 0.1” after a few seconds.

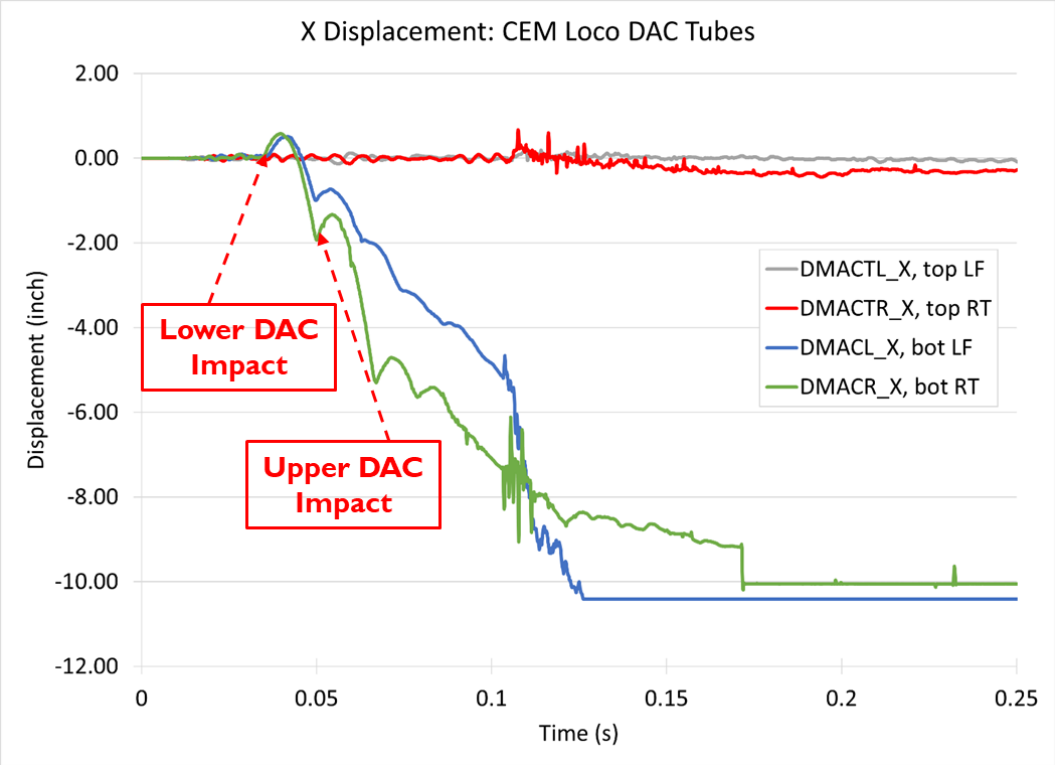

Figure 92. DAC longitudinal motion, as measured by string potentiometers DMACR_X and DMACL_X (lower DAC tubes) DMACTR_X and DMACTL_X (upper DAC tubes)

7.1.2 Vertical Motions

Recall that VTVT1 test videos indicated a noticeable cyclic pitch (bouncing) of the CEM locomotive carbody on the suspension system of the forward truck during the collision (nearly ±4”; see Figure 37). This was attributed to missing limit stops on the CEM truck-to-body connections. For VTVT2, the limit stops were in place, and the CEM pitch motions were much less pronounced, as indicated in Figure 93.

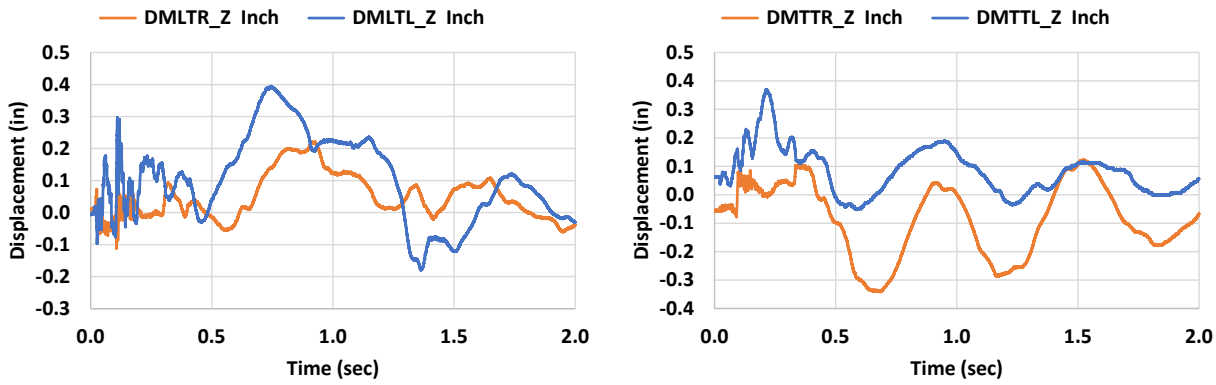

Figure 93. CEM forward (left) and rear (right) truck secondary suspension vertical displacements indicate less than 0.4” of body-to-truck relative displacement

The vertical motions of the cab car truck forward secondary suspensions were larger, as illustrated at left in Figure 94, but still less than about 1”. On the other hand, the relative vertical displacements between the rear cab car truck and body were more significant, reaching over 3” in magnitude, as shown at right in Figure 94. These higher displacements were likely the result of the high compressive force through the cab car center sill and the subsequent buckling of the center sill forward of the rear door. This appeared to have had the effect of raising the carbody, as indicated in an image taken from one of the high-speed videos (“South.mp4”) approximately 480 msec after impact (see Figure 95). The time at which this image was captured coincided with the initial positive displacement peaks indicated in Figure 94. Note that the wheels of the rear truck are off the rail in this image. The 3–4” positive displacement at this time was consistent with the researchers’ understanding of how the limit stops of the cab car trucks function, allowing for about 4” of stroke before lifting the truck with the carbody. The subsequent negative displacement was likely associated with the wheels again coming in contact with the rail and secondary suspension compression. This was followed by continued oscillation of the suspension, as is visibly noticeable in other test videos.

Further analysis of the “South.mp4” video indicated the buckle in the cab car underframe/body began to grow at about 140 msec after impact, peaking between 420 msec and 480 msec, and then decreasing. The absence of any significantly large acceleration signals during this time suggests that the growth of the buckle occurred at a very small longitudinal force, which was not surprising given the magnitude of the buckle, which appeared to be well over 18” and may have reached 2’ at its peak.

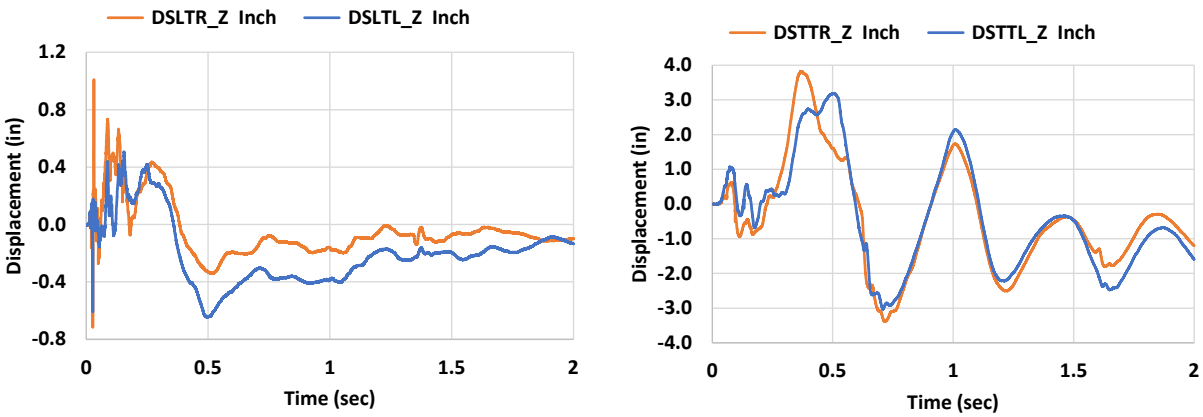

Figure 94. Cab car forward and rear truck secondary suspension vertical displacements

Figure 95. Image captured from high-speed video approximately 480 msec after impact, showing the upward folding of the cab carbody at the induced buckle just forward of the rear doors, causing the rear truck wheels to lift off the rail

7.1.3 Collision Forces

As noted, it is difficult to estimate collision forces based on vehicle accelerations due to the higher-frequency content of the pulses. The impacting coupler strain gages provided a good indication of the force between the two vehicles up to the point that the DAC impacted the buffer beam of the cab car. Averaged force time-histories estimated based on strain gage data and assumed coupler shank cross-sectional areas are shown for the respective couplers in Figure 96. These curves indicate:

- A build-up in force for about 0.015 seconds followed by a drop in force and a subsequent increase through approximately 0.022 seconds. This was likely due to the impact and failure of the coupler knuckle.
- Several milliseconds during which the force was relatively uniform, at about 600 to 800 kips. This was likely indicative of PBC push-back.
- A drop in load at about 0.080 seconds that appeared to be when the shear bolts failed. One would normally expect a sharp jump in load associated with impact of the coupler with the sliding lug, but this did not seem to have been the case. This may have been due to the interference from the failed coupler carrier that acted to cushion the impact.
- An abrupt impulse did, however, arise at about 0.105 to 0.110 seconds in the PBC only. Additional evidence (see below) suggested that this sharp rise in load was due to impact of the sliding lug with the back of the draft pocket.

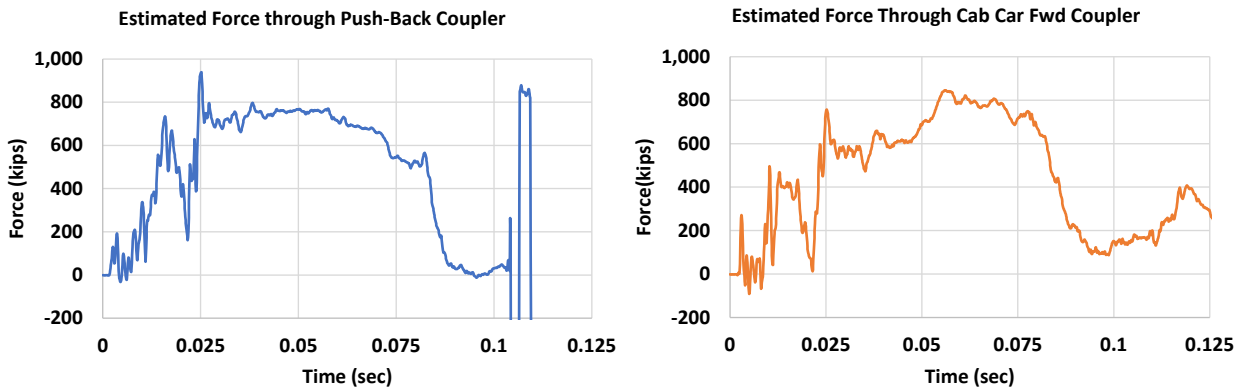

Figure 96. Force through impacting couplers estimated based on strain gage data and known coupler shank cross-sectional area

Once the lower DAC tubes impacted the end beam of the cab car, the load between vehicles quickly increased. Because of the oscillations in the colliding vehicle longitudinal accelerometer data shown in Figure 84, it was difficult to estimate a total force-crush curve for this test. Figure 97 shows a force-crush curve estimated from the longitudinal acceleration data. As is evident in this figure, even when a lower-frequency filter (CFC30) was applied to the data in lieu of the standard CFC60 in an effort to filter out the oscillations, it was difficult to interpret the curve. Nonetheless, the plot does show the force rising after about 20” of crush — to as much as 1,500 kips before falling. This was likely due to the build-up of force when the lower DAC tubes and then the upper DAC tubes impacted the end frame of the cab car.

The lower load levels evident in Figure 97 between 36” and 57” are consistent with the small forces that are typically associated with post-buckling behavior.

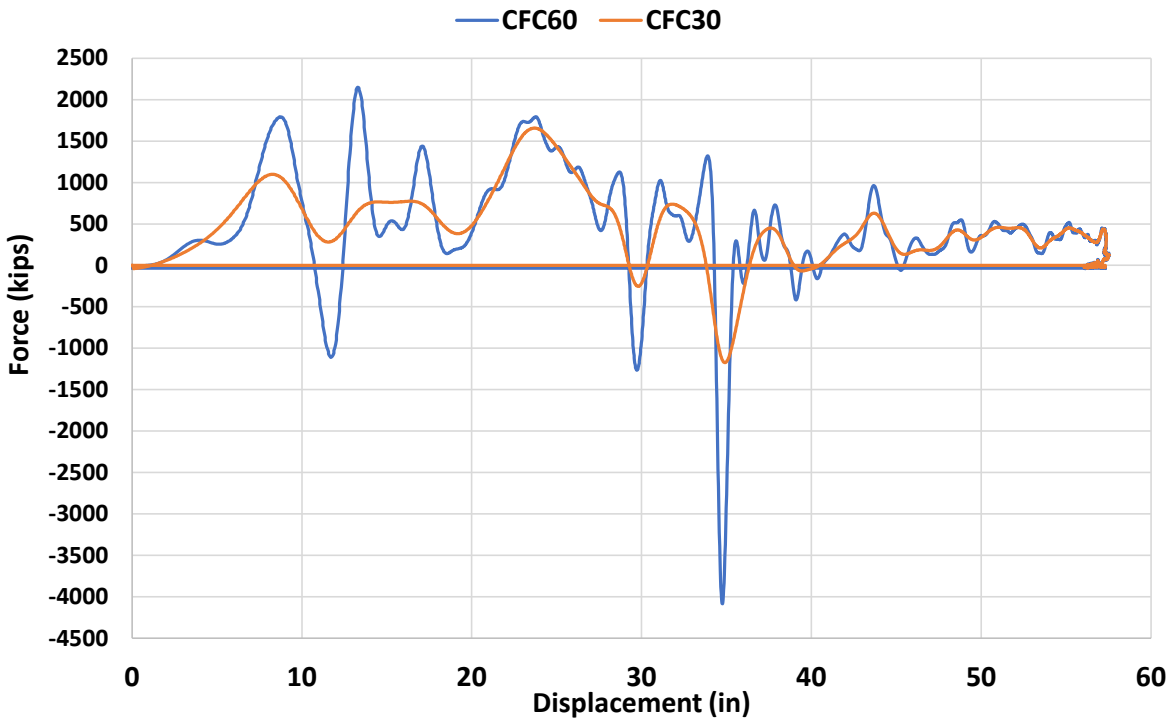

Figure 97. Colliding vehicle force-crush curve derived from CEM longitudinal acceleration data (Figure 84, left) and predicted relative displacement between the CEM locomotive and the cab car (Figure 86, right) presented for two filtering frequencies: CFC60 (standard) and CFC30 (non-standard)

7.1.4 Strain Near Shear Bolts

Time-histories of strain aft of the eight top and bottom shear bolts on the draft pocket side plates are shown at the left in Figure 98. Time-histories of strain forward of the eight top and bottom shear bolts on the sliding lug side plates are shown at right.

Table 3 reports averaged values (front and rear, top and bottom, and left and right sides) for the eight strain gages mounted to the draft pocket side plates and the eight gages mounted to the sliding lug slide plates. (Note that positive strain readings indicate compression.) Strain gage readings for the draft pocket and sliding lug bolt hole regions were reasonably consistent with results from VTVT1 and the 9-mph CEM coupling test [9] during which the PBC triggered. However, average peak strains (and, therefore, loads) for the draft pocket were higher because the load through the PBC increased to the point where the shear bolts failed.

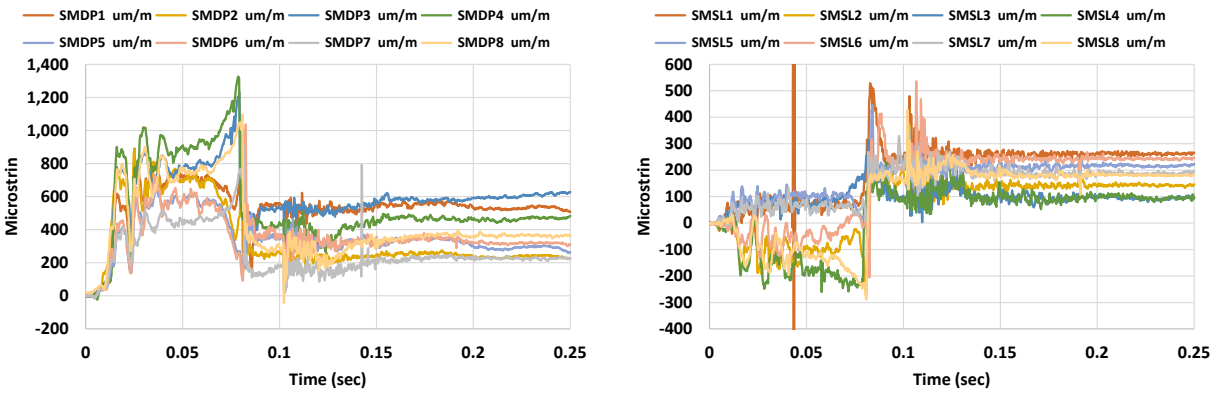

Figure 98. Left — time-histories of strain aft of the eight top and bottom shear bolts on the draft pocket side plates; right — time-histories of strain forward of the eight top and bottom shear bolts on the sliding lug side plates

Table 3. Comparison of averaged measured peak strain levels (microstrain) during vehicle-vehicle tests with those from 9-mph CEM coupling test[9]; note that positive strain gage readings were compressive

		Front	Rear	Left	Right	Top	Bottom
Draft Pocket Side Plate	9 mph Coupling Test	380	530	550	360	490	430
	VTVT1	550	670	530	700	600	630
	VTVT2	630	730	590	770	650	720
Sliding Sill Side Plate	9 mph Coupling Test	40	-150	-40	-60	-30	-70
	VTVT1	80	-130	-40	0	-20	-20
	VTVT2	60	-120	0	-50	-20	-40

Time-histories of strain near the top of the draft pocket sides plates (one positioned near the front of the side plate and one near the rear) are shown at the left in Figure 99. Time-histories of strain along the web of the underframe main I-beams, near where the lifting pads are positioned, are shown at the right. All these measured strains were relatively small, roughly 200 microstrain, until the sliding lug impacted the back of the draft pocket at about 0.105 seconds, at which point there was a large impulse applied to these strain signals. Prior to this impact, the strain levels at the front draft pocket side plate appeared to be compressive, while those at the back were tensile. The strain levels along the web of the main I-beams were mostly tensile, with the strain levels near the top of the web having a higher magnitude. It was difficult to draw conclusions based on these results, given the gradients in stress in these regions and the small magnitude of these strains. Nonetheless, they appeared to be consistent with FE model predictions, as discussed in Section 7.2.

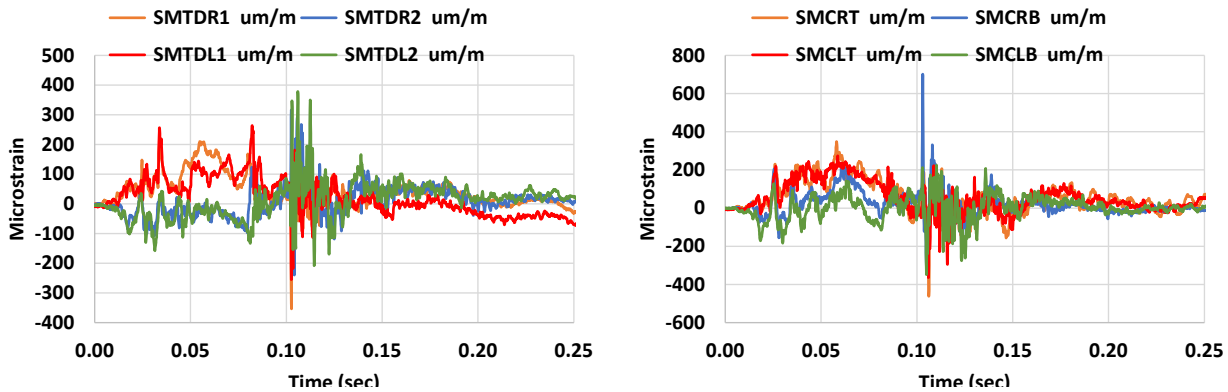

Figure 99. Left — time-histories of strain near the top of the draft pocket side plates ('1' front and '2' rear); right — time histories of strain along the web of the underframe main I-beams ('T' top and 'B' bottom)

7.1.5 Collision Sequence

Combining evidence from the CEM coupler strain gages, the string potentiometers on the push-back coupler and the sliding lug, and images from high-speed videos suggest the collision sequence summarized in Table 4.

Table 4. Estimated timing of key collision events

Timing (msec)	Event
0 – 15	Build-up of force in the colliding couplers
15	Failure of the cab car coupler knuckle
15 – 22	Decrease in force as the coupler heads moved past one another
22 – 25	Secondary build-up of force in the colliding couplers
25	Activation of the push-back coupler deformation tube
45	Impact of the lower DAC tubes with the cab car end frame
60	Impact of the upper DAC tubes with the cab car collision posts
45 – 120/160	Continued crush of the lower left and right DAC tubes
80	Impact of the PBC with the sliding lug limit stop and shear bolt failure
80 – 105	Post-bolt failure motion of sliding lug
105	Impact of sliding lug with back of draft pocket
100	Buckle in cab car side body became apparent
280	Maximum extent of crush
420	Maximum extent of cab carbody buckle
480	Maximum extent of cab car rear wheel lift
680	Cab car rear wheels returned to rail

7.2 Comparison of Test Results with Pre-Test Model Predictions

Pre-test predictions of behavior during the test are compared with test results in this section. In general, the outcome of the test was reasonably consistent with key model predictions. With respect to the target speed, the researchers recognized going into the test the need to balance the risk of two non-ideal outcomes: one in which the collision speed was not sufficient to meet targets with respect to CEM component activation and energy absorption, and the other where the damage to one of the vehicles would lead to derailment. The cab car was of particular concern, especially given (1) the asbestos remediation process that removed the floor and interior seating, both of which strengthened the car and increased its resistance to crippling; and (2) the age of the car, and the associated potential that its strength and stiffness had degraded over time, or that certain assumed properties, such as truck secondary suspension characteristics, do not match actual values.

The FE-based, 33-mph target speed was chosen so that, even at the low end of the expected speed range (31–35 mph), there was still some leeway with respect to having sufficient collision energy to completely exhaust the PBC and fail the shear bolts. FE model results indicated the bolts would fail at 29 mph, giving a 2-mph cushion. As noted above, simulations at lower speeds indicated non-ideal outcomes in which the cab car absorbed much of the collision energy due to collapse of the end frame and buckling of the draft sill and floor structures prior to the shear bolts' failure.

By and large, the key predicted test outcomes were realized, with shear bolt failure, DAC energy absorption of around 300 ft-kips, and no derailment and no indication of vehicle override. Differences between model predictions and test results can be largely attributable to three factors:

1. The knuckle of the cab car coupler failed, allowing the CEM coupler knuckle to move past it and seat the coupler heads together as if they had been open at impact. This caused the impacting vehicles to move closer to one another by about 7", with little or no stroke of the PBC deformation tube.
2. The upper DAC tubes did not crush extensively, and, instead, the collision posts which they impacted folded, causing the cab car end beam to rotate back significantly. It seems likely that the modeled strength of the collision post was greater than its actual strength. This was most likely due to the lack of a strong connection between the sheet that closed off the C-shaped post and the flanges of the post. These two parts of the posts separated completely from one another at the impact point. Because the upper DAC tubes did not absorb much, if any, energy, there was more extensive deformation of the cab car end structure than anticipated.
3. The plywood flooring that was added to replace the original plymetal floor of the cab car came completely loose during the collision. It appeared that the screw connections between the plywood and the floor stiffeners were not strong enough the keep these structures intact.

With these differences in mind, several comparisons between model predictions and test results are highlighted below.

7.2.1 Vehicle Motions

Post-test measurements indicated that the extent of crush between the CEM locomotive and the cab car was between 45.6” and 51”. Video evidence (see Figure 87 through Figure 89) indicated that the maximum penetration of the end frames was about 64”, with an extent of rebound in the range of 12” to 15”, yielding a crush of 49” to 52”.

The FE model prediction of peak relative displacement at 33 mph was 54.3”. (Interpolating results from the 31-mph analysis indicated that, at 32.8 mph, the extent of peak relative displacement would be 53.7”.) This was about 10” less than the relative displacement estimated from the high-speed video. The predicted extent of relative displacement after 0.25 seconds was 52.8” (and dropping), suggesting that the final displacement would likely be closer to about 51”.

Figure 100 shows the predicted relative displacement vs. time curve compared to both the raw and corrected estimates of relative displacement obtained from test data by double-integrating the longitudinal acceleration curves measured at the respective centers of each vehicle underframe, and then subtracting one from the other. Interestingly, while the corrected curve matched the predicted final crush reasonably well, the FE model prediction was actually more consistent with the uncorrected curve through the first 0.16 seconds following impact. It may have been the case that the longitudinal acceleration response of the cab car was affected by the buckling of the cab car underframe/body, which began at about this time.

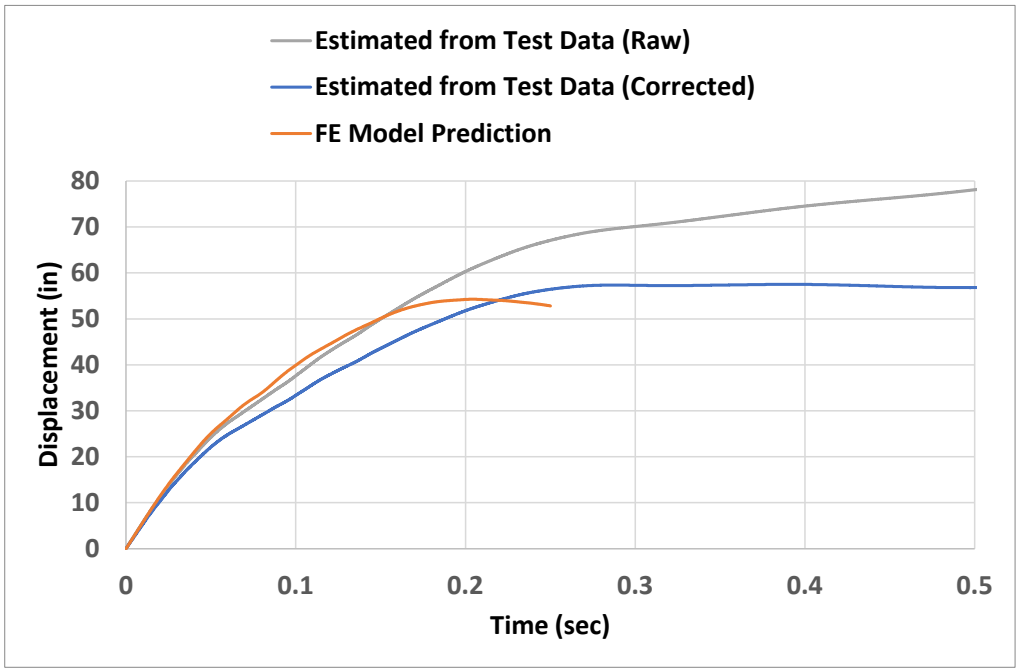

Figure 100. Comparison of predicted relative displacement vs. time curve with raw and corrected estimates obtained from test data

The FE model's under-prediction of crush by about 10" was likely due to three factors:

1. The 7" of additional travel of the impacting couplers with little energy absorption prior to knuckle failure
2. The additional cab car end frame deformation that arose because the collision posts were weaker than anticipated.
3. The shortening of the cab car associated with the crippling of the carbody.

7.2.2 Force-Displacement Curve

As noted above, the noise in the acceleration signals made it impossible to accurately estimate the total collision force. Moreover, the drift in the signal led to differences in vehicle velocities late in the test, when the CEM locomotive and cab car were locked together, making it difficult to accurately determine the relative displacement time-history of the colliding vehicles. At best, the force through the coupler could be compared, which was equal to the total force prior to the lower DAC tubes impacting the cab car end beam. This comparison is shown in Figure 101. The comparison was made more difficult by the failure of the cab car knuckle, which produced a large up and down spike in load between 8" and 12" of displacement and also affected the displacements associated with activation of the deformation tube. Nonetheless, there is some level of consistency between the curves.

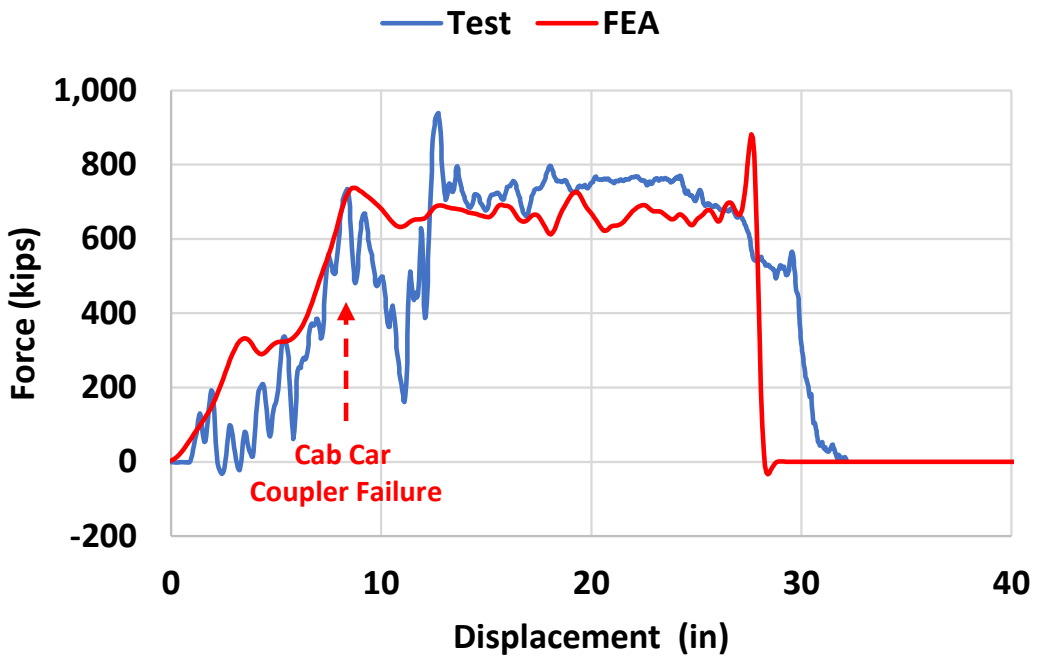

Figure 101. Comparison of force through the CEM coupler estimated based on coupler shank strain gage readings (see Figure 96, left) with FE model predictions

For completeness, a comparison of the estimated total force vs. crush is shown in Figure 102. As is evident, and for the reasons listed above, there is little agreement between these curves. In addition to the oscillations present, it appears that the buckling of the cab car collision post, which likely occurred at about 24" of crush, completely changed the character of the subsequent

force-displacement behavior, as very little force was required to produce additional end frame deformation.

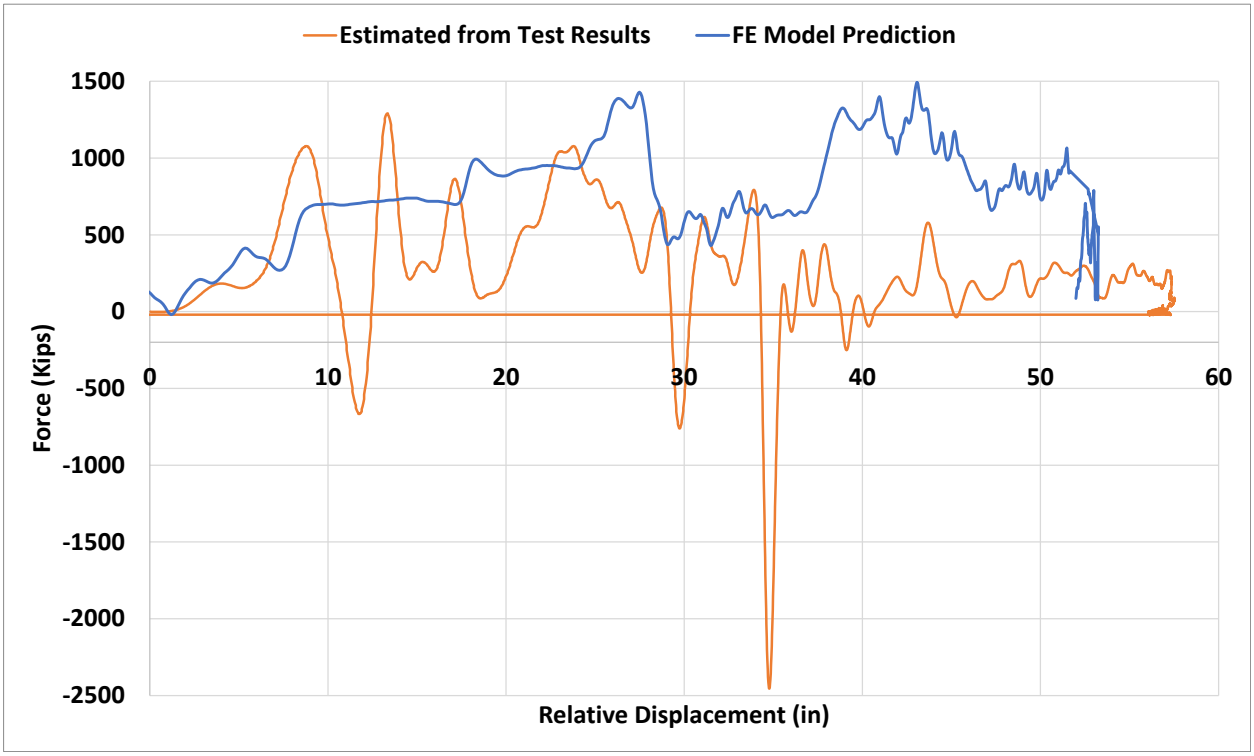

Figure 102. Comparison of total force vs. displacement derived from CEM longitudinal acceleration pulse with FE model predictions

7.2.3 Energy Absorption

Certain calculated/estimated energy absorption totals for the test and the model are compared in Table 5. Because reliably estimating the total force displacement curve was not possible, the total energy absorbed during the collision likewise cannot be accurately estimated. The PBC deformation tube energy absorption is assumed to be near its design value of 1,030 ft-kips. The estimate of DAC energy absorption was a little more difficult, particularly because the tubes did not compress uniformly. A rough estimate of DAC energy absorption was made based on measurements of DAC displacement at the four front corners of each lower DAC tube, yielding around 300 ft-kips – the test target. This was much less than the FE-predicted value of 710 ft-kips for the entire DAC assembly, and also significantly less than the predicted value of 500 ft-kips for the lower DAC tubes. It was likely that most, if not all, of this difference in predicted DAC energy absorption is attributed to the preferential deformation of the cab car underframe and collision posts, which were weaker than expected and clearly not able to withstand the forces transmitted through the anti-climbers. Note that, based on their force-displacement characteristics, each of the draft gears were expected to absorb about 70 ft-kips of energy when compressed to the push-back load. Draft gear energy was estimated based on integrating the coupler force-displacement curve over the first 12” of displacement, as the force rose to the push-back load. Based on this calculation, it appeared that the draft gears absorbed approximately 280 ft-kips of energy, almost twice as much as they otherwise would have

because they were loaded, then unloaded, as the cab car knuckle fractured, and then loaded again.

Table 5. Comparison of estimated CEM component energy absorption levels from the test with FE model predictions

Component	Test (ft-kips)	Model (ft-kips)
PBC Deformation Tube	1,030	1,030
PBC/Conventional Locomotive Draft Gears	280	140
DAC Lower Tube Assembly	300	500
DAC Upper Tube Assembly	0	220

7.2.4 Strain Near Shear Bolts

A contour plot of longitudinal strain in the draft pocket side plate during PBC pushback (see Figure 103) indicates the model predicted lower strain levels than were measured in the test, as was the case for VTVT1 (see Table 3). Strain levels were again greatest near the top-forward bolt hole, also contrary to test results. This is again likely the result of using connector elements to define the shear bolts and the associated difficulty in determining their influence on the stiffness of the structures surrounding the bolts.

The contour plot shows an area of compression near the top-front of the draft pocket side plate and an area of tension near the rear-top of the side plate. This is consistent with the test results. Because there was a sharp gradient away from the peak locations, it was not surprising the measured magnitudes were small.

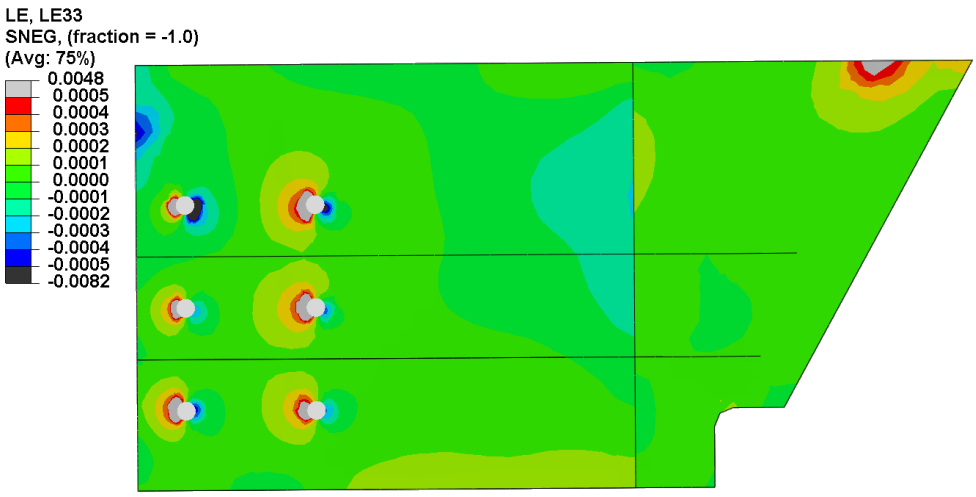

Figure 103. Contours of strain on the side of the draft pocket during deformation tube stroke

Expanding the contour plot to include the web of the underframe main I-beam (see Figure 104), it appeared there were pockets of tensile strain near the location of the lifting pad, as indicated. These pockets of tension, in the range 200 to 300 microstrain, seemed to be reasonably consistent with the measured values, but, because the values were small and the gradients sharp, it was not possible to make definitive conclusions regarding the consistency of model predictions and test results.

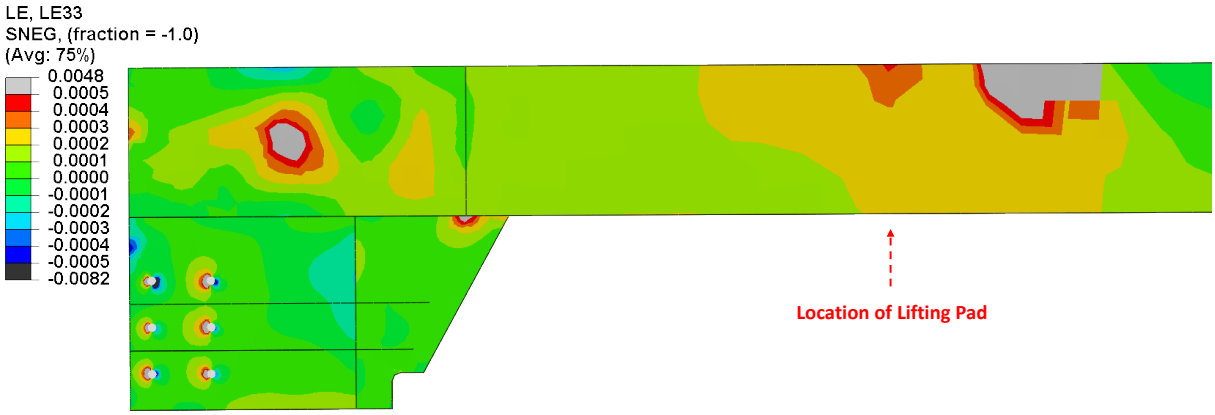

Figure 104. Contours of strain on the side of the draft pocket during deformation tube stroke

7.2.5 Modes of Deformation

As previously noted, key differences between the model predictions and the test results included the failure of the cab car knuckle, the extensive deformation of the cab car collision post with little deformation of the upper DAC tubes, and the crippling of the carbody near the rear door opening.

Figure 105 shows a comparison of predicted DAC crush with a post-test photograph. The noted differences are apparent. However, it appeared that the mode of deformation of the lower DAC tubes was consistent with the test result and was indicative of impact of the end beam with the lower inside regions of each lower DAC tube.

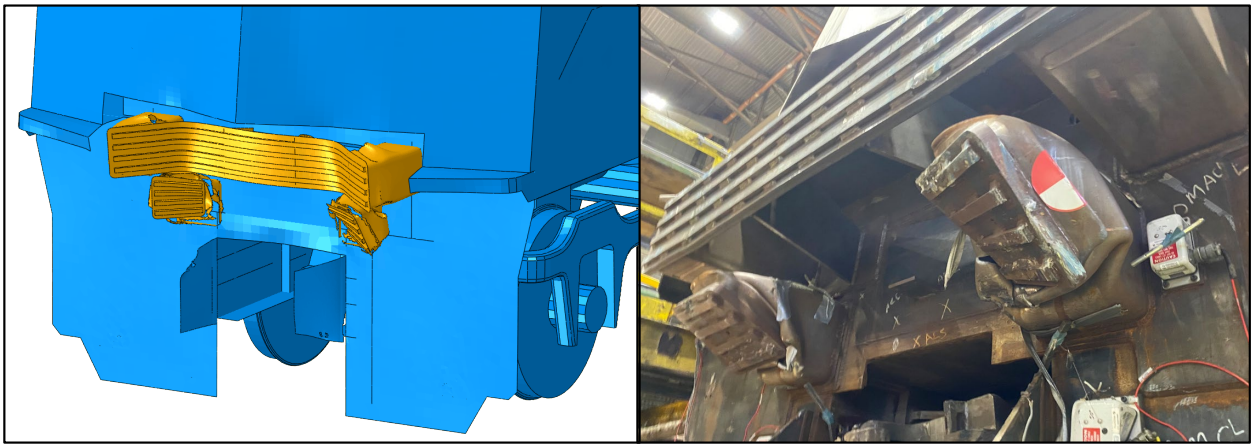

Figure 105. Comparison of FE model prediction of CEM end frame mode of deformation with a post-test photograph of the end frame (right)

The end frame of the cab car deformed extensively, with the collision posts folding back due to impact of the upper DAC tubes, which did not deform extensively, indicating the collision posts could not support a load sufficient to initiate DAC tube-folding. Figure 106 shows a comparison of the predicted cab car end crush with a photograph of the crushed end. The predicted folding back of the collision post and associated rotation of the end beam was consistent with the test result.

Figure 106. Comparison of FE model prediction (left) of cab car end frame mode of deformation with a post-test photograph of the end frame (right)

A graphic from the FE model highlighting the undeformed distance (approximately 70”) between the back of the cab car collision post to a vertical post below the middle of the endmost passenger window is shown at the top of Figure 107. A similar graphic shown at the bottom in Figure 107 highlights the predicted deformed distance (approximately 42”) as well as the height above the rail (71”) at which the maximum intrusion occurred. These results indicate that the predicted intrusion of the post into the vestibule of the cab car was about 28”.

A post-test measurement indicated that the distance between these two points was 41.5” (compared to the 42” predicted distance). A further measurement indicated that the maximum intrusion occurred approximately 66” above the rail, about 5” less than the FE model predicted.

The deformed plot in Figure 107 shows the draft sill was pushed down by the forces exerted upon it at the colliding interface. Post-test measurements indicated the minimum distance between the pushed-down draft sill and the rail was approximately 16” at a distance of 48” forward of the front wheel of the forward truck. The FE-predicted distance to the rail at this location was about 20.5”. Figure 108 shows a comparison of predicted draft sill deformation with a post-test photograph. The more extensive measured downward deformation of the cab car was likely the result of the more extensive deformation of the cab end relative to the model. The lower position of the fold in the collision post was consistent with this more extensive downward deformation.

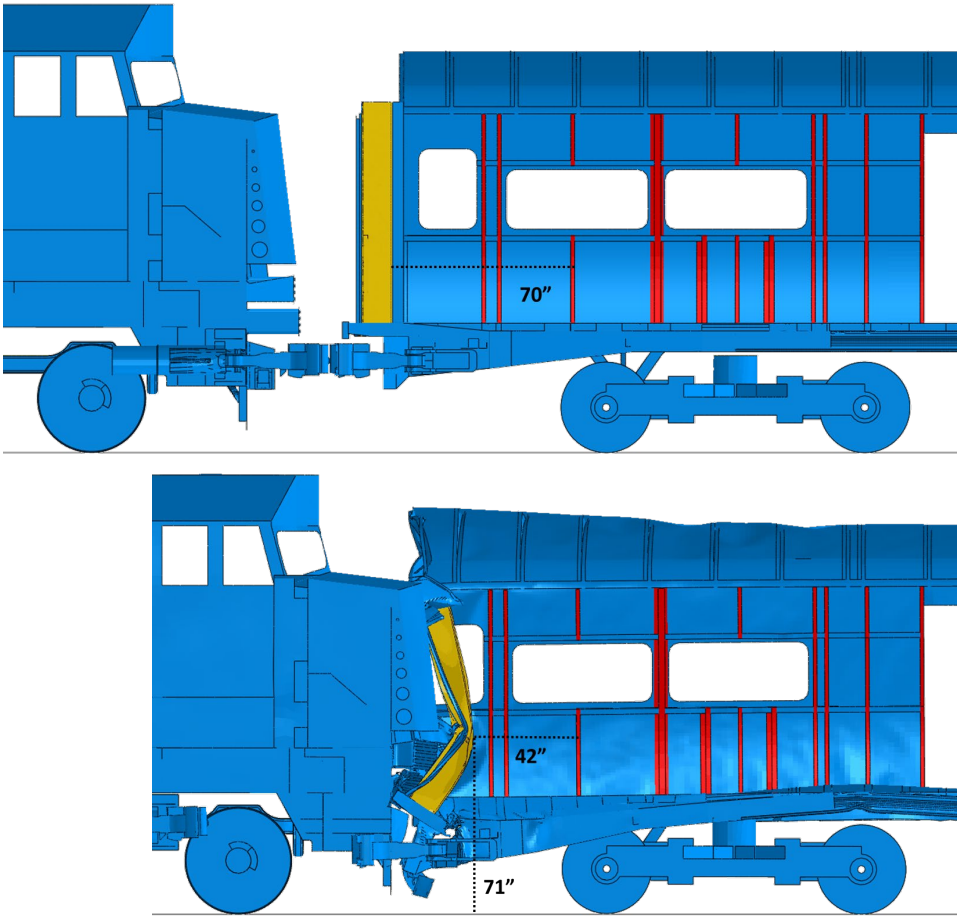

Figure 107. A graphic from the FE model showing the deformed cab, annotated with the undeformed distance from the back of the collision post to the middle of the endmost passenger window

Figure 108. Comparison of FE model prediction (left) of cab car draft sill mode of deformation with a post-test photograph of the draft sill (right)

7.3 Assessment of CEM Locomotive Damage/Repair Needs

The damage to the CEM vehicle was reviewed with test site personnel. The lower DAC tubes experienced extensive damage and will be replaced prior to the next test. As noted, the upper DAC tubes appeared to have deformed very little during the test, with only minor scratches visible, and will not be replaced.

The PBC was of course exhausted and will be replaced, as will the shear bolts and bushings. Likewise, the coupler carrier was destroyed, by design, and will be replaced.

Two additional components experienced extensive deformation:

- The sides of the end plate on either side of the draft pocket were bent backwards by several inches (see Figure 78). The extent of the deformation was exacerbated because the upward-angled tubes connecting the end plate to the underframe were missing. Test site personnel indicated it would be possible to bend these plates back. Note that these plates are not expected to be deformed during the upcoming train-to-train test.
- One of the two "rail stopper" plates bolted to the bottom plates of the draft pocket assembly and support the sliding lug was bent. It appeared the coupler carrier did not fall out of the way as intended and became wedged between this plate and the head of the PBC (see Figure 77). It is possible that the retention cables that were added to prevent the coupler carrier from falling to the track may not have had enough slack designed into them. Both support plates will be replaced for the next test.

In addition, it appeared that one of the holes in the draft pocket side plate through which the shear bolts were positioned became ovalized (see Figure 76) due to the high loads it experienced prior to and during shear bolt failure. This will be repaired for the next test.

To summarize, based on the post-test inspection of the vehicle and discussion with test site personnel, the following replacement/repair activities were recommended:

- Replace the PBC.
- Replace the shear bolts and bushings.
- Repair the ovalized shear bolt hole in the draft pocket side plate.
- Replace the lower DAC assembly.
- Replace the coupler carrier and add a few inches of cable to the coupler carrier retention device.
- Replace the draft pocket sliding lug support plates.

7.4 Lessons Learned/Recommendations for the Train-to-Train Test

In anticipation of the upcoming train-to-train test, a few lessons that can be taken from the post-test analysis of V2VT2 include:

- If the colliding couplers are placed in their "closed" position, it is likely that the knuckle of one of the two impacting couplers will fail. If the post-failure behavior of the colliding couplers is similar to what it was for this test, the heads of the couplers will continue to

move until they are effectively coupled. This additional relative motion (about 7”) changes the impact sequence in that contact of the DAC will occur at a lower level of PBC stroke. Given the uncertainties associated with knuckle failure, it may be worth considering having the couplers open as they were for VTVT1. In any event, the pre-test FE model calculations should accommodate this likelihood.

- The lack of upper DAC deformation suggests that it may be too strong for impact with cab cars. It may be worth revisiting the design strength of this sub-component, particularly with regard to the load required to buckle the angled support plates. This will not likely affect the collision behavior in the upcoming train-train test, as the conventional locomotive end frame is much stronger than that of the cab car.
- Researchers had difficulty replicating the inherent strength/stiffness of the original cab car flooring with retrofit plywood. For the train-to-train test, special care should be taken to ensure the plywood is well-connected to the flooring substructure. Also, FE models should explore the consequences of having flooring that is much weaker than what it otherwise would be if the plywood was well-connected to the rest of the carbody.
- The coupler carrier impeded the motion of the PBC into the draft pocket of the CEM. While it did not appear that this strongly affected the activation of the shear bolt failure process, the manner in which the coupler carrier is tethered to the front sides of the draft pocket, including the extent of slack in the connecting cable, should be reviewed prior to the train-to-train test.
- With regard to instrumentation, researchers found it difficult to estimate the collision force and relative displacement of the impacting vehicles. This may be made a little easier in the train-to-train test due to the heavier colliding vehicle weights; however, it will be critical to have reliable estimates of forces through all of the coupled interfaces. Also, alternative means of estimating displacements, such as high-speed video analysis, may be warranted.
- The strain levels measured on the sliding lug were small. If additional channels are needed, these gages are good candidates for elimination. The same can be said of the draft pocket side plate gages and the underframe gages, especially given the spatial gradients in strain in these regions.

8. Construction of Finite Element Models

The research team made a number of modifications to the FE model for analyses conducted to support the two vehicle-to-vehicle tests. In support of pre-test analyses conducted in support of V2VT1, the team made several changes to the FE model simulating the CEM locomotive-conventional locomotive collision. Each change was implemented in Abaqus/CAE [16]. Journal files (.jnl) documenting the interactive model development process were organized and edited so they could not only be used to re-create the model but also easily edited to implement modifications to the model.

8.1 CEM Locomotive Coupler Carrier

To increase its fidelity, the team modified the FE model of the CEM locomotive to include a more explicit representation of the coupler carrier. This allowed the impact between the coupler and the coupler carrier to be more directly modeled, as well as the failure of the coupler carrier. The modified CEM locomotive model with the more explicit representation of the coupler carrier is shown in Figure 109. In the figure, the sprung top box is shown in yellow, the bottom support box shown in red, and the side bolt locations shown in dark blue. The detailed side view (below right) of the modified CEM locomotive model illustrates the contact that will occur between the PBC head and the coupler carrier after about 8" of push-back.

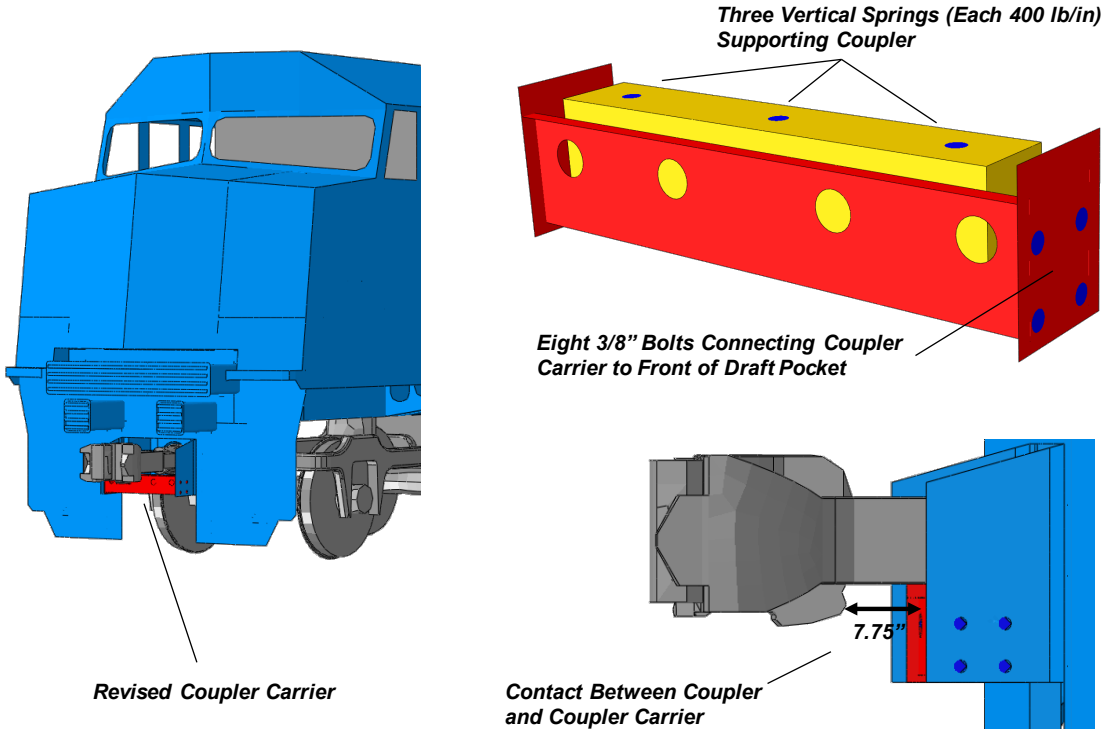

Figure 109. Left — the front end of the modified CEM locomotive model, with the new representation of the coupler carrier highlighted in red; above right — the new coupler carrier model; below right: detailed side view of the modified CEM locomotive model

The model for the coupler carrier featured an upper open box connected by three vertical springs (each with a stiffness of 400 lbf/in) to a lower open box into which it fit. The coupler rode on the upper open box, supported by the vertical springs, and pushed it down under its own weight. The sides of the lower box were connected to the extensions of the draft gear side plates with eight 0.375”-diameter steel bolts modeled with connector elements, each with a strength of approximately 8,000 lbf. Contact conditions were imposed between the coupler and the frangible coupler carrier so that it was impacted after about 8” of push-back, then failed, moving out of the way of the coupler head. Welded areas that ran across the lower box connecting its side plates to its bottom plate were defined to have reduced strength; these were intentionally designed to be weak to increase the frangibility of the coupler carrier when encountering a longitudinal load.

8.2 Conventional Locomotive Plow

Project researchers modified the FE model of the conventional locomotive to include a plow. Starting with an existing model for the plow developed in a previous program [17], they worked with engineers at the test site to incorporate measurements of key plow features from the locomotive to be used in V2VT1 (Locomotive 4117). The FE model of the plow is shown in Figure 110.

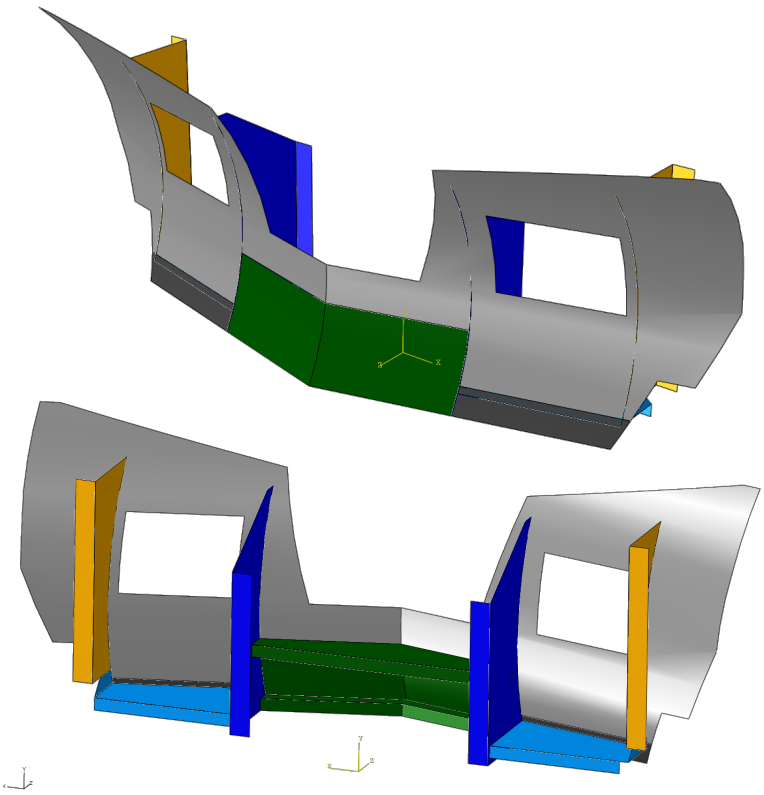

Figure 110. Front and back views of FE model for a conventional locomotive plow

Most of the curved plow, shown in light gray, was 0.25” thick steel. The center and lower few inches of the plow (dark gray and green) had doubling plates and were modeled as 0.5” thick. Behind the curved plow surface were vertical and horizontal gusset plates. The horizontal gusset

plates (dark blue and yellow), bolted to the end plate of the locomotive, were 1” thick. The horizontal stiffener plates (light blue and green) were 0.5” thick. Researchers integrated the plow model into the Abaqus/CAE [16] model of the conventional locomotive, as illustrated in Figure 111. The plow extended approximately 22” in front of the end plate, as indicated.

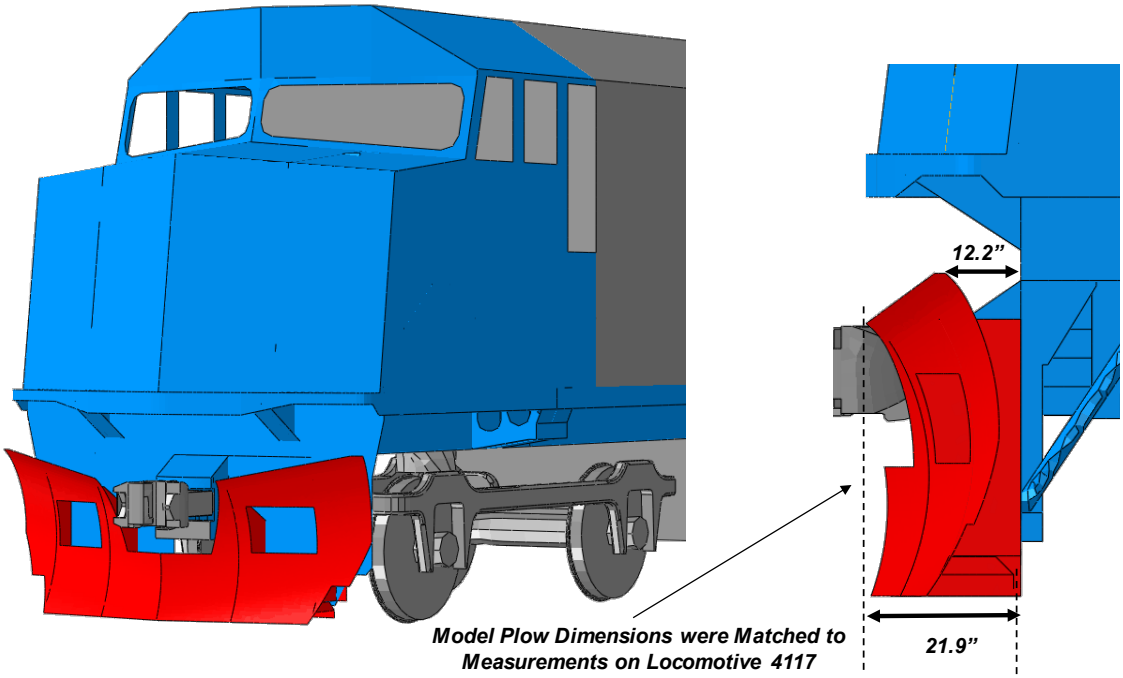

Figure 111. FE model of conventional locomotive with plow added

8.3 Modification of Collision Post and Other Short Hood Structures

Further revisions to the FE model of the conventional locomotive included modifications to the collision post and other structures inside the short hood to reflect the pre-S-580 [18] condition of Locomotive 4117 that would be used in V2VT1. These revisions included 0.375” collision posts with an angled flange and 0.125” sheets welded in front and behind that were determined based on measurements taken during an inspection of the inside of the short hood of Locomotive 4117. In addition, the thickness of the short hood was reduced to 0.125” to reflect its pre-S-580 construction. An image of the FE model of the conventional locomotive with the short hood skin removed is shown in Figure 112.

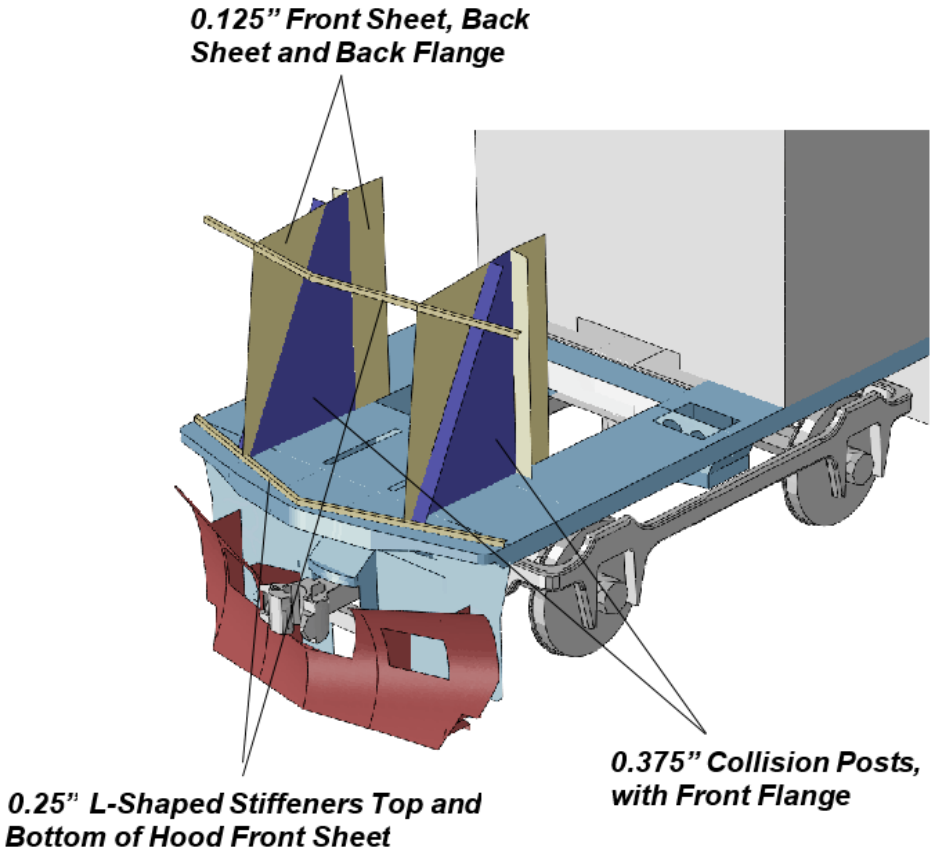

Figure 112. FE model with hood removed to reveal collision post modifications

8.4 Hopper Style Freight Car

An FE model for a hopper-style freight car that would trail the cab car and be ballasted to equalize consist weight during VTVT2 was developed and implemented in Abaqus/CAE. The geometry of this generic hopper-style car was based on photographs and dimensions of hopper cars from several manufacturers' web pages. For example, some dimensions were taken from specifications for the GBX 5200 covered hopper car [19]. Components for the car model include:

- A stiff, box-shaped center sill
- A frame consisting of side and end top rails, side and end sills, and side and end posts.
- Cross-bearers connecting the center sill and the side sills.
- A tub formed from thick plates, with the bottom of the tub having a serrated shape to represent the internal compartments and gravity outlet gates.
- Trucks
- A rigid-body representation of the connected rear cab car and forward freight car couplers, with compliance for the respective draft gears modeled with connector elements.

The car was assigned an empty weight of 60 kips, including 10 kips for each truck, consistent with specifications for the GBX 5200. Additional mass was added to bring the total weight of the cab car (about 90 kips) and the freight car to 232.6 kips (the weight of the CEM locomotive).

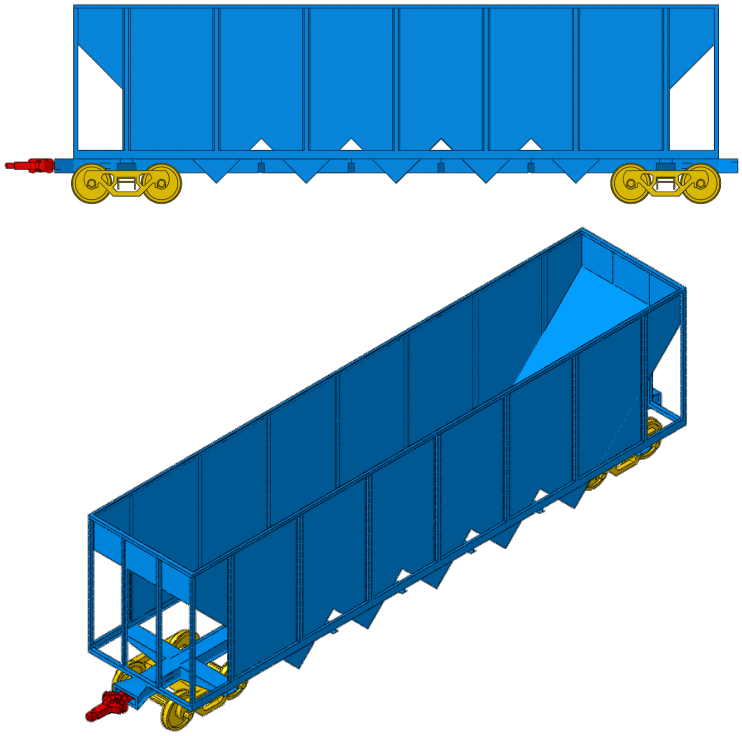

Figure 113. Side and isometric views of FE model of hopper-style freight car

8.5 CEM Locomotive Modifications

Based on the test results for V2VT1 and subsequent evaluation of damage, several changes were made to the CEM locomotive model that would be used in simulations of V2VT2. Two modifications were made to increase the stiffness and strength of the connection between the angled support plates:

- A 4”-deep by 9”-tall by 1”-thick stiffening plate was added behind the front plate where the DAC angled support plates were welded to the front plate, as highlighted in red at left in Figure 114.
- A 0.375”-thick bearing plate was added to the front plate where the angled support plates were welded, doubling the thickness in this region, as highlighted in red at right in Figure 114.

Cutouts were made to the floor sheets in this same area; these provided access to the back side of the front plate and had been made when the locomotive was first retrofit. These sheets were only 0.060”, so it was unlikely that these cutouts greatly affected the structural integrity of this region.

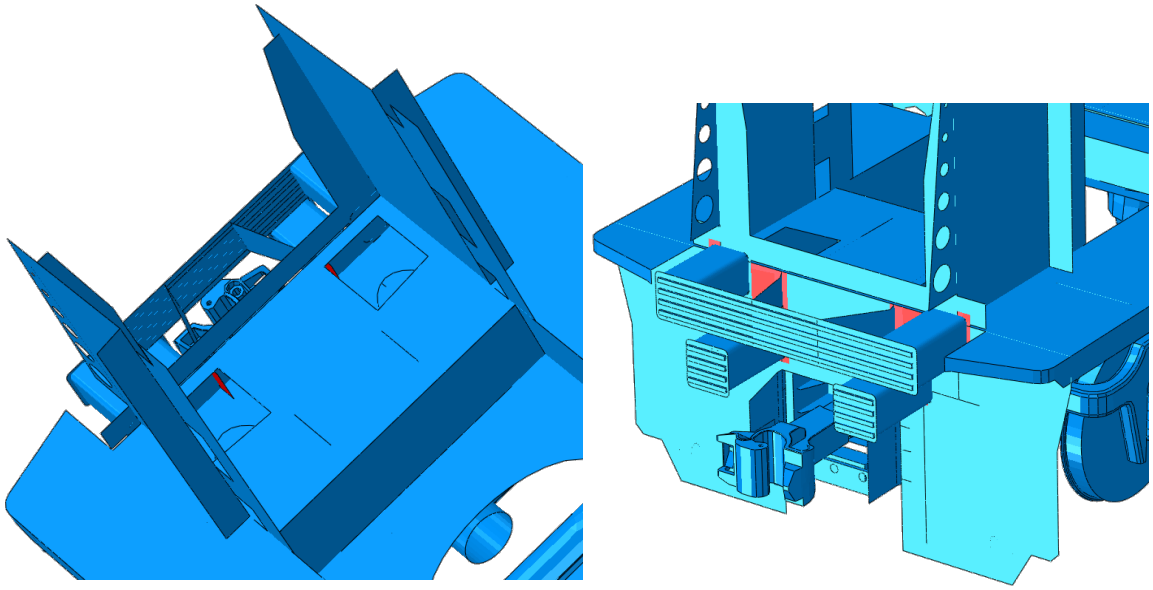

Added Stiffeners Behind DAC Angled Supports & Cut Hole in Floor Plate

Increased Size of Bearing Plate to Include DAC Angled Support Connection to Front Plate

Figure 114. Left — detail from FE model showing added stiffeners (red); right — size of bearing plate increased (larger rectangles highlighted in red) to include area where angled DAC supports were welded to front plate.

Informed by an analysis of differences between pre-test model predictions and V2VT1 test results performed as described in Section 4, the DAC tubes and the angled support plate were extended forward by 1.125” to account for use of shell elements to model the front plates and bearing plates (see Section 4.2).

An excerpt from a DAC drawing (14424-0400) [8] shows that the top DAC assembly extended 18.875” from the end plate, as illustrated in Figure 115.

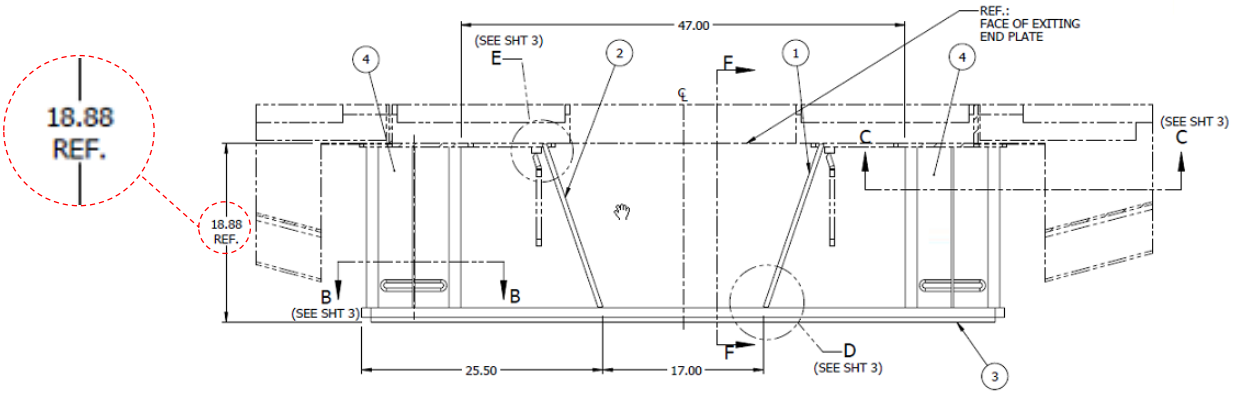

Figure 115. Excerpt from drawing 14424-0400 [8] showing that top DAC assembly extended 18.875” forward from the end plate of the CEM locomotive

Because the model used shell element representations of the DAC structures, the crush tubes and angled support plates had to be extended an appropriate distance forward from the end plate to permit contact with the colliding conventional locomotive end structures (note that, for contact, the half thickness of the bars welded to the upper DAC cross plate added another 0.25”). The 1.125” sections at the back of the four tubes and two angle plates, shown in Figure 116, were assigned properties that rendered them effectively rigid, so they just transmitted forces through to the end plate.

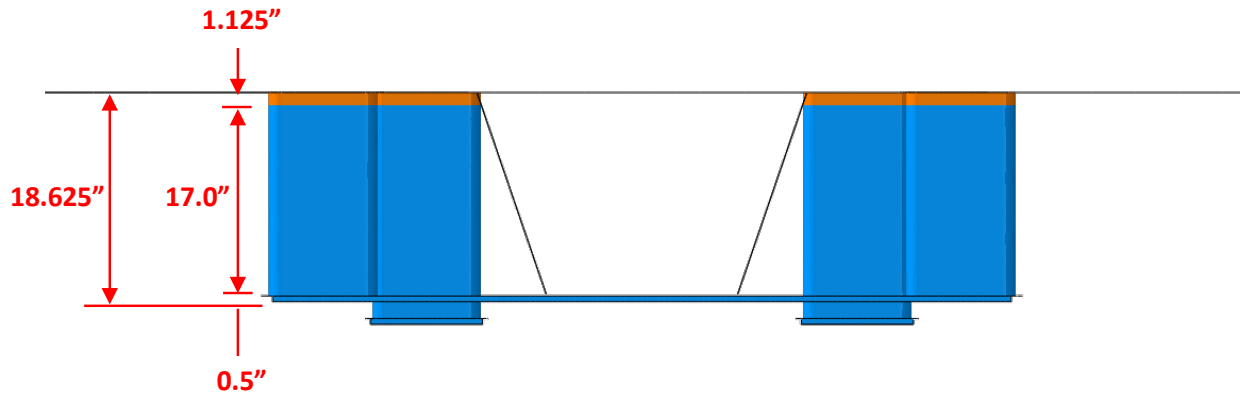

Figure 116. Detail from modified CEM locomotive model showing 1.125”-deep sections added to the four DAC tubes and the angled support plates

8.6 Cab Car Modifications

The FE model for the M1 cab car model was also modified.

A composite floor cover was added from the vestibule back to the end of vehicle. The floor cover, comprising a 0.72”-thick plywood sheet sandwiched between a 0.14”-thick plastic top sheet and a 0.03”-thick aluminum underlay sheet, was not included in the original M1 cab car model because the vehicle used in the coupling tests had been remediated to remove asbestos.

The original plan was for the cab car to be remediated only to the back of the front vestibule, so flooring was added from there to the end of the vehicle, as is shown in Figure 117. Note that, later, researchers decided the entire vehicle should be remediated, so the floor covering added here was removed for the later simulations of VTVT2. However, these simulations indicated that without the strength and stiffness provided by the floor cover, the cab car was susceptible to localized deformation of the sub-floor panels and sidewall structures, particularly near the open side doors. For this reason, the car was retrofitted with plywood panels (two 0.5” layers) to enhance the strength and stiffness of the floor. The floor structure was added back into the model, and the properties were modified so that they were representative of the plywood.

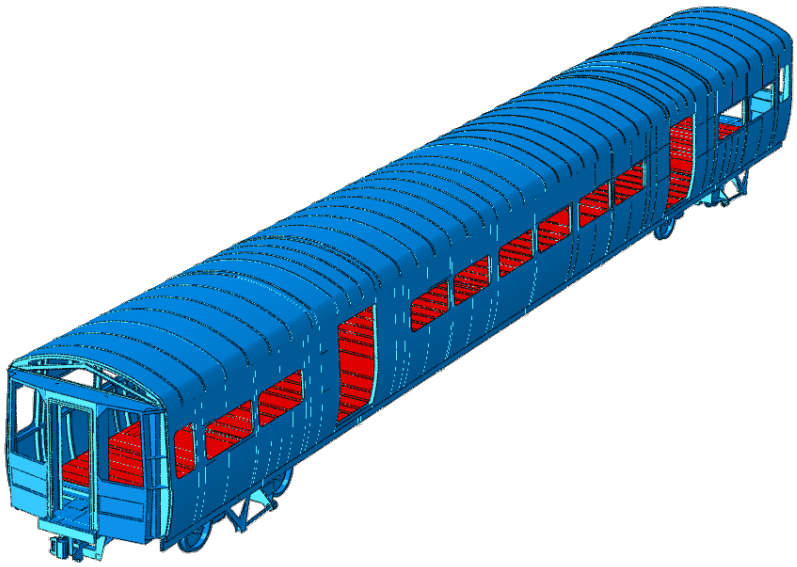

Figure 117. Modified cab car FE model showing added flooring, highlighted in red

In addition, an open, box-shaped buffer beam (not part of the M1 cab car used in the coupling tests) was added, along with spring connections to the end beam behind it, as illustrated in Figure 118. The spring connection was modeled in a fashion similar to what has been used for the CEM locomotive shear bolts and the cab car coupler carrier side bolts. Small, circular rigid disks were defined at the locations of the ends of the longitudinal springs connecting the buffer beam to the end beam of the car. These springs were somewhat arbitrarily defined, given the absence of specifications, to have a spring stiffness of 400 lbf/inch. With this small spring constant, it does not take much force to push the buffer beam back against the end beam.

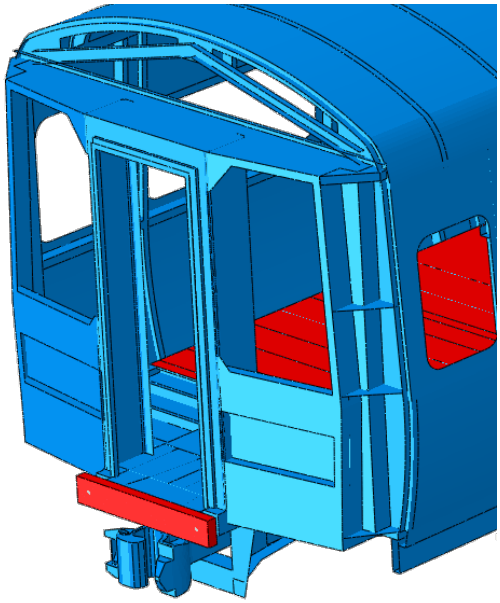

Figure 118. Detail showing front end of modified cab car FE model with added buffer beam, highlighted in red, and small round discs representing the ends of springs coupling the buffer beam to the end beam of the car, highlighted in yellow

Finally, a connector representing the aft draft gear was added. This connector was assigned the same properties as the forward draft gear. It connected the rear draft pocket of the cab car with the rigid body representation of the coupled rear cab car/forward freight car couplers.

8.7 New Coupler Models

In anticipation of VTVT2, one of the issues that arose was whether the couplers should be open or closed for the test. The couplers were open for VTVT1. This allowed for smooth push-back of the PBC, but, as noted in Section 4.1, decreased the extent of stroke of the PBC prior to DAC engagement by about 10.5". This significantly affected the outcome of the test and, in particular, increased the required impact speed for full activation of the PBC to shear the bolts connecting the sliding lug to the draft pocket side plates. This was one of the contributing factors that resulted in the shear bolts not failing during the test.

Partly for this reason, the research team decided the couplers would be closed for VTVT2. There is precedence for this, as the couplers appear to have been closed for both of two previous train-to-train impact tests[20][21]. Also, it is more likely that they would be closed during normal operation.

There was concern, however, about whether the impact of two closed couplers might cause one or both of them to rotate such that the longitudinal force through them would decrease to a point where it would be insufficient for push-back and failure of the shear bolts. Analyses conducted several years ago appeared to suggest the push-back of the PBC occurs so quickly that there is not enough time for significant rotation; however, the documentation of these analyses has been lost.

To help answer this question, the VTVT2 model was modified to first add a yoke behind the cab car coupler and partition the PBC to allow isolation of its yoke. It was then further modified to treat the couplers as deformable structures connected to their respective yokes through a pin that allows yaw rotation and vertical motion but no pitch/roll rotation or lateral/longitudinal motion.

The FE model for the yoke is shown in Figure 119.

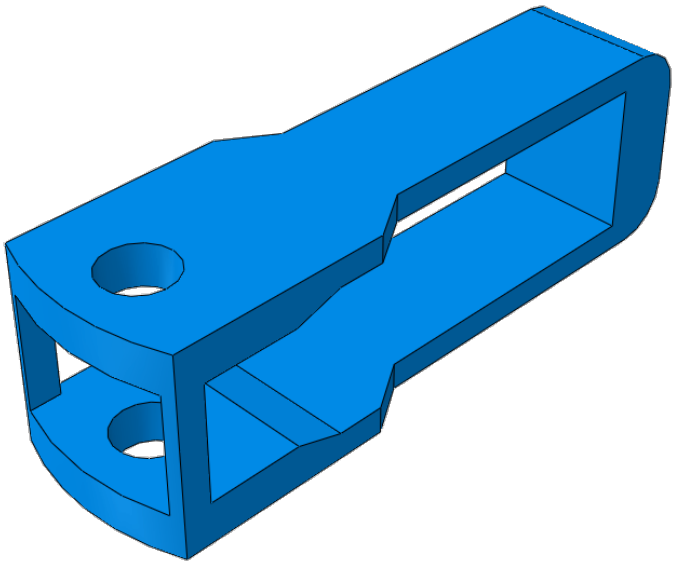

Figure 119. FE model of cab car yoke

Attempts to run simulations of VTVT2 with the modified coupler definition were not successful, due to runtime errors associated with poorly defined geometry (leading to poorly defined elements) in the respective couplers. The CAD model for the couplers was created in an earlier program [8] and were intended to be "looks-like" representations of the coupler rather than more exact geometries required for FE model creation. Prior to this recent change this had not been a problem, as the couplers had been modeled as rigid bodies.

To address this issue, both couplers were recreated in Abaqus/CAE, using the geometry of the existing couplers as a guide. The respective couplers are pictured in Figure 120. The cab car coupler was 28" long (longitudinal distance between coupler pin and knuckle pin, as indicated) and the CEM locomotive coupler was 31" long. The couplers were defined to have identical head geometries, differing only in the length of the shank and the presence of a feature on the underside of the longer CEM locomotive coupler to impact the frangible coupler carrier.

The FE model for simulation of VTVT2 were updated to incorporate these new coupler models.

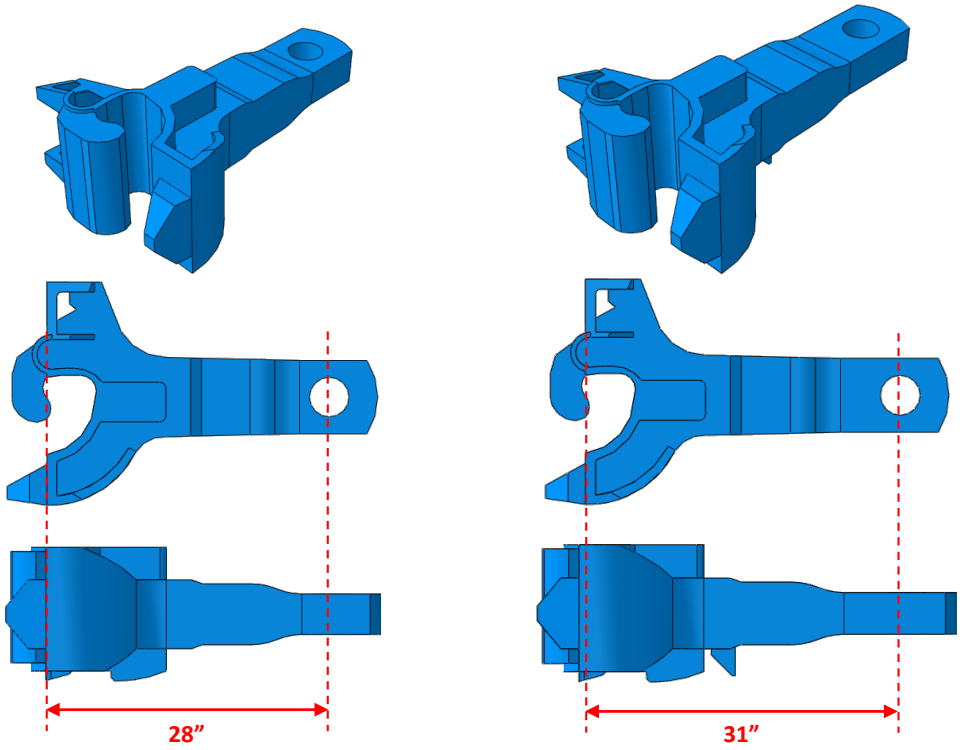

Figure 120. FE model of new cab car (28", left) and CEM locomotive (31", right) couplers

9. Conclusion

Two full-scale, vehicle-to-vehicle tests have been conducted that evaluated a CEM system retrofit onto a conventional passenger locomotive to enhance its crashworthiness. Pre-test activities in support of V2VT1 indicated a target speed of 21 mph ± 1 mph would meet test objectives of a complete PBC stroke with shear bolt failure and energy absorption in the DAC of at least 50 percent of the design specification, with some margin for error. The actual test speed was only 19.3 mph, well below the minimum expected speed. The various components performed as designed: the vehicles remained in-line with no derailment and no signs of override, the stroke of the PBC deformation tube appeared to have been exhausted, and the DAC energy absorption levels met test targets. However, due to the low test speed, there was not enough energy to fail the PBC shear bolts. Two FE model-related factors were identified as also contributing to the lack of shear bolt failure:

- The test was conducted with the couplers open. This effectively increased the closing distance between the vehicles prior to load build-up in the PBC and effectively reduced the extent of PBC deformation prior to DAC engagement, which altered the load path and caused significantly more energy absorption prior to PBC shear bolt failure.
- The DAC bearing plate and front plate were modeled as shells. This effectively reduced the extent to which they extended forward from the end plate of the locomotive, which also increased the extent of energy absorption prior to PBC shear bolt failure.

A post-test assessment of damage revealed one issue regarding the design of the CEM locomotive support structure that needed to be addressed prior to V2VT2. Welds at the connection of the DAC angled support plates to the end plate of the CEM locomotive were damaged. FE model results showed localized plastic deformation in this area. A repair was implemented in which a gusset plate was added behind the end plate, and a bearing plate was added in front of the end plate. Longer term, it is likely that increasing the size of the collision post flange/DAC bearing plate to include the region where the angled support plate is welded will be sufficient to alleviate this issue.

A post-test review of test data indicated that strain gages mounted to the surface of the coupler shank provided an excellent estimate of forces through the coupler and were generally better than accelerometers mounted near the center of the CEM locomotive carbody for determining force build-up during PBC deformation prior to engagement of the DAC. Post-test model simulations for relative vehicle displacement, vehicle speed, force-vs.-crush behavior, and mode of deformation compared quite favorably to test results.

Pre-test FE modeling in support of VTVT2 indicated a target speed of 33 mph ± 2mph would meet test objectives of complete PBC stroke with shear bolt failure and energy absorption in the DAC of at least 50 percent of the design specification, with some margin for error. These models further indicated that the collision forces that arise in this test might challenge the buckling resistance of the cab car, particularly because the original flooring was removed. Interestingly, these models indicated that this mode of deformation was less desirable at speeds where the shear bolts did not fail, leading to buckling of the carbody/underframe near the forward side doors of the cab car.

V2VT2 collision speed was 32.8 mph – very close to the target. The test was successful, with all key test objectives met, including exhaustion of the PBC deformation tube stroke and failure of the shear bolts. The colliding vehicles did not derail, nor did one override another. However, the cab car was "crippled," with a large buckle forming in the underframe just forward of the rear side doors. This caused the wheels of the rear truck to lift off the rail, and it was fortunate that they fell back onto the rail without causing a derailment.

The knuckle of the cab car coupler fractured just after impact. It appeared that the knuckle of the CEM locomotive pushed past the vertically oriented split in the cab car coupler knuckle and seated against the back of the coupler head as if the couplers had been open prior to impact. This changed the deformation mode, with the DAC loaded much earlier with respect to the stroke of the PBC. In addition, it appeared that the coupler carrier did not fall away fast enough and became trapped between the push-back coupler head and the support plates for the sliding sill. Despite these two unexpected events, the PBC performed as designed, suggesting that it has some robustness with respect to deformation modes at the collision interface that might differ to some extent from those of the idealized design.

The FE model captured certain aspects of the collision well, but there were some key differences in deformation mode, particularly because the upper DAC plate and tubes were barely damaged in the test. Instead, the cab car collision posts folded back at a lower load than expected, and the energy absorption in the upper DAC tubes was minimal. Revisiting the design of the upper DAC assembly may be warranted. Nonetheless, the predicted cab car end frame deformation was quite similar to that observed in the test.

The post-test review of test data again indicated that the strain gages mounted to the surface of the coupler shanks provided an excellent estimate of forces through the coupler and were generally better than accelerometers mounted near the center of the CEM locomotive carbody for determining force build-up during PBC deformation prior to engagement of the DAC. The data from string potentiometers were also very useful in determining the timing and magnitude of key component behavior.

Overall, the vehicle-to-vehicle impact tests were very successful. The primary objective to demonstrate the effectiveness of the components of the CEM system working together to absorb impact energy and to prevent override in two different vehicle-to-vehicle collision scenarios was met. The FE analyses predicted the behavior of the equipment in both collision scenarios with high fidelity. These results give researchers a high degree of confidence in the modeling and test preparation for the last test in the program, the train-to-train test.

10. References

[1] Mayville, R.A., Stringfellow, R.G., Rancatore, R.J., Hosmer, T.P. (1995). Locomotive Crashworthiness Research: Executive Summary [DOT/FRA/ORD-95/08]. Washington, DC: U.S. Department of Transportation, Federal Railroad Administration.

[2] Tyrell, D., Severson, K., Marquis, B., Martinez, E., Mayville, R., Rancatore, R., Stringfellow, R., Hammond, R., Perlman, A.B. (1999). Locomotive Crashworthiness Design Modifications Study. *Proceedings of the 1999 IEEE/ASME Joint Railroad Conference.* Institute of Electrical and Electronics Engineers, number 99CH36340.

[3] Mayville, R., Stringfellow, R., Johnson, K., Landrum, S. (2003). Crashworthiness Design Modifications for Locomotive and Cab Car Anticlimbing Systems [DOT/FRA/ORD-03/05]. Washington, DC: U.S. Department of Transportation, Federal Railroad Administration.

[4] Tyrell, D., Jacobsen, K., Martinez, E., (2006). A Train-to-Train Impact Test of Crash Energy Management Passenger Rail Equipment: Structural Results. American Society of Mechanical Engineers, Paper No. IMECE2006-13597.

[5] Llana, P., Stringfellow, R. (2011). Preliminary Development of Locomotive Crashworthy Components. *Proceedings of the 2011 ASME Joint Rail Conference*. Paper No. JRC2011-56104.

[6] Llana, P., Stringfellow, R. (2011). Preliminary Finite Element Analysis of Locomotive Crashworthy Components. American Society of Mechanical Engineers, Paper No. RTDF2011-67006.

[7] Llana, P., Stringfellow, R., Mayville, R. (2013). Finite Element Analysis and Full-Scale Testing of Locomotive Crashworthy Components. *Proceedings of the 2019 ASME Joint Rail Conference*. Paper No. JRC2019-1259.

[8] Stringfellow, R., Amar, G. (2016). Locomotive Crashworthy Components Retrofit for F40 Locomotive. Cambridge, MA: Volpe National Transportation Systems Center.

[9] Llana, P., Jacobsen, K., Stringfellow, R. (2019). Conventional and Crash Energy Management Locomotive Coupling Tests [DOT/FRA/ORD-19/36]. Washington, DC: U.S. Department of Transportation, Federal Railroad Administration.

[10] Rakoczy, P., Gorhum, T. (2019). Conventional Coupling Test Between Coach Car and Passenger Locomotive [DOT/FRA/ORD-19/06]. Washington, DC: U.S. Department of Transportation, Federal Railroad Administration.

[11] Rakoczy, P., Sciandra, E. (2021). Crash Energy Management Coupling Test between a Coach Car and a Passenger Locomotive [DOT/FRA/ORD-21/01]. Washington, DC: U.S. Department of Transportation, Federal Railroad Administration.

[12] Llana, P., Jacobsen, K., Stringfellow, R. (2019). Locomotive Crash Energy Management Coupling Tests Evaluation and Vehicle-to-Vehicle Test Preparation. *Proceedings of the 2019 ASME Joint Rail Conference.* Paper No. JRC2019-1259.

[13] Rakoczy, P., Gorhum, T. (2021). Conventional and CEM Passenger Locomotive Impact Test [DOT/FRA/ORD-21/02]. Washington, DC: U.S. Department of Transportation, Federal Railroad Administration.

[14] Llana, P., Jacobsen, K., Stringfellow, R., Locomotive Crash Energy Management Vehicle-to-Vehicle Impact Test Results. *Proceedings of the 2020 ASME Joint Rail Conference*, Paper No. JRC2020-8030.

[15] DeGeorge, M., Gorhum, T. (2022). F40 CEM Locomotive and M1 Passenger Car Impact Test", U.S. Department of Transportation [DOT/FRA/ORD-22/24]. Washington, DC: U.S. Department of Transportation, Federal Railroad Administration.

[16] Abaqus CAE Software.

[17] TIAX LLC (2007). Pilot for Rail Passenger Cab Cars. Phase I SBIR Report to the Federal Railroad Administration.

[18] Association of American Railroads, Technical Services Division, Mechanical Section. *Manual of Standards and Recommended Practices, Locomotive Crashworthiness Requirements.* Standard S-580. Adopted: 1989; revised, 1994, 2001, 2005, 2008.

[19] The Greenbriar Companies. 5200 Grain Covered Hopper.

[20] Tyrell, D. (2003). Passenger Rail Train-to-Train Impact Test Volume I: Overview and Selected Results [DOT/FRA/ORD-03/17].

[21] Tyrell, D., Jacobsen, K., Martinez, E. (2006). A Train-to-Train Impact Test of Crash Energy Management Passenger Rail Equipment: Structural Results. American Society of Mechanical Engineers, Paper No. IMECE2006-13597.

Abbreviations and Acronyms

ACRONYMS	EXPLANATION
ASME	American Society of Mechanical Engineers
CEM	Crash Energy Management
CG	Center of Gravity
DAC	Deformable Anti-Climber
FE	Finite Element
FRA	Federal Railroad Administration
TIP	Test Implementation Plan
TTC	Transportation Technology Center
TTCI	Transportation Technology Center, Inc.
PBC	Push-Back Coupler
V2VT1	Vehicle-to-Vehicle Test 1
V2VT2	Vehicle-to-Vehicle Test 2